

 Die approbierte Originalversion dieser Diplom-/Masterarbeit ist in der Hauptbibliothek der Technischen Universität Wien aufgestellt und zugänglich.  
<http://www.ub.tuwien.ac.at>

  Universitätsbibliothek

The approved original version of this diploma or master thesis is available at the main library of the Vienna University of Technology.  
<http://www.ub.tuwien.ac.at/eng>



FAKULTÄT  
FÜR INFORMATIK

Faculty of Informatics

# Automatisierte Messung funktionaler Parameter älterer Erwachsener basierend auf Tiefendaten

DIPLOMARBEIT

zur Erlangung des akademischen Grades

**Diplom-Ingenieur**

im Rahmen des Studiums

**Medizinische Informatik**

eingereicht von

**Ing. Michael Atanasov, BSc**

Matrikelnummer 01225770

an der Fakultät für Informatik

der Technischen Universität Wien

Betreuung: PD DI Dr. Martin Kampel

Mitwirkung: Mag. DI Dr. Rainer Planinc

Wien, 5. März 2018

---

Michael Atanasov

---

Martin Kampel



# Automated Measurement of Functional Parameters of Older Adults Based on Depth Data

DIPLOMA THESIS

submitted in partial fulfillment of the requirements for the degree of

**Diplom-Ingenieur**

in

**Medical Informatics**

by

**Ing. Michael Atanasov, BSc**

Registration Number 01225770

to the Faculty of Informatics

at the TU Wien

Advisor: PD DI Dr. Martin Kämpel

Assistance: Mag. DI Dr. Rainer Planinc

Vienna, 5<sup>th</sup> March, 2018

---

Michael Atanasov

---

Martin Kämpel



# Erklärung zur Verfassung der Arbeit

Ing. Michael Atanasov, BSc  
Waidhofnerstraße 5, A-3843 Dobersberg

Hiermit erkläre ich, dass ich diese Arbeit selbständig verfasst habe, dass ich die verwendeten Quellen und Hilfsmittel vollständig angegeben habe und dass ich die Stellen der Arbeit – einschließlich Tabellen, Karten und Abbildungen –, die anderen Werken oder dem Internet im Wortlaut oder dem Sinn nach entnommen sind, auf jeden Fall unter Angabe der Quelle als Entlehnung kenntlich gemacht habe.

Wien, 5. März 2018

---

Michael Atanasov





The research presented in this thesis was partially supported by the Austrian Research Promotion Agency (FFG) and the European Union (AAL-Joint Programme) under grant AAL 2015-056.





# Acknowledgements

It is an honor to acknowledge the persons who supported me throughout my studies and this thesis. I would like to thank my advisors Martin Kampel and Rainer Planinc, who shared their knowledge with me and gave precious advice and guidance. I would also like to acknowledge the help of the employees of cogvis by participating in the recordings. Additionally, I want to thank my colleague David Fankhauser for providing his knowledge and technical know-how.

Further, I want to express my deepest gratitude to my parents Anita and Johann, who enabled my academic studies and provided support, whenever needed. I would also like to thank my brother Alexander, who always listened to my problems and supported me with recommendations and motivation. Finally, I want to heartily thank Tamara for her patience and support during the time writing this thesis.



# Kurzfassung

Durch erhöhte Lebenserwartung, sowie die wachsende Weltbevölkerung steigt die Zahl der älteren Erwachsenen. Erhöhtes Alter bringt Herausforderungen, wie Verschlechterung kognitiver und physischer Fähigkeiten, mit sich, die sich in Gebrechlichkeit äußern können. Gebrechlichkeit ist ein Syndrom, welches durch geringere Resistenz gegenüber Stress, Krankheiten und anderen exogenen Einflüssen charakterisiert wird. Gebrechlichkeit ist reversibel und verhinderbar, wenn es früh genug erkannt wird, dadurch werden Methoden zur Erkennung von Gebrechlichkeit benötigt. Durch die Korrelation zwischen Gebrechlichkeit und körperlicher Leistungsfähigkeit, gibt es Tests, um die Mobilität einer Person, und in weiterer Folge das damit verbundene Gebrechlichkeits-Risiko, bewerten zu können. Die dadurch entstehende Prüfungssituation bewirkt allerdings, dass getestete Personen ihr Verhalten ändern, wodurch sich die Ergebnisse von den Leistungen im Alltag unterscheiden.

In dieser Arbeit wird das Fitnessniveau automatisch eingeschätzt, basierend auf der Messung von Gang-Parametern als zusammenfassenden Indikator des Gesundheitszustandes und Aufsteh-Leistung als Prädiktor für Balance-Defizite und Stürze. Für beide Messungen werden durch Tiefensensoren aufgezeichnete Bewegungsverläufe verwendet. Tiefensensoren ermöglichen unaufdringliche, Privatsphäre schützende Erfassung von Bewegungen in habitueller Geschwindigkeit. Die zugrundeliegende Methode zur Bewegungsverfolgung von Personen benötigt keine Konfiguration, wodurch eine einfache Installation in Wohnungen ermöglicht wird. Für die Evaluierung der vorgeschlagenen Mess-Ansätze wurden zwei Datensets aufgenommen und manuell annotiert. Das STS Datenset beinhaltet 137 Aufsteh-Sequenzen in Kombination mit alltäglichen Aktivitäten. Das 4-Paths Datenset enthält Gang-Sequenzen von 10 Personen auf 4 vordefinierten Pfaden.

Die erste Messmethode analysiert den Gang bezüglich Geh-Geschwindigkeit, Distanz, und Dauer. Weiters werden zwei Vorgehensweisen zur Bestimmung von Gang-Ereignissen verglichen. Eine verwendet Literatur-basierte scale-space Filterung, die andere verwendet maschinelles Lernen um die Gang-Ereignisse zu bestimmen und in weiterer Folge Komponenten des Gang-Zyklus abzuschätzen: Schrittzeit, Gangzeit, Schrittfrequenz, einfache Stütze, doppelte Stütze, Standphase. Für das Training des Lern-Algorithmus und die Evaluierung der gemessenen Parameter wird das 4-Paths Datenset verwendet. In diesem Datenset sind die Fersen-Auftritte und Zehen-Abhebungen manuell annotiert und die

Pfad-Distanzen sowie die Gang-Zeiten mittels Laser-Messung und Stoppuhr erfasst, um räumlich-zeitliche Evaluierung der gemessenen Gang-Parameter zu ermöglichen. Der Vergleich zeigt bessere Ergebnisse für den Maschinenlern-Ansatz und, dass die Bestimmung von Komponenten des Gang-Zyklus vergleichbar mit State of the Art Messungen mittels tragbaren Sensoren ist.

Die zweite Messmethode ist in zwei Probleme unterteilt: die Erkennung einer Aufsteh-Bewegung und die Messung der Aufsteh-Dauer. Zur Erkennung wird ein Literatur-basierter Schwellwert-Ansatz mit Maschinenlern-Ansätzen verglichen. Die Zeitmessung wird mittels Kurvendiskussion durchgeführt, um den steilsten Höhenanstieg in der detektierten Aufstehsequenz zu identifizieren. Die Maschinenlern-Algorithmen werden mit Aufsteh-Sequenzen des STS Datensets trainiert, in dem jeweils Beginn und Ende von Aufsteh-Bewegungen manuell annotiert sind. Das ermöglicht die Evaluierung des Detektierungsansatzes sowie der Zeitmessung. Die Aufsteh-Erkennung erzielt beste Ergebnisse mit einem Random-Forest-Algorithmus, die Ergebnisse der Zeitmessung sind vergleichbar mit State of the Art Ergebnissen.

Ein ganzheitliches System wird vorgestellt, welches die Messmethoden kombiniert und in Wohnungen von älteren Erwachsenen installiert werden kann, um Gang-Parameter und Aufsteh-Leistung zu messen. Die akquirierten Informationen werden aggregiert und für die weitere Verwendung durch z.B. medizinische Fachkräfte zur Verfügung gestellt. Das System wurde in einem 8-wöchigen Feldexperiment mit 4 älteren Erwachsenen getestet und mit Messungen einer Physiotherapeutin verglichen. Die Evaluierung zeigt einen klaren Unterschied zwischen habituellen Bewegungen zuhause im Vergleich zu den Leistungen in den Bewertungstests, was die Verhaltensänderung in Testsituationen aufzeigt, wie es auch in der Literatur demonstriert wird.

# Abstract

Due to increased life expectancy and growing world population, there is an increase in older adults. With increased age, challenges like cognitive and physical decline are more likely to occur and involve the age-related frailty syndrome, which is characterized by lower resistance against stress, diseases, and other exogenous influences. Frail older adults have an enhanced need of health care utilization, are more likely to fall and be hospitalized due to reduced cognitive and physical capabilities. Frailty is reversible and preventable, if detected early enough, thus methods to identify frailty are required. Due to correlation between frailty and physical fitness, there are physical performance tests, to assess a person's mobility, and the associated risk to become frail. However, the test situation causes tested persons to change their behavior which leads to different results compared to persons' performance in daily life.

In this thesis, the fitness level is automatically assessed based on measurement of gait parameters as summarizing health indicator, as well as sit-to-stand performance as predictor for falls and balance deficits. For both measurements, person tracking data from depth sensors are utilized, which allows non-intrusive, privacy protecting capturing of motion at habitual speed in the homes of older persons. The underlying person tracking method allows plug and play, which enables easy installation in apartments. For evaluation of the proposed measurement approaches, two datasets have been recorded and manually annotated. The STS dataset contains 137 sequences of persons performing sit-to-stand transitions in combination with activities of daily living. The 4-Paths dataset contains gait sequences of 10 persons walking on 4 predefined paths.

The first measurement method analyses human gait for walking velocity, distance, and duration. Further, two approaches for gait event demarcation are compared. One uses literature-based scale-space filtering, the other approach uses machine learning to determine gait events, which are further used to estimate gait cycle components: step time, stride time, cadence, single support, double support, stance phase. For training of the machine learning algorithms, and for evaluation of the measured parameters, the 4-Paths dataset is used. In this dataset heel strike and toe off events are manually annotated and the walking distances and durations were acquired using laser measurement and a stop watch, which allows spatio-temporal evaluation of the measured gait parameters. The comparison shows better results for the machine-learning approach, and gait cycle

component estimation comparable to state-of-the-art measurements using wearable accelerometers.

The second measurement method is split into two problems: the detection of sit-to-stand movements and the measurement of sit-to-stand transition durations. For detection, a literature-based threshold approach is compared to different machine-learning algorithms. The duration measurement is approached using curve-sketching to identify the steepest height increase in the sequence where the stand-up is detected. The machine learning algorithms are trained using stand-up sequences of the STS dataset, where start and end of sit-to-stand transitions are manually labeled. This enables the evaluation of the detection approaches, as well as the duration measurement. Stand-up detection achieves best results using a random-forest algorithm, the duration measurement achieves results comparable to state-of-the-art methods.

A holistic system combining the measurement methods is presented, which is installable in the homes of older adults to measure gait parameters and stand-up performance. The acquired information is aggregated and provided for further usage by e.g. health professionals. This system was tested in an 8-week field trial with 4 older adults and compared to measurements conducted by a physiotherapist. The evaluation shows a clear difference between habitual in-home movements to the performance in the conducted assessment tests, showing the behavior change in test situations, which is also demonstrated in literature.

# Contents

<b>Kurzfassung</b>	<b>xi</b>
<b>Abstract</b>	<b>xiii</b>
<b>Contents</b>	<b>xv</b>
<b>1 Introduction</b>	<b>1</b>
1.1 Problem Definition . . . . .	1
1.2 Contributions . . . . .	3
1.3 Structure . . . . .	4
<b>2 Related Work</b>	<b>5</b>
2.1 Definition of Frailty . . . . .	5
2.2 Mobility Assessment . . . . .	10
2.3 Technology Supported Assessment . . . . .	16
2.4 Depth-Based Motion Tracking . . . . .	25
<b>3 Methodology</b>	<b>31</b>
3.1 Gait Velocity, Distance, and Duration Analysis . . . . .	32
3.2 Gait Event Analysis . . . . .	34
3.3 Stand-Up Detection . . . . .	37
3.4 Stand-Up Duration Measurement . . . . .	40
3.5 Implementation . . . . .	44
<b>4 Results and Discussion</b>	<b>49</b>
4.1 Datasets . . . . .	49
4.2 Gait Velocity, Distance, and Duration Evaluation . . . . .	51
4.3 Gait Event Evaluation . . . . .	55
4.4 Stand-Up Detection Evaluation . . . . .	57
4.5 Stand-Up Measurement Evaluation . . . . .	58
4.6 Field Test . . . . .	59
<b>5 Conclusion &amp; Future Work</b>	<b>65</b>
	xv

<b>List of Figures</b>	<b>67</b>
<b>List of Tables</b>	<b>69</b>
<b>Bibliography</b>	<b>73</b>



# Introduction

Due to advantages in medicine, life expectancy is increasing [1], together with the growing world population, there is an increase of people over 60 years, as shown in Figure 1.1 [2]. Increased age involves challenges like cognitive and physical decline, chronic diseases and age-related limitations, such as impairments in hearing and vision [3]. This raises the demand on health care systems to adapt to the requirements of a growing amount of elderly persons [3]. Hence, services and devices are developed to support the independence of older adults. These systems are called active and assisted living technologies and aim at construction of (connected) environments that assist older adults in their homes [4, 5]. The number of information and communication technologies supporting (self-)monitoring of health conditions and providing alert functionality is increasing [6, 7], leading to a change of traditional care processes in the direction of patient self-care and the possibility for older adults to remain independent and to age in their own homes [5, 6, 8].

## 1.1 Problem Definition

With increased age the risk to become frail is higher [9–11]. Frailty is a medical syndrome caused by multiple contributors [12] and has diversified indicators, such as weight loss, decline in physical activity, or decreased walking speed [13]. Frail older adults have an enhanced need of health care utilization, which leads to higher costs due to therapy, medication, and need for health professionals. Additionally, frail people are more likely to fall and be hospitalized due to reduced cognitive and physical fitness [11]. Since frailty can be reversible, if detected early enough [12], there is a demand for reliable and valid methods to identify frailty on the one hand, but also to detect pre-frailty on the other hand [10] in order to prevent further increase of frailty and set appropriate counteractions, like certain diets, cognitive and physical activity [14, 15]. The main objectives of frailty prevention are improved health at an advanced age as well as decreased demand on the health system [15]. Since there is a correlation between physical performance and the

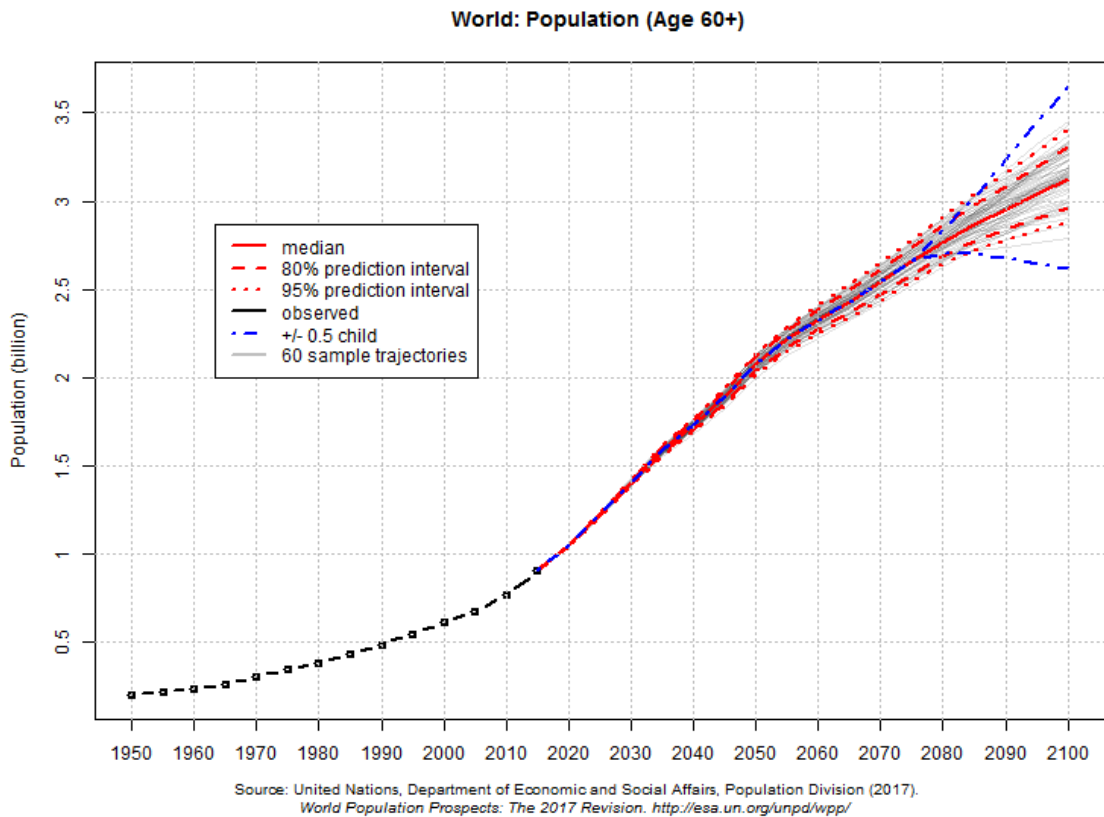


Figure 1.1: The United Nations prospects of world population show an increase in people of age 60 and above [2].

overall frailty level [16], there are physical tests for assessment of a person's physical fitness indicating whether a person is frail [17]. For example, the Timed Up and Go Test (TUGT) [18] measures the time a person needs to stand-up, walk 3m, turn around, walk back to the chair and sit down again. This test estimates balance and gait performance, which are used to distinguishing features between non-frail, pre-frail, and frail persons [19] and increased fall risk [20]. Although the assessment of mobility only is not sufficient to define a person as frail, it is a reliable indicator [10, 16]. Due to the test situation, tested persons change their behavior which leads to different results compared to persons' performance in daily life [21]. There are tests conducted in the home of test persons (e.g. [19, 22]), which attenuates the test persons' behavior adaption, but there is still a difference to habitual behavior [23]. However, passive observations without supervision by e.g. physiotherapists, allows to obtain activities at habitual speed, which is considered to mediate the inverse correlation of cognitive decline and age emerging during functional tests [23]. In order to measure habitual movement of persons at home without supervision, wearable devices are used (e.g. [24]). These devices, however, are intrusive as they change



Figure 1.2: Visualization of depth information obtained from a 3D sensor as gray values: the closer the object the darker the representation. The person’s face is not visible.

persons’ everyday life, sensors have to be placed correctly [25], and people forget to attach them [26]. 3D sensors offer an unobtrusive way to capture habitual movements, when stationary mounted in certain rooms [25]. By the use of depth data only, no texture details, such as faces, are visible when visualizing the depth information as shown in Figure 1.2, which preserves persons’ privacy in comparison to [27].

## 1.2 Contributions

The possibility of unobtrusive and unsupervised measurement enables monitoring of health-related parameters in the homes of persons [25]. Gait is a summarizing vitality indicator, since it requires the interaction of multiple organic systems [28]. The execution of Sit-To-Stand (STS) transitions provides information about balance and lower body musculature, which correlates with the risk of falling [29, 30]. Hence, gait and STS transitions are analyzed in this thesis to obtain information about a person’s fitness level. Using movement trajectories provided by a depth-based person tracking method, following approaches are developed and described:

- An approach for measurement of walking velocity, distance, and duration is devel-

oped, additionally two approaches for gait event demarcation are compared. One uses literature-based scale-space filtering, the other approach uses machine learning to determine gait events, which are further used to estimate gait cycle components: step time, stride time, cadence, single support, double support, stance phase.

- Before measuring STS durations, a literature-based threshold approach is compared to different machine-learning algorithms to detect stand-ups. The duration measurement is approached using curve-sketching to identify the steepest height increase in the sequence where the stand-up is detected.
- A system combining the described measurement approaches is presented, which is installable in the homes of older adults to measure gait parameters and stand-up performance. The acquired information is aggregated and provided for further usage by e.g. health professionals.

### 1.3 Structure

This thesis is structured as follows. Chapter 2 focuses on frailty and its correlation with mobility parameters and fall risk. Due to this correlation, tests to assess persons' mobility and fall risk are described and compared. Additionally, mobility assessment tests advanced by technological assistance using state-of-the-art wearable and non-wearable technologies are presented. Studies using these technologies to examine functional parameters, such as gait velocity, and stand-up velocity, in supervised and unsupervised settings are shown. In addition, person tracking based on depth data is explained.

Based on the evaluation of physical assessment tests and state-of-the-art algorithms, approaches are developed for the measurement of human gait parameters and STS performance. These are described in Chapter 3. Walks are analyzed in order to extract average velocity, duration, and distance of walks, as well as gait cycle components, like stride and step length. Methods to detect STS sequences are described and used as starting point for stand-up duration measurement. Further, a holistic system is shown, that combines the presented algorithms and generates a mobility model that can be used to access the aggregated information.

In Chapter 4 the performance of the gait and STS movement analysis methods are evaluated and the respective results compared to related work based on the Mean Average Error (MAE). Additionally, the evaluation of the holistic system in an 8-week field trial is presented. Chapter 5 closes the work with a conclusion and a view on future work.

## Related Work

Modern society faces economic and social challenges caused by population aging: higher age increases the possibility to be frail, including impaired mobility and cognitive decline, which causes Activities of Daily Living (ADL) to become a challenge and increases the need for assistance [9–11]. The probability to become hospitalized is four times higher for frail people and twice as high for pre-frail than for healthy people [11]. The recognition of frailty and pre-frailty is of particular importance since the progress of frailty can be damped or even reversed by application of appropriate treatment [12]. This chapter describes frailty itself and tools to assess it, as well as its correlation with mobility. Ways to assess a person's mobility status are explained and how these measurements are supported by technology using sensors and automated analysis methods.

### 2.1 Definition of Frailty

Until 2013 there existed no consensus definition of frailty [31–33], but various individual descriptions have emerged: Lang et al. [34] describe frailty as lengthy process with increased vulnerability and predisposition to functional decline that may lead to death. According to Sales [35] frailty represents multiple co-morbidities over time and Fried et al. [36] describe frailty as the reduced resistance to stressors. In 2013 a consensus group of major international societies defined physical frailty as medical syndrome caused by multiple contributors and characterized by reduced endurance, strength, and physiologic function resulting in increased vulnerability to develop dependency or death [12]. They define frailty further as indicator for a higher vulnerability to stressors than non-frail persons, causing adverse health issues and functional deterioration, however, it might be reversible due to interventions [12]. Frail people are restricted in executing ADL or have limited mobility; they show higher fall risks and hospitalization probabilities [13]. Adults older than 65 years have a higher probability to become frail as Bandeen-Roche et al. [11] show evaluating 7,439 non-nursing home persons. 15.3% of the persons analyzed

were frail and 45.5% pre-frail [11]. The vulnerability of a frail person in comparison to a healthy person is illustrated in Figure 2.1, showing the impact of a minor health problem on healthy and frail elderly persons. The event has more effect on the health state of frail persons, which may cause that this person becomes dependent, immobile, or delirious [10]. Since frailty can be prevented or delayed [12, 37], it is necessary to identify the risk of frailty for early application of preventive interventions, which leads to a demand for methods to detect frailty in a valid and reliable manner [10, 37]. There are two major assessment tools, which have emerged in the past decade [31, 32, 38]: the **frailty phenotype** of Fried et al. [13], and the **frailty index** of Searle et al. [39].

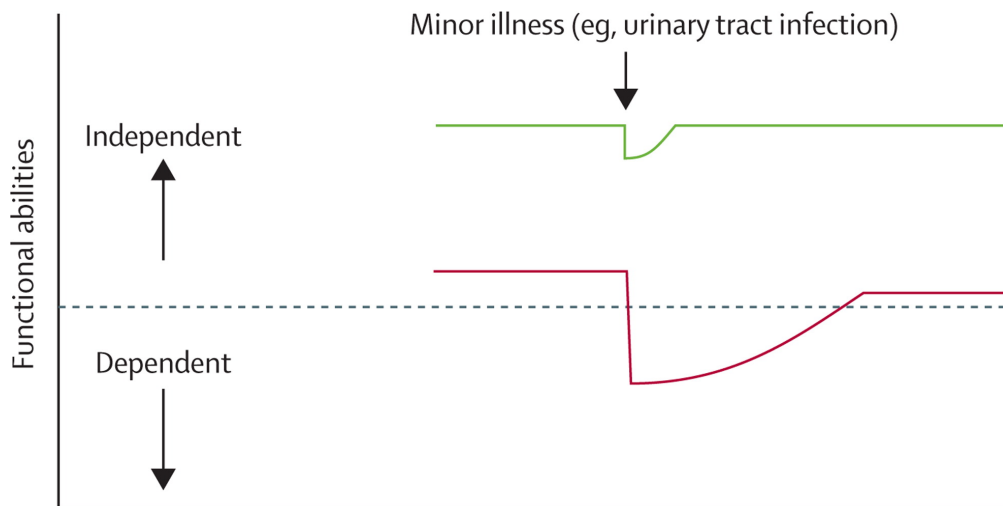


Figure 2.1: Vulnerability of elderly people to minor health problems: red line shows a frail elderly person becoming dependent due to this event, whereas the same event has less effect on a healthy person. (Image from [10])

### 2.1.1 Physical Frailty Phenotype

Fried et al. [13] investigate frailty in a cohort-study of 5,317 community-dwelling adults of 65 years and older. In their study frailty is operationalized as clinical syndrome based on five criteria: 1) weight loss: unintentional loss of more than 4.5kg (or 5% of body mass) in preceding year, 2) exhaustion: the person reports having low energy and being easily exhausted, 3) low physical activity: no recent physical activities nor walks for exercise, 4) weakness: grip strength is below or at 20% baseline, adjusted for body mass index and gender, and 5) slow walking speed: time required to walk 4.6m, baseline is defined as the slowest 20% of the population considering age and gender. A person is considered frail if three or more of these criteria are present, pre-frail if one or two criteria are met and robust if none are present. Fried et al. [13] distinguish between frailty, disability, and co-morbidity, which are all predictors for adverse health outcomes [32]. If frail persons suffer from impairments in ADL, they are identified as disabled, while impairments in ADL only do not identify a person as frail [32]. For example, an older person suffering

from disability after an accident maintaining functions in other physiological systems, is not considered frail [32]. Further, co-morbidity - the presence of multiple chronic diseases - does not automatically identify a person as frail, but worsening of these diseases, inappropriate treatment, or additional diseases constitute a higher risk to become frail [40]. The relation between frailty, co-morbidity, and disability in the study of Fried et al. [13] is illustrated in a Venn diagram shown in Figure 2.2. Bandeen-Roche et al. [41] verify the validity of the physical phenotype in a study with women between 70 and 80 years, and confirm the occurrence of the five criteria, which supports the characterization of frailty as clinical syndrome with manifestations as frail, pre-frail and nonfrail [13,32].

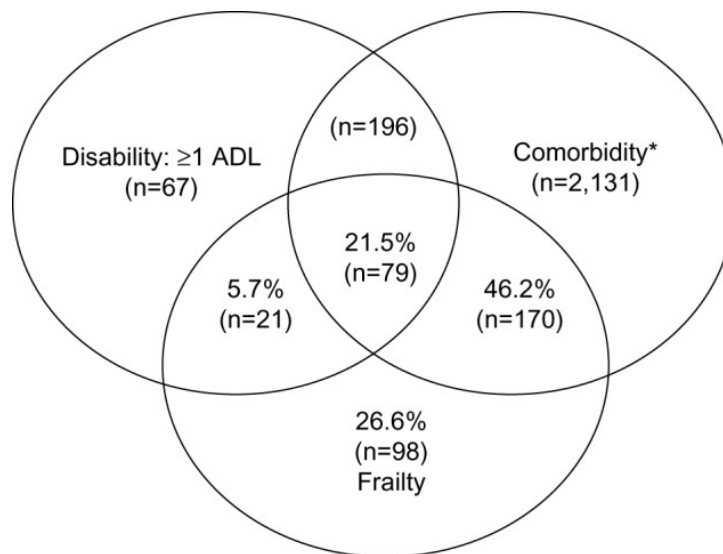


Figure 2.2: Frailty syndrome, disability, and co-morbidity as predictors for adverse health outcomes have to be distinguished. \*At least two of following diseases: angina, arthritis, cancer, claudication, congestive heart failure, COPD, diabetes, hypertension, myocardial infarction. (Image from [13])

### 2.1.2 Frailty Index

Searle et al. [39] describe an index to measure frailty, which is based on social factors, physical, and psychological parameters. The Frailty Index combines multiple clinical state variables into a single number, which quantifies the possibility of adverse events [16]. It is defined by Searle et al. [42] as

$$\text{Frailty Index} = \frac{\text{number of deficits}}{\text{number of considered variables}} .$$

The chosen variables are not predefined but must follow five criteria: 1) chosen variables have to be health-related, 2) their prevalence has to increase with age, 3) they should not saturate too early (e.g. age-related eye lens change), 4) the variables must cover a range to ensure a general frailty index (otherwise it is only e.g. a cognitive index), 5) if several

people are tested with the same index, the variables are required to remain the same [42]. The higher the number of deficits, the higher is a person's frailty index. Following list shows suggestions for deficit variables from Searle et al. [39]: need help getting in/out of chair, need help with housework, need help walking around house, walk outside, lost more than 4.5kg in last year, feel everything is an effort, had heart attack, has arthritis. The number of considered variables should range from 13 to 100, although the optimal number lies between 40 and 50 variables as Davis et al. [16] investigated. Davis et al. [43] describe the construction of a Frailty Index based on the Comprehensive Geriatric Assessment [44], which allows to use variables obtained routinely by geriatricians and are reliable for risk stratification of possible adverse events. Due to the inclusion of deficits with relationship to adverse events, the Frailty Index is considered to be more sensitive as predictor for adverse health issues [45].

### 2.1.3 Comparison

Due to different characteristics, the Frailty Phenotype and the Frailty Index are not substitutable but considered to be of complementary use as Cesari et al. [38] describe by comparing these instruments. An overview of the differences based on the observations of Cesari et al. [38] is given in Table 2.1. While the Frailty Phenotype is applicable to immediately identify the possibility of adverse events for non-disabled older adults, the Frailty Index gives a deficit summary by accumulating results of a comprehensive geriatric assessment [38].

Table 2.1: Characteristics of the Frailty Index and the Frailty Phenotype [38]

	<b>Frailty Phenotype</b>	<b>Frailty Index</b>
<b>Investigates</b>	symptoms and indications	ADL, diseases, clinical test results
<b>Application</b>	before clinical tests	after comprehensive clinical tests
<b>Variable types</b>	categorical, predefined	continuous, unspecified following criteria
<b>Frailty considered as</b>	pre-disability syndrome	accumulated deficits
<b>Significant results</b>	primarily for non-disabled older adults	independent of age or functional status

### 2.1.4 Correlation With Mobility Parameters

As shown by these assessment instruments, multiple variables and criteria, such as diseases, mobility decline, or impairments in ADL, have to be observed in order to



identify a person as frail. However, covered variables show high correlation with frailty in general: Davis et al. [16] evaluate 1,295 people of 70 years and above having a Frailty Index between 0 and 51% to investigate the relation between frailty and mobility. They created 5 classes of 259 persons each, with ascending frailty indices: Q1) 0-8%, Q2), 8-12%, Q3) 12-17%, Q4) 17-23%, and Q5) 23-51%. In Q5 37% showed difficulties with mobility, while none of Q1 had mobility impairments. Davis et al. [16] state that although mobility impairment only is not sufficient to classify a person as frail, it is a predictor for frailty due to its correlation. Delbaere et al. [46] also show a correlation between mobility and frailty: the avoidance of activities due to fear of falling increases physical frailty. By reducing the ADL and outdoor activities, the muscle strength is reduced, which increases the risk of falling and slows the speed of walking [46]. The correlation between falls and frailty is also shown by Davis et al. [16]: persons of Q5 reported 3 times more falls than those in Q1. This corresponds with the results of Bandeen-Roche et al. [11], who describe that the fall risk is three times higher for frail people than for non-frail people.

Montero-Odasso et al. [47] define gait speed below 0.8m/s as pathological and show a correlation between this slow walking speed and the occurrence of falls: persons (70+ years) with pathological gait speed fall twice as much as persons with normal gait speed. Studenski et al. [28] describe a correlation between gait speed and mortality at a certain age, based on nine cohort studies with data of 34,485 individuals. Figure 2.3 shows the relation between age, gait speed and life expectancy. The lower the walking velocity, the higher the risk of early mortality [28]. Reasons for that are the need for energy and movement control during walking [28]. Further, walking requires interaction of multiple organ systems in the body, e.g. lungs, heart, circulatory, nervous system, and muscles [28]. Damages in those systems can result in slow gait speed, hence gait velocity is a summarizing indicator for vitality [28].

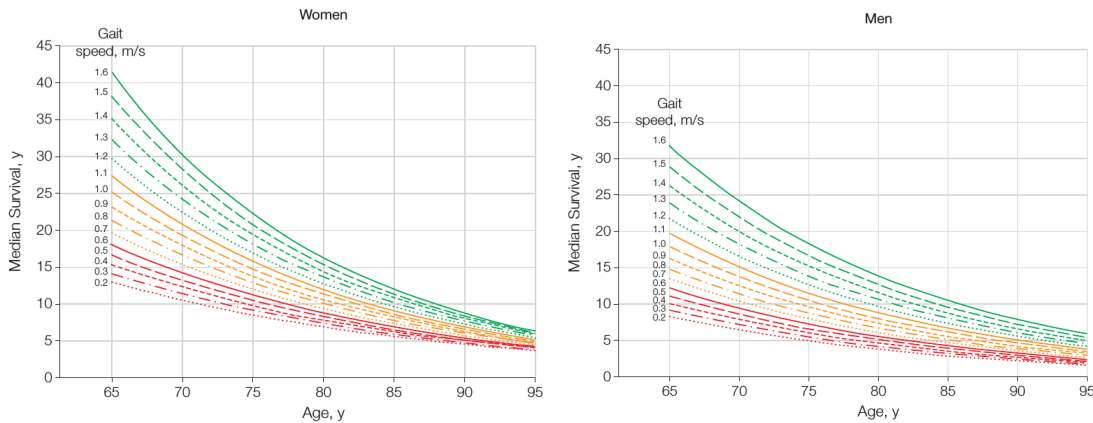


Figure 2.3: Median life expectancy in relation to age and gait speed of men and women. (Image from [28])

A significant association between gait velocity and persons' balance is reported by Montero-Odasso et al. [47]: 79% of 92 observed persons with pathological gait speed had

problems maintaining balance on one leg, while only 40% of persons with normal gait speed had these problems. Balance deficits indicate decreased power of the lower body muscles, which correlates with higher fall risk and results in problems when standing up [29, 30]. Cheng et al. [29] examine the stand-up duration of 105 persons (young, non-fallers, fallers) and show that the time required to stabilize oneself after a STS movement is 0.83s longer on average for fallers than for non-fallers, and hence, also the average of the total STS duration is 2.13s longer [29].

Zhang et al. [48] examine STS times of 948 adults (60+ years) using the 5 times Sit-To-Stand test (5tSTS), which consists of 5 successive stand-ups without use of upper extremities. They conducted further a 3-year follow-up showing following results: For persons incapable of performing the 5tSTS the probability of falling was 4.22 times higher at the follow-up than those having the fastest stand-up times (<11.2s). The probability to fall was 1.09 times higher for the slowest group able to perform the test (>16.6s) than the fastest group. Further, persons not able to perform the test showed 24.70 times higher probability to develop impairments performing ADL, than the fastest group. Hence, problems performing STS movements are a significant predictor for ADL-related disability and increased fall risk [48].

## 2.2 Mobility Assessment

Mobility parameters and fall risk correlate with a person’s frailty state [10, 49] and are thus used as predictors for frailty [16, 48]. In medicine, mobility is measured using mobility assessment tests [50]. There exist technology assisted versions of these tests as shown in the next Section. Six examples of the medical assessment tests are described in Table 2.2. The tests are selected since they require no special equipment, and their conduction requires only short time (<30min) [50]. In the TUGT [18] and the Six-metre-walk test [51] the test persons are told to conduct the test at “habitual speed”, instead of “as fast as possible”, which means performing the movements like in everyday life. Performing geriatric tests at habitual speed partially mediates the inverse function between disability of elders and cognitive function [23]. Further, there is a significant correlation between changes in habitual walking velocity and cognitive decline [52]. Persons still change their behavior and do not execute the movements at habitual speed as in daily life, due to the created test situation [21].

Table 2.2: Examples of mobility assessment tests

Test	Description	Reference Values
<b>TUGT [18]</b>	The subject has to stand-up without assistance, walk 3m, turn around, walk back and sit down. The time needed is measured. Examines: gait velocity, balance, lower extremity.	<ul style="list-style-type: none"> <li>• 60 - 99 years: 9.4s [53]</li> </ul>

Continued on following page

Table 2.2, continued

Test	Description	Reference Values
<b>Half turn test [54]</b>	The subject walks a few steps, then has to turn 180° around. The number of steps needed to turn around is counted. Examines: mobility, balance.	<ul style="list-style-type: none"> <li>• 74 - 98 years: 4.5s [50]</li> </ul>
<b>Alternate-step test [54]</b>	The subject has to place both feet on a step, beginning with left and right alternating. The time needed to complete 5 steps is measured. Examines: lateral stability.	<ul style="list-style-type: none"> <li>• 74 - 98 years: 10.8s [50]</li> </ul>
<b>5tSTS test [55]</b>	The subject has to perform five stand-ups and sit-downs consecutively from a chair without arm rest. A variation of this test is the STS 1, where the subject has to stand-up only once [50]. The total time needed is measured. Examines: lower limb strength.	<ul style="list-style-type: none"> <li>• &gt; 60 years: 11.4s</li> <li>• &gt; 70 years: 12.6s</li> <li>• &gt; 80 years: 14.8s [53]</li> </ul>
<b>Six-metre-walk test [51]</b>	The subject has to walk at normal walking speed for 10m in total, 2m before and after the 6m walk to ensure a constant speed. The time needed for the distance is measured to calculate the velocity. Examines: gait velocity, fall risk	<ul style="list-style-type: none"> <li>• &gt; 60 years: 1.36±0.21m/s (men)</li> <li>• &gt; 70 years: 1.33±0.2m/s (men)</li> <li>• &gt; 60 years: 1.30±0.21m/s (women)</li> <li>• &gt; 70 years: 1.27±0.21m/s (women) [56]</li> </ul>

Continued on following page

Table 2.2, continued

Test	Description	Reference Values
<b>Short Physical Performance Battery (SPPB)</b> [57]	The subject has to perform certain standing positions for 10s each. Further, either a 2.44, 3 or 4m walk has to be done twice, as well as five STS transfers. The durations to hold the positions, to walk the pre-defined path, and to perform the stand-up are measured and individually scored from 0 to 4 (12 points in total). Examines: balance, gait velocity, lower body strength, overall physical fitness.	<ul style="list-style-type: none"> <li>• &gt; 70 years: <math>8.4 \pm 2.7</math> points [58]</li> </ul>

### 2.2.1 Human Gait Analysis

As an indicator of a person's health condition, human gait is analyzed for diagnosis and monitoring, as well as rehabilitation [59]. One way to analyze gait is visual observation by a human of a person walking or running, and for repeated viewing without exhausting the patient, video recordings of the walk are recorded. This method depends highly on the subjective rating and personal experience of the observing clinician. Spatio-temporal measures (e.g. gait velocity) allow to obtain quantitative parameters [60]. In order to perform objective gait analysis, spatio-temporal parameters of gait cycles have to be obtained and analyzed [61]. Figure 2.4 illustrates a gait cycle of a healthy adult, which is defined as the interval between two consecutive floor contacts of one foot partitioned into two main phases: stance and swing. During stance phase the foot is in constant contact with the floor beginning with the heel, followed by the flat foot and ending with the push off from the ground, which itself starts from the heel to the toes. During swing phase the foot is brought to the front, while the other foot is in stance phase. When the toes are pushed off, the other foot regains floor contact which causes both feet to touch the floor at the same time, called double support. The event when a foot touches the floor is defined as Heel Strike (HS) and the event when the foot leaves the floor as Toe Off (TO). Other gait parameters are derived from these gait events: from HS to the second following TO (the TO event of the same foot) represents a stance phase. The duration between two consecutive HS events is defined as the step time. The stride time is the duration between an HS event and the next HS event of the same foot, which corresponds to the total gait cycle duration [62]. The phase of both feet touching the ground is defined as double support, while single support defines the phase of only one foot being in contact with the floor.

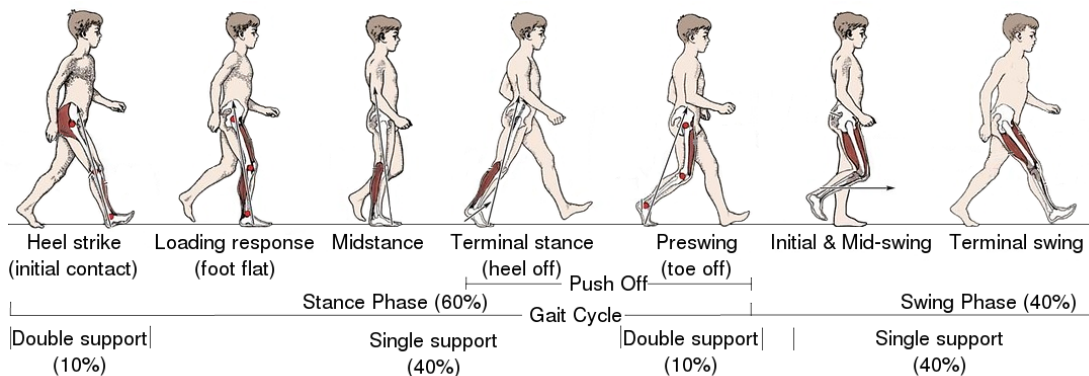


Figure 2.4: The gait cycle consists of two main phases: stance phase where the foot has permanent contact to the ground, and the swing phase where the foot is brought forward to begin the next step.<sup>1</sup>

### 2.2.2 Sit-To-Stand Analysis

STS transitions consist of three phases, which are depicted in Figure 2.5: I) weight shift and begin of trunk flexion, II) knee extension and end of trunk flexion, III) lifting the weight, extension of the trunk flexion and full extension to standing position [63]. The performance of STS movements is determined by an interaction of multiple physiological and psychological factors: knee extension and flexion, dorsiflexion strength of the ankle, foot reaction time, body weight, sway of posture, reported pain, sensitivity to visual contrast, proprioception of lower limb, anxiety, and general vitality [64]. STS performance is further influenced by the chair height, position of the feet, as well as the use of armrests [65]. Examination of the stand-up performance by recording the required duration is used in mobility tests, as described in Table 2.2: TUGT [18], sit-to-stand test [55], and SPPB [57]. These tests have in common, that the measurement begins, when the subject is advised to start, which includes the person's reaction time. Depending on the evaluation method, there exist different reference values for stand-up durations in literature ranging from 1.51s to 2.42s on average for healthy young adults [29,66–68] and 1.56s to 2.54s for healthy older adults [67,69–71]. Pathologic durations for STS transfers are specified from  $2.73 \pm 1.19$ s to  $4.32 \pm 2.22$ s [29,68,72]. In contrast to the STS movement, the Sit-To-Walk (STW) transition is partitioned into four phases: 1) initiation: forward movement of the center of mass, 2) seat-off and peak of vertical velocity: body rises, lower limb joints and trunk are extended, 3) initialization of the gait and swing phase: unloading, weight shift, 4) stance phase: end of swing phase, walk [73]. The center of gravity moves higher but less forward in STS than in STW movements. To perform an STW motion, a forward impulse has to be created using the upper body (head, trunk,

<sup>1</sup>Image adapted from <https://www.physio-pedia.com/File:Gait-Cycle.jpg> (accessed 03-2018), Copyright 2011 Wolters Kluwer Health | Lippincott Williams and Wilkins, usage permitted for non-commercial and/or educational purposes.

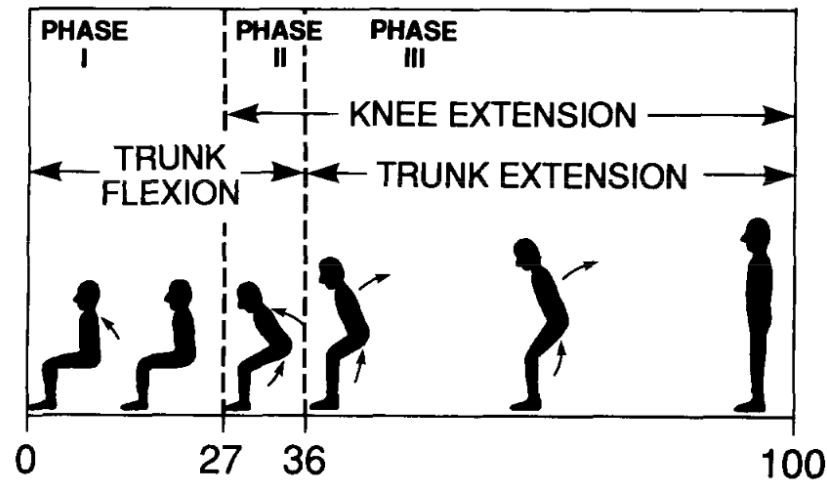


Figure 2.5: Phases of the STS transition. (Image from [63])

and arms) resulting in a higher horizontal velocity. The STW movement requires more advanced motoric control than the transition from sitting to standing [74]. Especially the momentum created in the third phase, when the transition to walking takes place, requires balance control [75].

### 2.2.3 Fall Risk Assessment

Falls represent a serious obstruction for elderly to live independently and are the major reason for injury related deaths for adults of the age 79 and above [76]. The inability to stay upright while standing or walking is the result of a complex system failure. To maintain balance, interaction of multiple muscles is required and controlled by commands from the motor cortex reacting to sensory signals from the spinal neurons. This activity is coordinated from the central nervous system, which reacts to the respective terrain conditions. Maintaining balance is a cognitively challenging task and confrontation with additional cognitive load results in higher fall probabilities also for healthy, young persons as shown by Templer and Conell [77]. Hence, frail persons suffering from multiple physiological impairments and vulnerable to stressors are prone to falling when exposed to exogenous stress and having no physical assistance available in their vicinity [12, 78, 79]. Table 2.3 shows an overview of assessment tests, which are used to determine a person's fall risk [80].

Table 2.3: Examples of fall risk assessment tests

Test	Description	Reference Values
<b>Get-up and go [81]</b>	The subject has to stand up from a chair and walk a short distance (e.g. 3m), turn around, walk back to the chair and sit down again. Observers rate the subject's performance on a 5-point scale. Examines: gait and balance.	<ul style="list-style-type: none"> <li>• Gait abnormalities: ataxia, apraxia, shuffle</li> <li>• require arms for stand-up</li> <li>• require assistive devices [80]</li> </ul>
<b>TUGT [18]</b>	The subject has to stand-up without assistance, walk 3m, turn around, walk back and sit down. The time needed is measured. Examines: gait velocity, balance, lower extremity.	<ul style="list-style-type: none"> <li>• <math>\geq 13.5</math>s: increased fall risk [82]</li> </ul>
<b>extended TUGT [83]</b>	The subject has to perform the TUGT with a 10m walking path. The durations of multiple components are measured individually: stand-up, gait initiation, walk to turning point, turn, walk to starting point, sit-down. Examines: gait velocity, balance, lower extremity as in TUGT but more sensitive.	<ul style="list-style-type: none"> <li>• first walk is most sensitive</li> <li>• 70 - 79 years: <math>1.18 \pm 0.15</math>m/s (men)</li> <li>• 70 - 79 years: <math>1.11 \pm 0.13</math>m/s (women) [83,84]</li> </ul>
<b>Functional reach test [85]</b>	The subject has to stretch the arms out frontward and lean as far forward as possible without losing balance. The maximum possible distance is measured. Examines: balance.	<ul style="list-style-type: none"> <li>• <math>&lt; 0.15</math>m: 4 times higher fall risk in succeeding half year</li> <li>• 0.15 - 0.25m: 2 times higher fall risk in succeeding half year [86]</li> </ul>
<b>Morse fall scale [87]</b>	The scale consists of six variables, which are rated using scores. The variables are assessed by observer(s): history of falls, number of medical diagnoses, ambulatory aids (e.g. wheelchair), application of intravenous therapy, gait, and mental status. Examines: fall risk on three-level scale (no, low, and high risk).	<ul style="list-style-type: none"> <li>• 45 - 55 points (and above): increased fall risk [88]</li> </ul>

## 2.3 Technology Supported Assessment

Based on the described medical assessment tests, instrumented and automated versions are developed, assisting the acquisition of functional parameters, such as gait velocity or STS duration. The use of technology to automate the analysis of persons' mobility allows increased measurement efficiency and objective evaluation [89]. Additionally to the application in supervised tests, the application of automated measurement technology is used for passive observation either in laboratory or in-home settings [19, 22]. Passive observation without direct supervision of clinicians enables the obtainment of activities at habitual speed, without behavior change of the tested persons [21]. The sensors utilized to measure mobility metrics are classified into **wearable** and **non-wearable** [89, 90]: while former consist of devices attached to a person's body or garment, the latter are integrated into the infrastructure of residences or a person's environment [91].

### 2.3.1 Wearable Sensors

Wearable sensors are placed at certain parts of the body, e.g. knees, ankles, but also inside of clothes, belts, watches or shoes [89, 90]. In order to obtain mobility parameters uni- or multiaxial accelerometers, gyroscopes, and magnetometers are used either solely or in combination to track spatio-temporal motion information and are called inertial sensors. Pedometers for step counting, electromyography-sensors to obtain muscle nerve activity, goniometers to record angles, and force sensors are additional examples for wearable sensors used to measure mobility metrics [92–94]. Figure 2.6 shows inertial sensors attached to certain parts of the body for kinematic measurement. The benefits of wearable sensors include that they are not restricted to a certain test environment or a Field Of View (FOV), further, the direct measurement allows elimination of errors in velocity data [95]. In order to obtain objective and additional quantitative measures, wearable sensors are used to support mobility assessments evident by instrumented versions of assessment tests: instrumented Timed Up and Go Test (iTUGT) [96], instrumented 5tSTS [97].

### Supervised Assessments

Salarian et al. [98] present an instrumented version of the TUGT using seven inertial sensors on forearms, legs, and sternum. Analysis of yaw angular velocity from the sternum gyroscope allows detection of turns which enables automatic separation in subcomponents. Gait is analyzed for temporal measures (the amount of steps per minute - cadence, gait cycle parts), lower and upper limb performance, as well as trunk performance. STS motion detection is performed searching the peak angular velocity and analyzed for average angular velocity, duration and range of motion of the trunk. They evaluate this approach with 24 persons split into two groups - twelve with Parkinson's Disease (PD), twelve as control group - resulting in full detection of all turns. Gait measurement shows more reliability in the test-retest than STS measurement with an intraclass correlation of  $\rho=0.94$  for cadence, and  $\rho=0.78$  for stride velocity, while stand-up duration received





Figure 2.6: Example for wearable sensors placed on various body parts. Correct placement before every usage disqualifies them from everyday usage [25]. (Image from [89])

$\rho = -0.42$ . This is associated with different stand-up strategies of the subjects. Salarian et al. [98] state that the instrumented version is not limited to subjects suffering from PD, but any persons with impairments of gait or balance. The test is further validated by Kleiner et al. [99] with 30 subjects to compare the instrumented results with Stop-Watch (SW) measurement. The mean total duration obtained by the instrumented measurement is  $20.8s \pm 14.3s$ , while the SW approach recorded a mean of  $19.9s \pm 14.9s$ , with a mean difference of  $-1.048$ . Besides this result Kleiner et al. [99] describe that the instrumented approach allows for more detailed assessment by measuring subcomponents than the SW method, and further removes subjectivity in the measures. Mellone et al. [100] conduct the iTUGT utilizing the accelerometer of a smart phone and compare it with the results of a tri-axial accelerometer, both worn in an elastic belt on the lower back. For evaluation 49 subjects performed the TUGT with 7m walking path. The means of the total duration showed the same outcome of 18.46s for the smart phone and the accelerometer, which shows that wearable sensors are replaceable by a smart phone in order to conduct the iTUGT.

Van Lummel et al. [22] describe a variation of the 5tSTS using three accelerometers embedded in a flexible belt attached around the waist. The test is conducted as part of

the SPPB and the STS phases are automatically detected and measured by identification of upward followed by downward motion, which completes an STS cycle. For evaluation the results of 63 elders performing the 5tSTS - manually and instrumented measured - are split into a fast and a slow group by median split and compared with the health status which is assessed using the European Quality of Life questionnaire [101]. This questionnaire comprises self-care, usual activities, mobility, pain, and anxiety. For the comparison the the Mann-Whitney U-test [102,103] is used with a p-value  $<0.05$  considered as statistically significant. It shows significant correlation between the health status and the instrumented measurements ( $p=0.009$ ), while the manually measurements show no significant association ( $p=0.457$ ). Van Lummel et al. [22] explain these results with more accurate measurements of the dynamic phases of the STS transitions using the accelerometers. The manually recorded time fully includes static phases (standing, sitting), which are described to be clinically less relevant than the dynamic phases containing the actual motion.

Schwenk et al. [19] describe the use of inertial sensors to assess the frailty status of 125 older adults, visited by clinicians in their own homes. The participants are grouped into frail, pre-frail and non-frail groups using the definition of Fried et al. [13] and wore tri-axial accelerometers, gyroscopes, and magnetometers placed on the legs and the lower back in order to obtain gait and balance parameters. The participants were recorded walking a distance of 4.6m at self-selected velocity for extraction of following gait parameters: velocity, stride length and time, proportion of double support from stride time, and gait variability. To evaluate the balance, the sway was obtained while the participants had to stay 15s with legs and eyes closed. The results are compared using the Games-Howell test due to unequal class sizes. The gait velocity evaluation shows best relationship to the respective frailty group and significant association with p-values of  $<0.001$  between non-frail and frail, as well as non-frail and pre-frail, and 0.033 between pre-frail and frail persons. The average gait speed of non-frail people results in  $1.17\text{m/s}\pm 0.15\text{m/s}$ ,  $0.94\text{m/s}\pm 0.23\text{m/s}$  for pre-frail, and  $0.71\text{m/s}\pm 0.36\text{m/s}$  for frail persons. Also the balance assessment (hip sway) is able to distinguish between non-frail and pre-frail ( $p=0.004$ ), but not between frail and pre-frail ( $p=0.999$ ).

### Unsupervised Assessments

Van Lummel et al. [22] tested their approach in everyday life for one week. With the exception of activities where the sensors would get wet (e.g. shower) the subjects had to wear the belt continuously and the activities are classified as standing, sitting, lying, shuffling, and movement to calculate the respective durations. The results of the physical activities are compared with the outcomes of the STS assessments: The slow group shows longer mean sitting durations per day (slow: 486s, fast: 287s), and shorter mean standing durations (slow: 123m, fast: 169m), which represents a significant association ( $p=0.001$ ). Due to the possibility that the belt can be worn beneath clothes, van Lummel et al. [22] describe this wearable to be unobtrusive and suggest to use it to automate the assessment of the health status.

Schwenk et al. [19] tested the association of the frailty status to physical activities in a 24-hour in-home assessment utilizing a shirt containing a tri-axial accelerometer and distinguished between lying, sitting, walking, and lying. Using step detection, less than three consecutive steps are considered standing otherwise walking; the other activities are obtained by the postural gesture. The evaluation shows less physical activity with increased frailty level, especially a decreased number of steps strongly correlates with presence of (pre-)frailty compared to non-frailty with  $p=0.001$  ( $p<0.001$ ). The strongest association between pre-frail and frail persons is shown by reduced walking durations with a reduction of 53%, which is explained by increased exhaustion in frail persons [13]. However, the study lacks of a longer test period in order to compensate day-to-day variability.

El-Gohary et al. [104] evaluate the use of a wearable inertial sensors in-home by investigating turns during walks of 21 subjects suffering from PD and 19 healthy subjects as control group which is used to identify fall risk. The participants wear the inertial sensors for one week during daytime on both feet and on the hip; the measuring device is a combination of tri-axial accelerometers, magnetometers, and gyroscopes. During night-time the sensors have to be re-charged. Persons suffering from PD show difficulties when turning and walking, which results in a higher fall risk of over 50% due to PD. Hence, the walks and turns during the recording period are identified in order to analyze certain turning characteristics: duration, frequency, jerk and rate of the rotation, number of steps required to perform a turn. The results are compared to the outcomes of experiments conducted in laboratory conditions resulting in slower turning rates at home (2.2s for control group, 2.0s for PD group) than in the laboratory (1.4s). Except for the number of turns ( $p=0.445$ ), all other metrics show significant differences between the control and PD group with  $p=0.001$  and  $p=0.002$ , using a *t*-test with 5% level of significance. The described technology is used by Mancini et al. [105] to monitor 35 persons over 77 years classified in fallers and non-fallers for one week. The analysis of the turn metrics show significant differences between fallers and recurrent fallers: mean turning duration is 0.3s longer for recurrent fallers ( $p=0.01$ ), more steps (+0.75 steps on average) are required to perform a turn ( $p=0.004$ ), and also the mean peak of the rotation velocity is slower by  $0.7^\circ/s$  ( $p=0.009$ ). In a follow-up examination 6 months after the evaluation, those participants who had higher variability in the number of steps required to perform turns show one or more falls. Since the result has as significant correlation ( $p=0.01$ ), this can be used to predict falls.

## Summary

Table 2.4 summarizes the characteristics of the described assessments using wearable sensor and outlines the respective main outcome. The usage of wearable sensors enables stronger correlations with health status than manual measurements, and discrimination between non-frail and pre-frail persons. Additionally, the application of these sensors allow the indication of increased fall risk.

Table 2.4: Summary Wearable Assessments

Reference	Assessment	Sensors	Outcome
<b>Supervised</b>			
Salarian et al. [98]	TUGT	gyroscopes	reliable estimation of gait and turns, least reliable STS
Van Lummel et al. [22]	5tSTS	accelerometers	stronger correlation with health & functional status than manual measurement
Schwenk et al. [19]	frailty status	accelerometers	pre-frailty identified by gait & balance
<b>Unsupervised</b>			
Van Lummel et al. [22]	5tSTS	accelerometers	stronger correlation with physical activity than manual measurement
Schwenk et al. [19]	frailty status	accelerometers	non-frail/pre-frail best discriminated analyzing walks
El-Gohary et al. [98] & Mancini et al. [105]	fall risk	accelerometers	high step variability when turning indicates increased fall risk

### 2.3.2 Non-Wearable Sensors

Wearable systems are intrusive as they change the everyday life of a person wearing the sensors [25] and older adults perceive wearable sensors as invasive, inconvenient, and obtrusive [8, 106]. Further, they require correct placement before every usage [25]. Non-wearable sensors are installed in a person’s environment or placed in their vicinity [90]. Examples to obtain mobility information include infrared sensors, audio recorders, proximity sensors, vision-based sensors, and sensitive floors [107]. Sensitive floors or force platforms are used to measure the force of steps which allows to analyze pressure patterns and quantification of horizontal or shear components of gait [89]. Further, fall detection is performed by estimation of a person’s posture and impact recognition by measuring vibration [108, 109]. Vision-based systems using RGB or depth cameras are utilized to detect persons in their field of view, which allows to obtain gait information [89], estimate a person’s pose [110], and detect falls [111, 112]. This thesis focuses on vision-based depth sensors to assess mobility aspects in a non-wearable way due to their advantages: no external light source required and thus robust to changes in ambient illumination conditions, algorithms from computer vision of RGB cameras can be used, and privacy is protected due to the procession of depth information only [113].

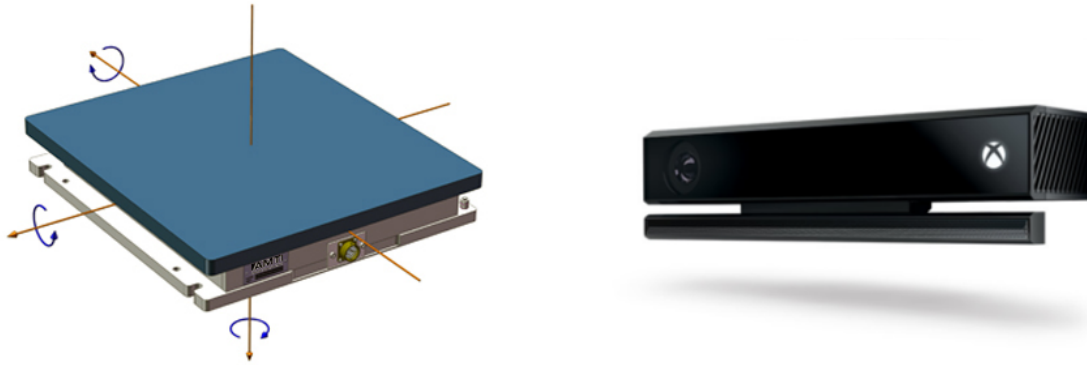


Figure 2.7: Examples for non-wearable sensors: Force sensing element for sensitive floors<sup>2</sup> (left), combination of RGB and depth camera for vision-based analysis<sup>3</sup> (right).

### Supervised Assessments

Instrumented assessments are also conducted using non-wearable sensors: Vernon et al. [114] use a depth sensor (Microsoft Kinect<sup>4</sup>) to conduct the iTUGT. Due to the depth sensor's limited field of view of 3.8m maximum, the depth camera is placed to record the stand-up from the chair and the walking path, except for the last meter and the turn area. The installation height of the Kinect is not specified. In order to detect and track and their respective joints and anatomical landmarks of persons within the field of view an algorithm provided by Microsoft [115] is used. To perform measurements, certain events are defined, which are used to extract information. The defined events are: start (frame before trunk movement), stood-up (peak height of shoulders), first step and first stride (heel strike), 2m distance to the depth sensor heading towards it, 2m distance heading to the chair, end of the test (end of trunk movement when sitting). The extracted features comprise peak velocity and peak angle of the trunk's flexion when standing, length of first step and stride, walking velocity, time to turn around as duration between both 2m events, as well as the duration required to complete the test. Visual inspection of depth images and plots of the anatomical landmarks are used to obtain these variables. Vernon et al. [114] evaluate the Kinect assisted TUGT with 30 subjects who had a stroke and perform a re-test one week later. The test-retest intraclass correlation coefficients show results between 0.93 and 0.99 for the extracted features except for the angle of trunk flexion (0.73). Further, the results are compared SW measurement. The total duration measured with the SW is  $17.21s \pm 9.89s$  and  $18.70s \pm 10.48s$  measured with the depth sensor, which corresponds to  $p < 0.001$  (significant correlation at  $p < 0.05$ ).

A conduction of the 5tSTS with assistance of the Microsoft Kinect is described

<sup>2</sup>Image from <http://www.amti.biz/fps-guide.aspx> (accessed 03-2018)

<sup>3</sup>Image from <https://www.xbox.com/de-AT/xbox-one/accessories/kinect> (accessed 03-2018)

<sup>4</sup><https://developer.microsoft.com/en-us/windows/kinect> (accessed 03-2018)

by Ejupi et al. [116]. The setup consists of the Kinect depth sensor which is placed in front of a monitor or television at a height of 0.8m and 2m distance to the subject performing the test. Start and end of the measurement are defined as the first increase respectively the last decrease of height exceeding a threshold of 0.05m. STS phases are partitioned into sitting, transition to standing, standing, transition to sitting. For analysis of the participant's performance, following features are automatically extracted: average duration of standing and sitting, average vertical velocity of the transitions, and the total duration required from start to end. 94 community-dwelling adults were classified as fallers and non-fallers if they experienced a fall in the preceding year and conducted the STS test, which is compared to SW measurement. The average velocity of the STS transition is reported to be most discriminative in order to distinguish between the two groups with  $p=0.019$  ( $p<0.05$  considered as significant). Overall duration measured by SW results in an average duration of  $16.8s\pm 5.68s$  ( $p=0.028$ ), while the depth sensor measurement results in  $15.33s\pm 5.45s$  ( $p=0.034$ ).

Gianaria et al. [17] describe automated frailty assessment by gait analysis based on the Microsoft Kinect version 2, while participants perform the TUGT. The sensor is set up at a height of 2m and 4m away from the chair, where the person starts the test. To track the person during walks, the skeleton map of the Kinect software is used. When the person is sitting, Gianaria et al. [17] report problems since the skeleton data becomes unreliable due to the limited range. Hence, the total test duration is measured manually and the depth sensor is only used to obtain features while the person walks. The features comprise as follows: gait velocity, duration of swing phase and double support, change in stride speed, average time and variability of walking sequences, and balance features extracted from posture (whether the torso is tilted forward). For evaluation, 30 older adults and 6 young persons perform the test while recorded with the depth sensor. There are visible differences in the results of the old and young adults: old adults require an average total time of  $11.42s\pm 3.22s$ , young adults require  $9.66s\pm 2.09s$ ; walking time of older adults is  $9.31s\pm 3.11s$  on average, while younger adults walk  $7.16s\pm 1.66s$  on average; average gait velocity of elders is slower ( $0.75m/s\pm 0.19m/s$ ) than the younger participants ( $0.92m/s\pm 0.07m/s$ ). The older adults further answer the Tilburg Frailty Indicator questionnaire [117] to assess their frailty level with following outcome: 17 frail and 13 robust subjects. Gianaria et al. report that the Timed Up and Go (TUG) time significantly correlates ( $p=0.012$ ) with the Tilburg Frailty Indicator score. Except for posture tilt, all automatically extracted features show significant correlation with the Tilburg Frailty Indicator score: gait velocity  $p=0.009$ , walking duration  $p=0.025$ , swing phase duration  $p=0.040$ , double support duration  $p=0.037$ .

Doppelbauer [118] describes mobility assessment based on gait analysis and an automated version of the TUGT. For both approaches, he compares two sources from the Microsoft Kinect version 2: depth data estimating the point cloud of the person and skeleton data provided by the Kinect SDK. The extracted gait parameters comprise gait speed, step and stride length, as well as step and stride time. For evaluation, three pre-defined walking paths are defined: frontal, diagonal, and orthogonal. Performance on

circular walks are not investigated. 13 subjects aged 24-77 years walk the paths multiple times, summing to a total of 234 sequences. Doppelbauer [118] compares four methods to estimate parts of the gait cycle: horizontal oscillation, vertical oscillation, feet distance, and correlation coefficient. Using these methods, the gait parameters are estimated, while the best results achieved measuring the gait speed, having MAE of 0.009m/s-0.0281m/s using depth data and 0.0152m/s-0.0347m/s using skeleton data. The automated TUGT is evaluated with 11 elderly persons. The MAE of the total TUG results in 0.29s for depth data and 0.23s for skeleton data. Doppelbauer [118] concludes that depth data is preferable when measuring gait parameters, while skeleton data is preferable for analysis of the joints.

### Unsupervised Assessments

Stone and Skubic [24] compare the TUG time to In-home Gait Speed (IGS) captured with a Kinect. To this end, a Kinect is installed at a height of 2.7m in the living room of an apartment and tracks persons within their field of view. Movements exceeding 1.2m and 0.127m/s are identified as walks and used to extract height and velocity. Further, stride parameters are extracted, but only when more than four steps are recognized to reduce the impact of lower extremity occlusion. Since it can not be assured in real-world installations that only one person is tracked, but also visitors and other residents, Stone and Skubic describe a gaussian mixture model to cluster tracked persons [119]. The features to fit this model comprise person height, gait velocity, as well as mean stride time and length if available.

The system was installed in 14 apartments for a duration of 2 to 16 months capturing 15 participants of 68 years and above. This is possible by inclusion of one multiperson household, others were excluded since the residents' models were not distinguishable. During this evaluation phase, monthly assessments were conducted, consisting of: 1) Habitual Gait Speed (HGS) test: average of two times 3m walk, measured with SW, 2) TUGT. The average gait speed of the HGS test is 0.65m/s $\pm$ 0.18m/s and the mean duration required to perform the TUGT is 19.5s $\pm$ 7.8s. The average IGS velocity equals 0.49m/s $\pm$ 0.12m/s. The Pearson correlations are used by Stone and Skubic [24] to compare the association between HGS and TUGT resulting in  $r=0.82$  ( $p<0.001$ ), while the correlation between IGS and TUGT results in  $r=0.91$  ( $p<0.001$ ), which suggests a better association between TUGT to IGS than to HGS. In order to estimate a mapping between TUG time and gait velocity, a non-linear neural network is used. The resulting mapping is shown in Figure 2.8. The results of the TUGT are filtered using 95% confidence boundaries to minimize intra-individual variation. The mapping shows an increase in the required TUG time, when persons walk below 0.5m/s on average. Velocities above 0.5m/s map to a TUG time between 12 and 15s. According to Alexandre et al. [20], TUG times above 12.5s are a predictor for fall risk in older adults. Hence, 0.5m/s IGS can be used as cut-off value to classify an elderly person as prone to falling.

The recorded IGS is further used by Stone et al. [120] to create a weighted average as metric for mobility and fall risk, called Average In-home Gait Speed (AIGS). The system

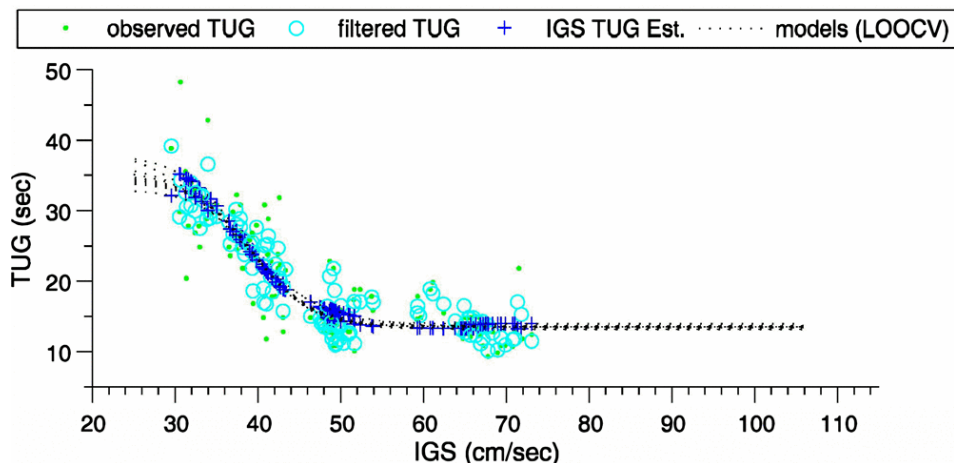


Figure 2.8: Mapping of TUG time to IGS learned with a non-linear neural network using leave-one-out cross validation (LOOCV). (Image from [24])

setup is identical to the setup in [24], and hence, also the extracted features describing a walk are the same: gait velocity, person height, time and length of stride. To build the AIGS the average velocity is weighted by the likelihood of the walk belonging to a certain resident. This likelihood is given by the probabilistic model [119] generated from the walk features of the preceding 8 weeks. This metric is compared to a set of clinical check-ups, which are conducted monthly: 1) HGS, 2) TUGT, 3) SPPB, 4) multidirectional reach test [121]: the person has to reach for- and backwards, as well as sideways, 5) short form of the Berg balance scale [54]: 7 balance examinations measured with SW. Stone et al. [120] use a neural network to analyze correlations between these tests and find mappings among each other, as well as to the AIGS. The best mapping is obtained between TUGT and AIGS with an intraclass correlation coefficient of 0.95, followed by TUGT and HGS with 0.88, and sideways reach and AIGS with 0.86.

Ejupi et al. [116] evaluated their Kinect based version of the 5tSTS in the homes of 18 test persons supervised and unsupervised with 10 participants. Compared to the performance in laboratory setting ( $13.42s \pm 5.3s$ ), the subjects performing the supervised version required a total duration of  $11.01s \pm 2.97s$  on average, which corresponds to  $p=0.008$ . The persons performing the unsupervised version required  $11.82s \pm 2.04s$  in laboratory and  $11.82s \pm 2.04s$  in-home, which corresponds to  $p<0.001$ . Ejupi et al. [116] report that every phase of the test is correctly identified and the sit-to-stand velocity can be used to classify fallers from non-fallers on retrospective fall reports:  $0.78 \pm 0.20m/s$  for fallers and  $0.94 \pm 0.24m/s$ . Due to the strong correlation between laboratory and in-home conditions ( $p<0.001$ ), this can also be applied to unsupervised settings at home.



## Summary

In Table 2.5 the main characteristics and outcomes of the described non-wearable assessments are listed. Although, the amount and health status of tested persons, as well as the set-ups vary, tendencies are recognizable: automated estimation of TUG parts is reliable, gait velocity and STS velocity are able to distinguish between fallers and non-fallers.

Table 2.5: Summary Non-Wearable Assessments

Reference	Assessment	Sensor	Outcome
<b>Supervised</b>			
Vernon et al. [114]	TUGT	Kinect	except trunk flexion, reliable TUG part quantification
Ejupi et al. [116]	5tSTS	Kinect	average STS velocity best discriminator between fallers/non-fallers
Gianaria et al. [17]	TUGT	Kinect 2	except posture tilt, significant correlation with Tilburg Frailty Indicator
Doppelbauer [118]	gait & TUGT	Kinect 2	depth data preferable for gait parameter measurement
<b>Unsupervised</b>			
Stone and Skubic [24]	TUGT	Kinect	higher correlation between TUGT and IGS than HGS
Stone et al. [120]	AIGS	Kinect	best mapping between TUGT & AIGS, AIGS allows continuous assessment
Ejupi et al. [116]	5tSTS	Kinect	STS velocity able to classify fallers & non-fallers

## 2.4 Depth-Based Motion Tracking

The described approaches using vision-based depth measurement to obtain person movement parameters utilize two versions of active optical depth acquisition methods: Structured Light (SL) and Time-Of-Flight (TOF). Both methods are active distance sensing technologies as they emit light to obtain depth information of the scene, which provides independence from external light sources and allows operation in darkness. Since sunlight interferes with the emitted light, the usage is limited to indoor application [113, 122]. The parallel use of multiple sensors emitting infrared light can cause interference between the systems [123]

### 2.4.1 Sensor Operating Principles

In order to obtain 3-dimensional information, SL depth sensors project a certain known light pattern onto the scene which is reflected by the objects of the scenery. A camera observing the scene captures the reflected pattern from a different angle, which differs from the original pattern due to deformation by the geometry of the scenery objects. This principle is depicted in Figure 2.9a. To calculate distance  $d$  from the disparity  $m$  of the reflected light pattern, the camera's focal length  $f$  and the distance between camera and projector (baseline  $b$ ) have to be known, as shown in Equation 2.1 [123].  $f$  and  $b$  are intrinsic camera parameters, which are calculated by transforming the camera coordinates of a 3D point to image coordinates. This method yields problems with reflective and transparent/light-absorbing surfaces, as the light is either reflected non-deformed (the spatial information is lost) or no light is reflected at all [89]. Further, sunlight illuminating the scene covers the projected light pattern, hence the pattern is difficult or impossible to capture [124], thus, outdoor installation and indoor environments where strong sunlight shines into the room impairs the function of this sensor type.

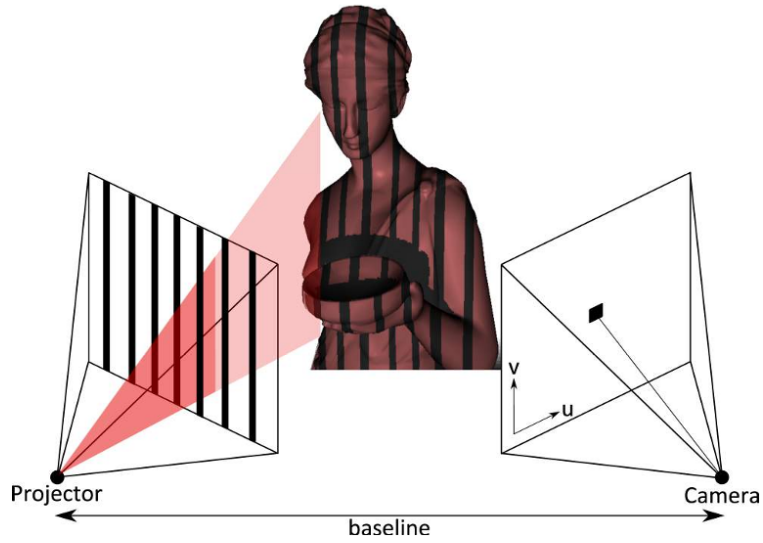
$$d_{SL} = \frac{f * b}{m} \quad (2.1)$$

TOF systems measure distances using signal modulation. Similar to the structured light method, the field of view is illuminated with modulated light and the reflected signal is captured using a sensor matrix. The received signal has a phase shift in comparison to the emitted signal, which is proportional to the traveled distance. The underlying principle is depicted in Figure 2.9b. The phase shift is used to determine depth as shown in Equation 2.2, where  $d$  corresponds to the distance,  $\lambda$  to the wavelength of the emitted signal, and  $\phi$  to the shift of phase in the signal [89, 125]. This method offers advantages as it requires only one camera and allows acquisition of depth information. Due to the superposition of the light on the individual pixels of the sensor matrix, it has aliasing effects and lower image resolution compared to structured light systems [89]. Since it uses infrared light, sunlight is as problematic as to the SL depth sensor.

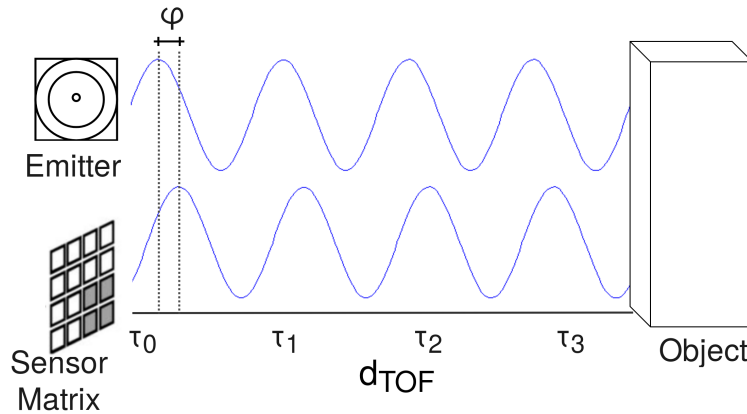
$$d_{TOF} = \frac{\lambda}{2} * \frac{\phi}{2\pi} \quad (2.2)$$

### 2.4.2 Person Tracking

In order to analyze motion patterns (e.g. gait) automatically, a way to detect persons within the field of view is required, as well as a method to track them over time. Pramerdorfer et al. [122] describe a person tracking method for fall detection using depth data only, hereinafter called the Depth based Person Tracker (DPT). Since this approach extracts motion features during tracking, it is also applicable for enhanced motion analysis based on the generated features. The DPT uses an auto-calibration algorithm: for self-calibration of the system, the sensor is required to face at least part of



(a) SL: Certain light pattern is reflected by scene objects. Deformed pattern is captured by the camera and analyzed to reconstruct scenery. (Image from [123])



(b) TOF: The emitter projects modulated infrared light onto the scene; the reflected signal shows a phase shift  $\phi$ , which is direct proportional to the distance  $d_{TOF}$ . (Image adapted from [89])

Figure 2.9: Operating principles of SL and TOF depth sensor.

the floor. In order to find the ground plane, the depth values obtained from the sensor are converted to a point cloud in camera coordinates. The RANSAC [126] algorithm, which utilizes depth points for plane-fitting, results in several planes, whereas the plane with the greatest distance to the origin corresponds to the ground floor, since the sensor's position is at the origin of the camera coordinate system. This plane is utilized to obtain the extrinsics: height of the sensor and orientation. The depth map is further converted to a point cloud in world coordinates, which is used to detect objects within the scene

by classification of grouped points with a size of 0.3-0.9m. Due to the integration of auto-calibration, the DPT supports plug-and-play, which enables to install the sensor inside an apartment without further interaction.

In a second step a background model of the scenery is generated. To this end, the pixel values of the first frame are used as background model, which represents the static objects. Subsequently, frames are compared to the background model using subtraction; the resulting differences correspond to moving voxels. Since the scenery may change over time (e.g. a door is opened, a chair is moved), the background model generation is conducted periodically. The scene is projected into a synthetic top-view using orthographic projection [127]. This allows to store the scene geometry in a compact way, enabling fast computation on low-end hardware according to Pramerdorfer et al. [122]. Further, this representation allows to extract features invariant to the orientation and position of the sensor, which is useful for person detection and tracking. In order to convert foreground pixels to plan-view coordinates, they are projected to world coordinates, followed by downsampling to the ground plane and discretization. This procedure results in mapping multiple points to the same plan-view point; the number of points mapped to the same plane-view pixel is encoded in an occupancy map, whereas the respective highest occurred points are stored in a height map. The conversion from depth map to plan-view is depicted in Figure 2.10.

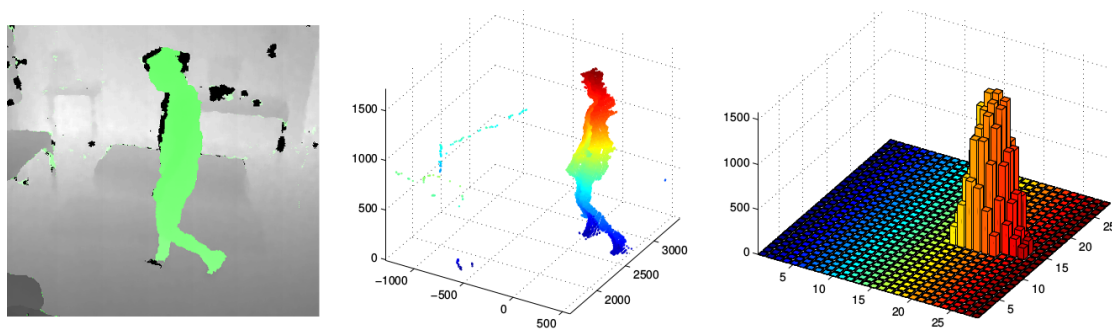


Figure 2.10: After background subtraction, the depth map (left) obtained by the sensor is converted into a point cloud (middle) followed by a projection to plan-view (right) resulting in an occupancy map and a height map. (Image from [122])

For the purpose of person detection every frame is analyzed individually by thresholding the height map generated in the preceding step to find connected components (connected pixels with a height  $> 0$ ). These regions are described by feature vectors composed by the number of connected pixels, height of the object, density of the object, and shape of the object. The resulting feature vectors are classified using a Random Forest (RF) classifier [128] to predict whether the object is a person. In order to track a person over time,  $n$  detected person regions of a frame have to be associated with  $m$  person regions of the subsequent frame. Pramerdorfer et al. [122] define a cost function considering proximity and similarity of the feature vector generated of a person region.

For efficient calculation of this optimization problem,  $m$  is equated with  $n$  resulting in a linear assignment problem. Since a person may enter or leave the scenery,  $m$  and  $n$  can diverge; this is compensated by the introduction of dummy regions [129]. Pramerdorfer et al. [122] extend their method by a fifth step performing fall detection using state prediction to estimate whether the person is resting, active or fallen.

Based on medical assessment tests for estimation of persons' mobility and fall risk, approaches utilizing wearable and non-wearable sensors to assist the measurement of these tests were developed. Due to the technological assistance, unsupervised assessments are enabled, allowing measurement of movements at habitual speed in persons' homes. Habitual gait and STS movements are identified as main source of information for overall fitness and fall risk. The application of non-intrusive, plug-and-play sensors facilitate the measurement of these movements in the homes of older adults, which are described in this work.



## Methodology

In order to assess a person's health and frailty status in a non-invasive way, approaches to measure physical parameters correlating with overall fitness are developed. Stationary in-home mounted depth sensors allow for non-intrusive, privacy protecting motion tracking [25]. Based on captured depth information, person detection and movement tracking is performed using the DPT [122]. This algorithm provides tracking information of moving objects and persons - either online, when the system is installed in the apartment of older adults, or offline using recorded depth streams. The output of the DPT is the input for the proposed approaches in this work, as shown in Figure 3.1. The provided trajectories are used for gait and STS transition analysis.

For every moving object the tracker provides a time stamp when the track began, a time stamp when the track ended, and for every tracking point:

- $x$ : x-coordinate of the tracked object's Center Of Mass (COM) in cm
- $y$ : y-coordinate (height) of the COM in cm
- $z$ : z-coordinate of the COM in cm
- $\dot{x}$ : x-velocity from the previous point in cm/s
- $\dot{y}$ : y-velocity in cm/s
- $\dot{z}$ : z-velocity in cm/s
- $t$ : time stamp of current tracking point

Figure 3.2 shows the orientation of the tracker's coordinate system. Although the depth sensor has to be mounted at a height between 2 and 3m, the image coordinates are converted to world coordinates and projected to plan-view (see Section 2.4.2), which allows to perform calculations in real world distances. Every moving object is classified by the tracker, if it is a person.

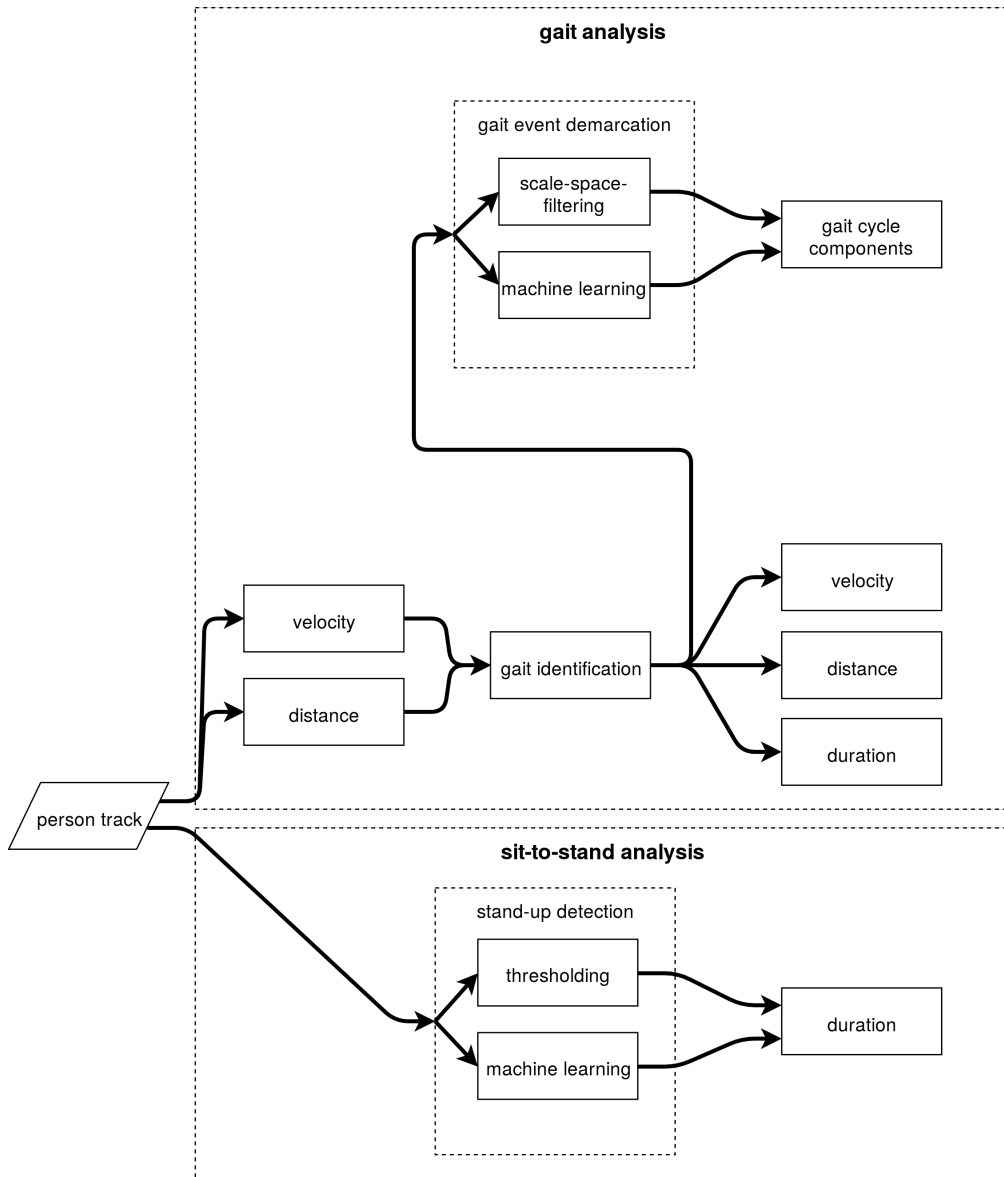


Figure 3.1: Overview of the proposed approaches, the output of the DPT are used as base for the gait and STS transition analysis. If the track is identified as walk or detected as STS movement, further analysis is performed.

### 3.1 Gait Velocity, Distance, and Duration Analysis

Gait velocity is recognized as predictor for overall fitness [28], health [47], frailty [10], and mortality [130]. Movement into the same direction for more than 1.2m with a minimum of 0.127m/s is taken into account for gait measurement as described by Stone and Skubic [119]. For this measurement the magnitude  $\|\vec{v}_{planar}\|$  of the horizontal velocity



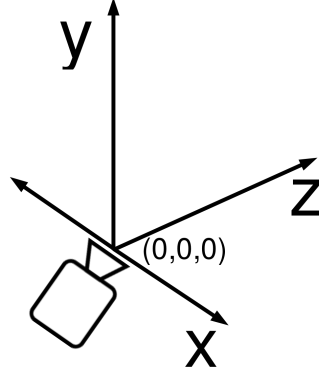


Figure 3.2: Orientation of the coordinate system after projection to plan view.

$\vec{v}_{planar}$  is used since the movement is independent of direction. The calculation of the planar velocity is shown in Equations 3.1 by multiplying the horizontal velocity vectors ( $\dot{x}$  and  $\dot{z}$ ). Equation 3.2 shows the calculation of the resulting vector's magnitude.

$$\vec{v}_{planar} = \dot{x} * \dot{z} \quad (3.1)$$

$$\|\vec{v}_{planar}\| = \sqrt{\dot{x}^2 + \dot{z}^2} \quad (3.2)$$

To ensure the person is moving into the same direction, the relative change of the active person's motion orientation is observed to detect if the person made a sharp turn. If the orientation exceeds a certain threshold, the current walk ends. In order to obtain the horizontal walking path, the  $x$  and  $z$  coordinates of three consecutive tracking points need to be observed:  $A = (x_i, z_i)$ ,  $B = (x_{i+1}, z_{i+1})$ , and  $C = (x_{i+2}, z_{i+2})$ . Figure 3.3a visualizes the coordinates and the connecting vectors in spatial representation. Since, height information is not required for analysis of the walked path, the height information  $y$  can be neglected. The person moves from point  $A$  to  $B$  to  $C$  and thus the walking path forms the direction vectors  $\vec{AB} = B - A$  and  $\vec{BC} = C - B$ . The scalar product of these vectors is equal to their length and the enclosed angle  $\theta$  as shown in Equation 3.3.

$$\vec{AB} \cdot \vec{BC} = \|\vec{AB}\| \|\vec{BC}\| \cos \theta \quad (3.3)$$

The angle  $\theta$  can be obtained using substitution as shown in Equation 3.4.

$$\theta = \arccos \left( \frac{\vec{AB} \cdot \vec{BC}}{\|\vec{AB}\| \|\vec{BC}\|} \right) \quad (3.4)$$

When a walk is recognized, following parameters are measured: 1) duration  $\Delta t$ : begin of movement until direction change, person inactive, or track ends, 2) distance  $d$ : during walk as shown in Equation 3.5, and 3) average velocity  $\bar{v}$ : as shown in Equation 3.6.

$$d = \sum_{i=1}^{n-1} \sqrt{(x_i - x_{i+1})^2 + (z_i - z_{i+1})^2} \quad (3.5)$$

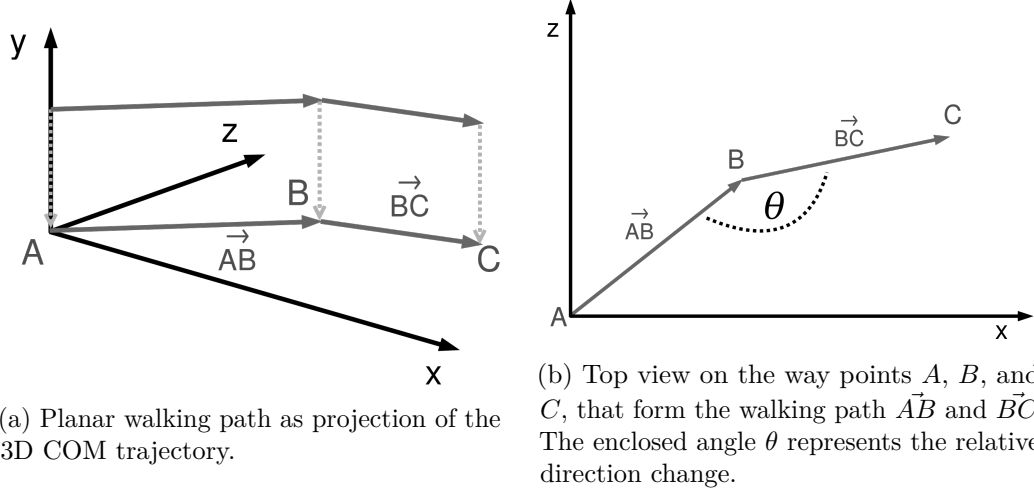


Figure 3.3: Illustration of walking path and its enclosed angle to compute change of direction.

$$\bar{v} = \frac{1}{n} \sum_{i=1}^n \|\vec{v}_{planar_i}\| \quad (3.6)$$

## 3.2 Gait Event Analysis

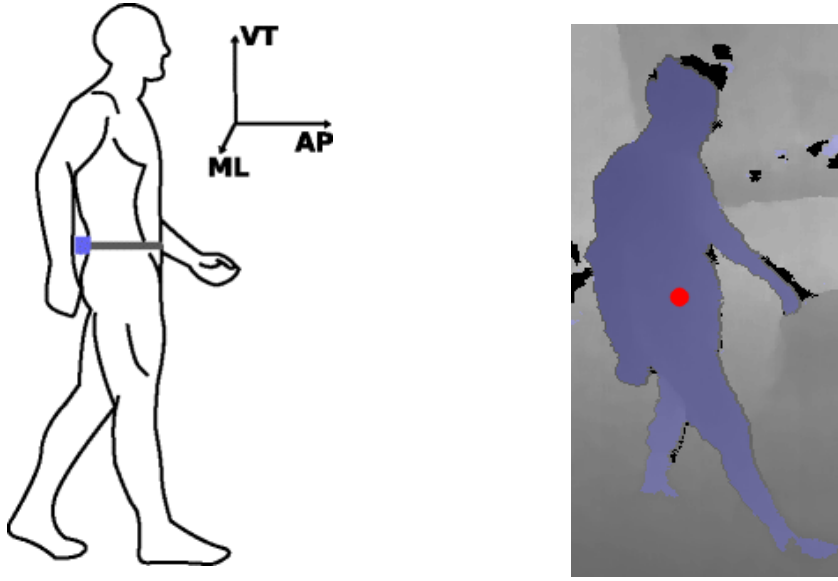
Gait velocity and gait cycle components are shown to be predictors for falls [131]. In functional assessment tests that examine human gait, persons have to walk a certain distance into one direction (e.g. TUGT [18]: 3m; SPPB [57]: 2.44m). Thus, quantitative gait parameters are a source of information to assess persons' mobility.

### 3.2.1 Scale-Space Filtering Approach

In order to estimate temporal gait parameters, González et al. [132] describe an approach based on a single three-dimensional accelerometer attached to the back at the height of the second lumbar vertebra. This position is comparable to the position of the COM provided by the DPT as shown in Figure 3.4a and 3.4b. The directional acceleration values of a tracking point  $\ddot{x}_i$ ,  $\ddot{z}_i$ ,  $\ddot{y}_i$  are calculated using the velocity difference of two consecutive points as shown in Equation 3.7, where  $i \in \mathbb{N}_{\geq 0}$  refers to the number of the respective tracking point.

$$\ddot{x}_i = \frac{\dot{x}_{i+1} - \dot{x}_i}{t_{i+1} - t_i}, \quad \ddot{z}_i = \frac{\dot{z}_{i+1} - \dot{z}_i}{t_{i+1} - t_i}, \quad \ddot{y}_i = \frac{\dot{y}_{i+1} - \dot{y}_i}{t_{i+1} - t_i} \quad (3.7)$$

The main difference of this method compared to the approach of González et al. [132] is the sampling rate: the depth sensor captures 30 frames per second and the DPT provides information at 15 frames per second; the accelerometer used by González et al. [132]



(a) The accelerometer is attached at the lumbar spine (Image from [132])

(b) Position of the COM used by the DPT

Figure 3.4: Comparison of the signal origins: accelerometer mounted to the waist and COM of person track

reaches a frequency of 70Hz. In order to estimate temporal gait parameters, González et al. [132] begin with demarcation of HS and TO as relevant gait events using three signals: I) the energy signal  $e_i$ , which corresponds to the 3D acceleration's magnitude (Equation 3.8), II) the vertical acceleration  $\ddot{y}_i$ , and III) the antero-posterior acceleration  $a_i$ . In order to calculate  $a_i$  from the tracking points, it is assumed that the movement of a walk is mainly forward. Hence the magnitude of the planar acceleration is used as shown in Equation 3.9.

$$e_i = \sqrt{\ddot{x}_i^2 + \ddot{z}_i^2 + \ddot{y}_i^2} \quad (3.8)$$

$$a_i = \sqrt{\ddot{x}_i^2 + \ddot{z}_i^2} \quad (3.9)$$

In a first step,  $e = \{e_0, e_1, \dots, e_{n-1}\}$  and  $\ddot{y} = \{\ddot{y}_0, \ddot{y}_1, \dots, \ddot{y}_{n-1}\}$ , which correspond to the whole signals of the track with  $n \in \mathbb{N}$  as the length of the track, are filtered with Gaussian kernels of different sizes, which allows to emphasize high concentrations of energy in these signals. A scale-space filter with three levels is used to filter the energy  $e$ . The levels represent small, medium and large step sizes. They are determined from gait cycle observations by González et al. [132] and define the  $\sigma$  of the kernels as follows: small steps  $\sigma=125$ ms, medium steps  $\sigma=281$ ms, large steps  $\sigma=438$ ms. This corresponds to 3.75, 8.43, 13.14 frames respectively. After filtering the signal, the product of the resulting smoothed signals  $\hat{e}_{\sigma=125}$ ,  $\hat{e}_{\sigma=281}$ ,  $\hat{e}_{\sigma=438}$  is obtained as shown in Equation 3.10. The signal  $\hat{e}_{\sigma=438}$  is subtracted from the product  $p$  resulting in signal  $s$  and used to

detect peaks above a certain threshold of 0.13.  $P_s$  is the set containing these peaks.

$$p = \hat{e}_{\sigma=125} \times \hat{e}_{\sigma=281} \times \hat{e}_{\sigma=438} \quad (3.10)$$

$\ddot{y}$  is filtered with  $\sigma \in \{50ms, 100ms\}$  to generate the smoothed signals  $\hat{y}_{\sigma=50}$  and  $\hat{y}_{\sigma=100}$ , which emphasizes peaks corresponding to steps. The signals captured by González et al. [132] are compared to those captured by the DPT in Figure 3.5. The smoothed signals intersect between local minima and maxima and limit the area where HS events can be found. After subtraction of  $\hat{y}_{\sigma=100}$  from  $\hat{y}_{\sigma=50}$ , the resulting signal  $s_{\ddot{y}}$  is used to

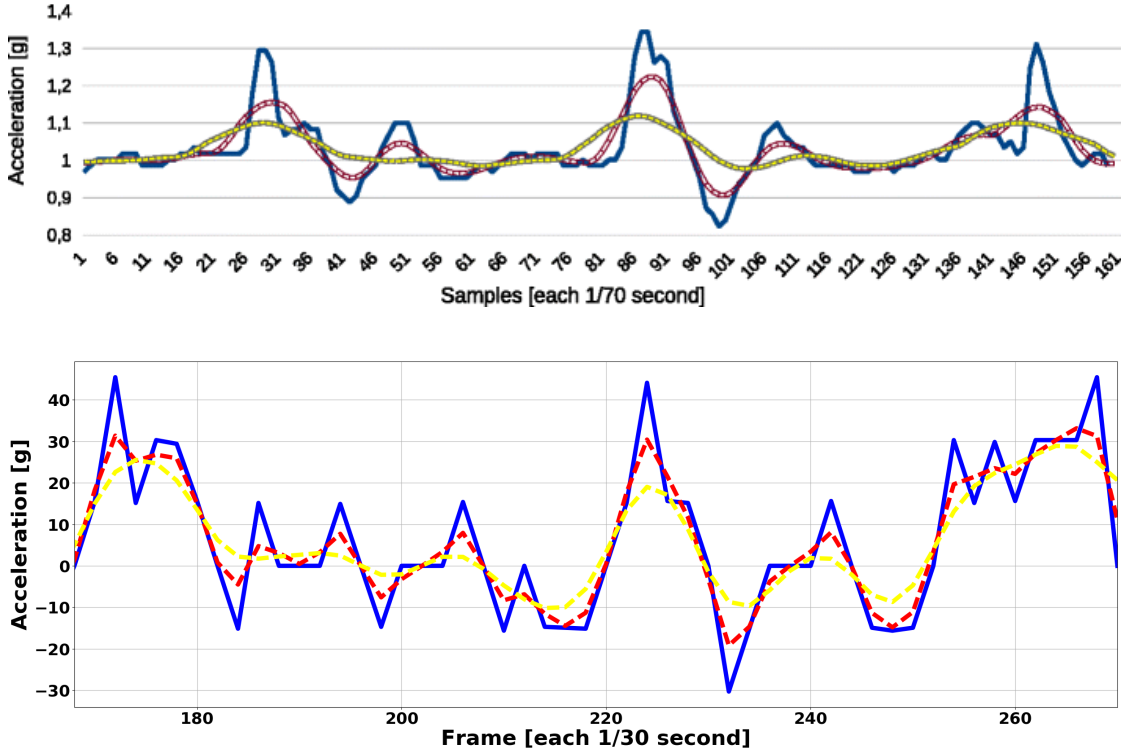


Figure 3.5: Vertical acceleration  $\ddot{y}$  (blue), and the smoothed signals  $\hat{y}_{\sigma=50}$  (red),  $\hat{y}_{\sigma=100}$  (yellow). Top: Signals from González et al. [132]. Bottom: Signals of DPT.

find zero-crossing points  $Z_{s_{\ddot{y}}}$  and peaks  $P_{s_{\ddot{y}}}$ . Only zero-crossing points next to peaks of  $P_{s_{\ddot{y}}}$  and  $P_s$  are considered. An HS event corresponds to the highest peak in the antero-posterior acceleration  $a_i$  in the vicinity of the remaining zero-crossings and the associated TO event to the subsequent valley in the signal. When HS and TO events are identified, other temporal gait parameters can be calculated, as described in Section 2.2.1.

### 3.2.2 Machine Learning Approach

Based on the experiments of González et al. [132], the magnitude of all directional accelerations  $e$  is used to generate a feature vector. In order to provide context information

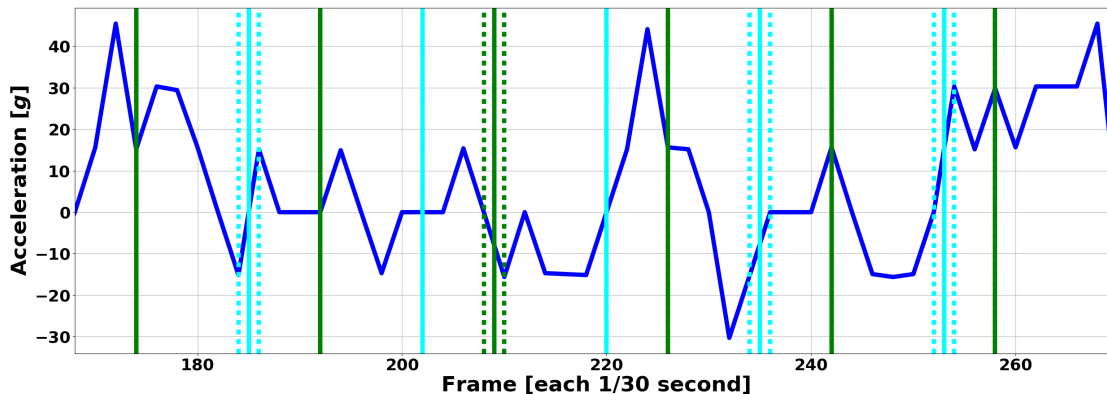


Figure 3.6: HS (cyan) and TO (green) events: annotated (solid) and predicted (dashed).

to the RF, a feature vector consists of 6 consecutive tracking points ( $=0.4s$ ), hence  $\vec{X} = \{e_i, e_{i+1}, \dots, e_{i+5}\}$ . The RF is trained with vectors from three classes, containing HS events, TO events, as well as NO events. Since a healthy gait cycle consists of only 2 HS and TO events, the classes of a track are unbalanced. The RF provides a probability for each class of every vector  $f_{RF}(\vec{X}_i) = (P_{i_{HS}}, P_{i_{TO}}, P_{i_{NO}})$ , which sum to 1. Figure 3.6 shows the output of the classifier applied to every vector of a track. Since information about the healthy sequence of a gait cycle is known, this information can be used to optimize the outcome of the RF predictions. For example, an HS event is followed by a TO event. Using the minimum (0.5s) and maximum (1.75s) length of a gait cycle observed by González et al. [132], weight arrays for all classes are generated, with the sum of elements at every index add up to 1. Since the duration of the double support (HS to next TO occurrence) corresponds to 10% of the gait cycle, this equals 0.05-0.175s or 1.5-5.25 frames. Within these boundaries the arrays are altered to generate a grid with all possible event occurrences. Further alterations comprise repetitions of the gait cycle and permutation of the events. The resulting grid is applied to the probabilities. To that end, a loss function is defined as shown in Equation 3.11,  $i$  refers to the current frame of the track,  $W$  is the current weight array. The loss for every weight array in the weight grid is calculated and the array with the least loss is used to calculate temporal gait parameters derived from HS and TO events.

$$\mathcal{L} = \sum_{i=0}^n \left\{ (1 - P_{i_{HS}}) * W_{i_{HS}} + (1 - P_{i_{TO}}) * W_{i_{TO}} + (1 - P_{i_{NO}}) * W_{i_{NO}} \right\} \quad (3.11)$$

### 3.3 Stand-Up Detection

Since the STS performance is determined by the lower body musculature, it is an indicator for balance, and fall risk [29, 30]. Physical assessment tests, like the TUGT [18], the

SPPB [57], or the STS test [55], use this for prediction of physical fitness and fall risk. Hence, measuring the time required for an STS transfer, and the number of stand-ups within a certain amount of time are valuable indicators for a person's mobility. Before measuring the STS transfer time, stand-ups have to be detected. For this, two different approaches are described: one approach uses machine learning, the other uses a thresholding technique.

### 3.3.1 Threshold Approach

This approach is based on the stand-up detection of Banerjee et al. [133], who detect sitting and standing separately. Hence, the height of the COM ( $y$ ) is used to distinguish between sitting and standing, as well as the intermediate transition. The approach aims to find all height differences in the track exceeding a certain threshold. Further, the higher value has to occur later in the signal than the lower value, to exclude sit-downs. To search for these values a time window 8 seconds is slid over the height values of the track. This time window covers the maximum length specified in literature for STS transfer times [72]. Every value higher/lower than the currently stored minimum and maximum is replaced. A new minimum always resets the current maximum too, to ensure a height increase. The difference between the current extrema is compared to the threshold. If it exceeds the threshold, a stand-up is registered. A suppression ensures the window is slid further for a certain amount of time to detect a possible higher maximum. This approach depends highly on the height of a person, respectively the COM of this person, since a tall person's COM may increase more during stand-up, then a small person's COM, depending on the stand-up technique. Hence, the threshold is selected dynamically as certain proportion of the maximum height value of the whole track. To find the optimal values for the suppression time and threshold, a grid search with following parameter space is conducted:

- suppression time: 0.5s, 1s, 1.5s, 2s, 2.5s, 3s
- threshold: 15 - 60% of max. COM

For the grid search a validation set consisting of 12,010 feature vectors (6,005 each class) is used. Best results are obtained using a suppression of 2.5s and a threshold of 50% of the maximum COM. Figure 3.7 shows an example of a height feature track, with detected stand-up.

### 3.3.2 Machine Learning Approach

In order to detect STS transitions automatically, different sets of features in combination with two Machine Learning (ML) techniques are used to identify which combination achieves the best results. A Support Vector Machine (SVM) [134] and an RF [135] are trained with following tracking sequences respectively: one time the classifiers are trained on the whole STS transition, and one time on the start sequence and end sequence separately. Allin and Mihailidis [30], who also use a decision tree as ML approach to detect STS transfers use relative distances between head, torso, and ground as features.

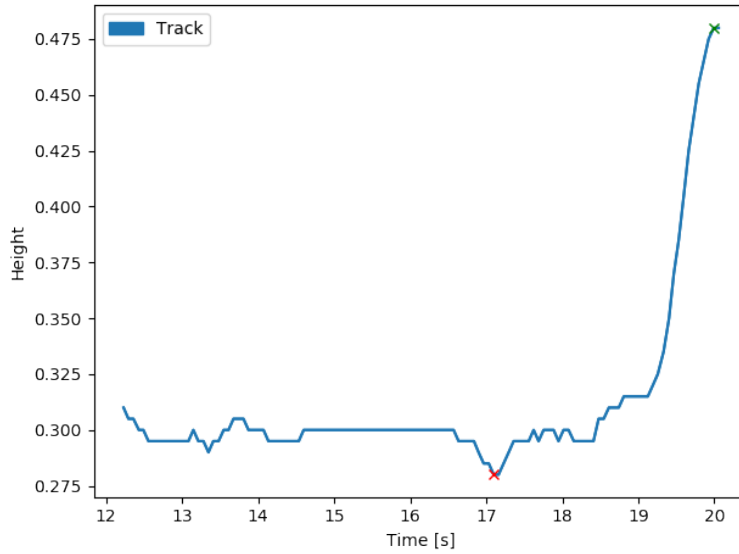


Figure 3.7: Height track with minimum (red mark) and maximum (green mark) of the detected stand-up using the threshold approach.

However, these features are different from the tracking information obtained and provided by the DPT and used to build feature vectors composed as follows:

- horizontal velocity magnitude  $\|\vec{v}_{planar}\|$  normalized between 0 and 1 with a maximum height of 2m/s
- height  $y$  normalized between 0 and 1 with a maximum height of 2m
- vertical velocity  $\dot{y}$  normalized between -1 and 1 with a maximum of 2m/s

The complete feature vector is composed of 8s to include the maximum STS transfer duration [72]. This leads to a total feature vector length of 360:

$$8s * 15 \text{ frames per second} * 3 \text{ features.}$$

The vectors containing only the start/end sequences comprise a length of 90 (=2s) The tracking information obtained from depth sequences is used to build these feature vectors and split into training and test set at a ration of 80 to 20. As soon as a person is considered active, the mentioned features are gathered to build a complete feature vector of length 360. This is necessary due to training of the ML algorithms with feature vectors of this size. When the length is reached, the current vector is used for prediction whether it contains a stand-up. After the vector is tested for a stand-up, the next features are added and the first ones are removed to ensure a fixed size of 360. If the current active track ends before the size is reached, the vector is zero-padded.

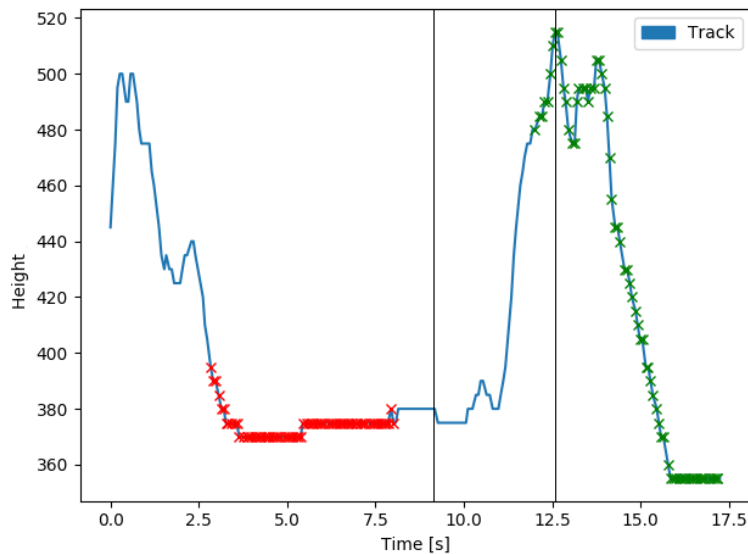


Figure 3.8: Beginnings (red marks) and endings (green marks) of feature vectors with predicted stand-up, and actual stand-up (black vertical lines).

### 3.4 Stand-Up Duration Measurement

After positive stand-up prediction, it is known that there is a stand-up within a certain time window, but not the duration of the actual STS transfer. Figure 3.8 depicts this problem showing the respective begin (red marks) and end (green marks) of all feature vectors, when a stand-up was predicted. To ensure the whole STS transfer is used for measurement, the examined window is sliced from the first feature point of the first feature vector the stand-up was detected to the last feature of the last vector the stand-up was continuously detected. To measure the duration of an STS transfer, the steps shown in Figure 3.9 are successively conducted.

In a first step the Savitzky-Golay filter [136] is used, which uses polynomial regression for smoothing and considers high frequencies as well, and thus preserves local minima and maxima. The filter is applied with

$$\text{window size} = \frac{\text{slice length}}{2},$$

which corresponds to an intentional wide window. The wide window together with a low polynomial degree of 2 results in strong smoothing which is required for the next step. In order to perform calculations like curve sketching, the smoothed track has to be polynomial fitted, which is done using a polynomial degree of 8 and results in a function  $f(t)$ . The results are shown in Figure 3.10. A key characteristic of a stand-up is the steep height increase in phase III in comparison to the other phases [63]. Hence, curve sketching is used to identify extreme values:



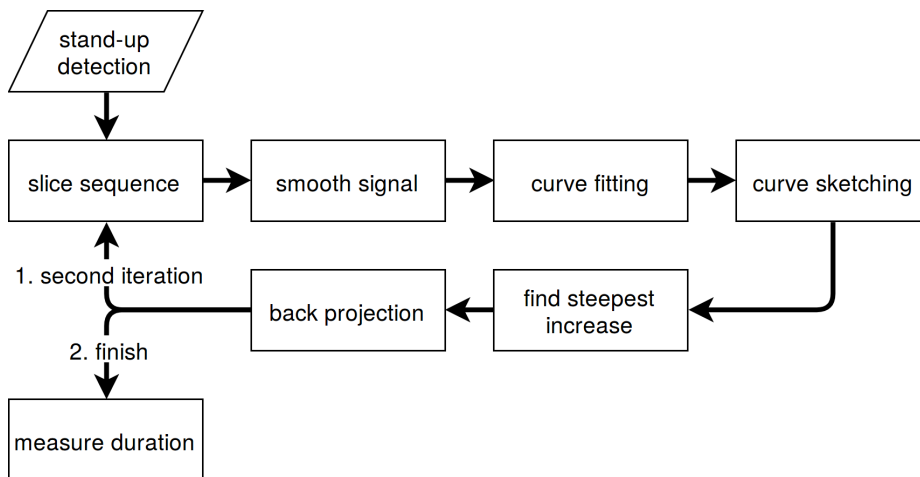


Figure 3.9: Overview of the STS duration measurement steps.

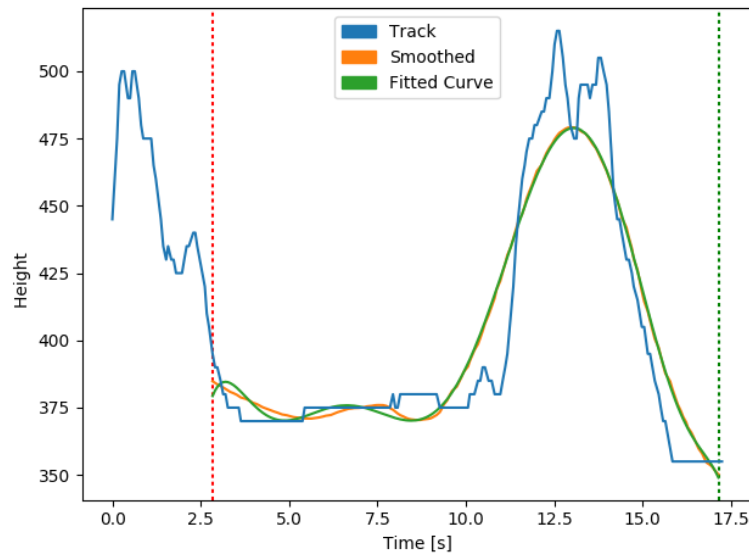


Figure 3.10: The selected track slice is strongly smoothed from start (red line) to end of last feature vector (green line). The smoothed track is polynomial fitted to enable further analysis on the curve.

1. First of all, the three derivatives  $f'$ ,  $f''$ ,  $f'''$  are calculated.
2. To find the steepest increase, a maximum value in  $f'$  has to be found. Hence,  $f''$  is equated to zero to find the roots indicating extrema (maxima or minima). The results are real and complex roots, thus the latter are filtered out.
3. Substituting the result into  $f'''$  shows whether the zero point is a maximum value.

4. From the resulting maxima, the global maximum is chosen, indicating the steepest part of the curve.
5. In the last step borders are set to the curve, thus the previous and following inflection points are selected. These correspond to the previous and next maximum of the global maximum. The result is shown in Figure 3.11.

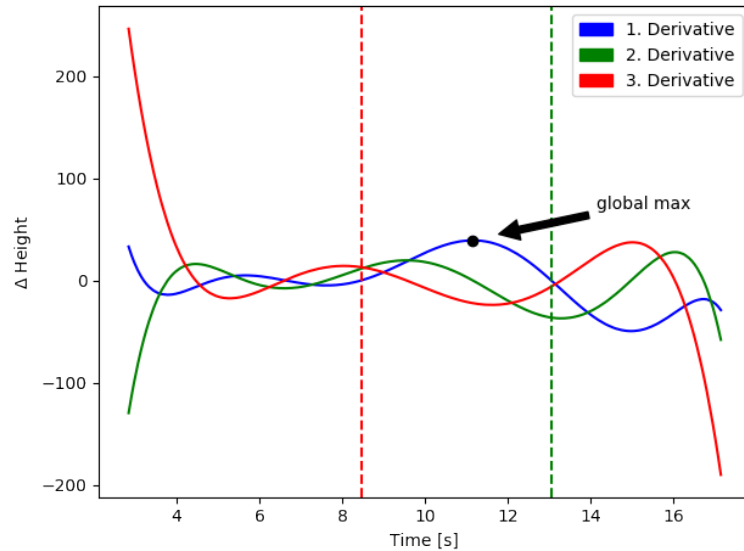


Figure 3.11: First three derivatives with the global maximum of the first derivative indicating the steepest increase. The red and green line mark the previous and next extremum used as borders.

When projecting the resulting time window back to the normal track, it can be seen that it approximates the actual stand-up in a narrow way. Figure 3.12 shows the projection onto the initial track. The window containing the result of curve sketching, approximates the actual stand-up already in a narrow way. However, performing a second iteration of the steps from smoothing to back projection using the narrow window and other parameters shows an even better approximation. This time the filter is applied using a smaller window of

$$\text{window size} = \frac{\text{newly obtained slice width}}{10}$$

and a linear function. Polynomial fitting is conducted using a polynomial of degree 5. The resulting curve fits the original track as can be seen in Figure 3.13, which also shows the resulting time window (i.e. stand-up borders) of the second curve sketching.

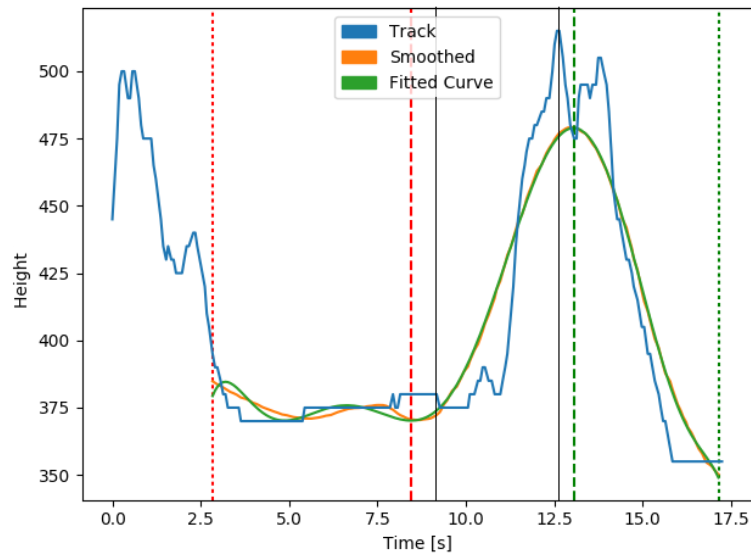


Figure 3.12: The inner dashed red and green line indicate the time window resulting from curve sketching. The black lines show the actual stand-up.

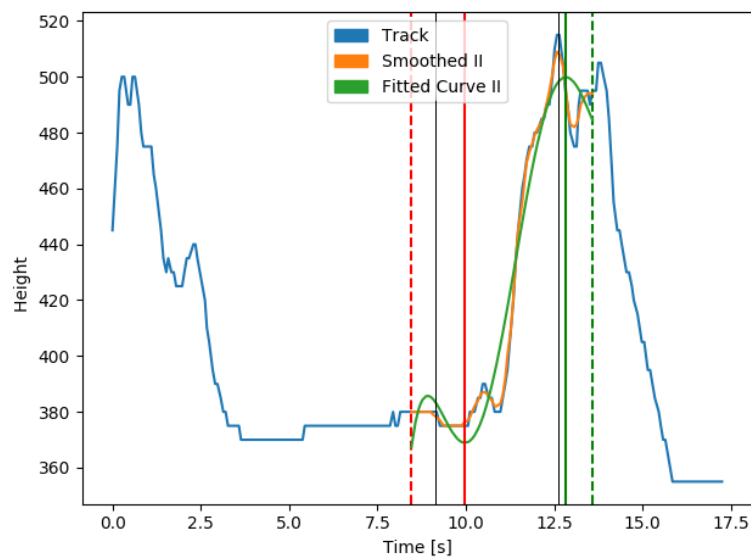


Figure 3.13: The dashed lines show the beginning and ending of the second time window (i.e. result of first iteration). The solid line shows the result of the second iteration (i.e. measured STS transfer). The black lines indicate the actual stand-up.

### 3.5 Implementation

The described algorithms are combined to a holistic system to analyze the tracking data automatically. The extracted mobility parameters are aggregated and provided for further use by e.g. clinicians or relatives. The setup consists of a Single Board Computer (SBC) and a depth sensor attached to it. Figure 3.14 shows examples of the hardware setup.

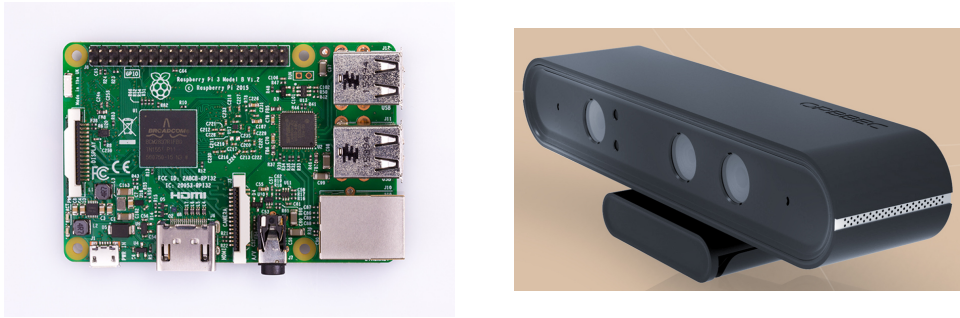


Figure 3.14: Hardware example: Single board computer Raspberry Pi 3 Model B<sup>5</sup> (left) and depth sensor Orbbec Astra<sup>6</sup> right.

For best results of the DPT, the sensor is required to face at least part of the floor. Additionally, to analyze a person's gait, a straight walking path of minimum 2m has to be within the FOV, as well as a sitting area, to measure STS movements. Since there is no distinction between different persons, the system is required to be set up in a one-person household or a single apartment of a nursing resident to work properly and avoid ambiguities between persons' mobility model. There is only one system installed per apartment unit, thus it is important to cover an area, the person spends most of the time (e.g. living room). On the SBC three main modules are deployed: I) Track Storing Module, II) Analysis Module, and III) Interface Module. This modular design allows individual activation of the respective modules, as well as replacement and/or extension of the existing modules and adding new ones. Figure 3.15 shows this modular architecture, consisting of the mentioned modules plus a local database, which holds the tracking information temporarily and the aggregated movement parameters.

The Track Storing Module interacts with the depth sensor and performs person tracking using the DPT. Tracks of moving objects classified as persons are stored to a local database on the SBC for later analysis. This module is kept lightweight, since it should not influence the tracker by reserving an inappropriate amount of resources. The Analysis Module analyzes the tracking information of a certain day to generate diurnal statistics that can be used for further analysis (e.g. progress over several weeks). This

<sup>5</sup>Image from <https://www.raspberrypi.org/products/raspberry-pi-3-model-b> (accessed 03-2018)

<sup>6</sup>Image from <https://orbbec3d.com/product-astra> (accessed 03-2018)

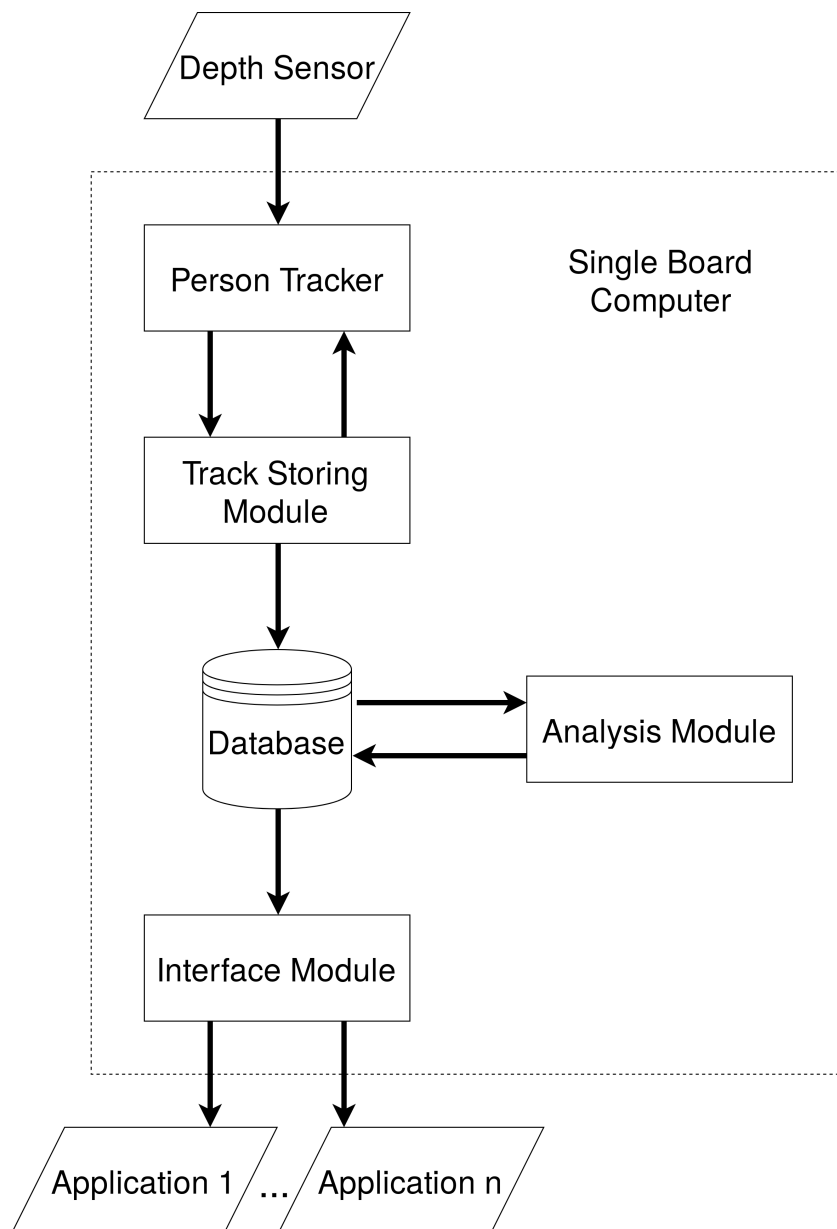


Figure 3.15: Modular Architecture: The depth sensor is connected to the person tracker, and the Storing Module decides which tracks to save. The Analysis Module extracts movement parameters periodically and the obtained results are provided via the Interface Module.

module integrates the analysis algorithms described in the previous sections. All tracks of the day of interest are processed and analyzed for an active person. If the person is active, the respective duration is measured and cumulated. Further, if the active

person is considered walking, all gait statistics are measured and evaluated: temporal gait parameters, distance, and velocity. Additionally, the features for stand-up detection are generated and used for prediction. Detected stand-ups are counted and measured for their respective duration. The obtained measurements are aggregated and composed to a mobility model. This mobility model comprises the average and total values of several measurements. Table 3.1 describes the obtained values of the mobility model. For reliable estimation of habitual movements, Scheers et al. [137] propose a measurement period of at least 3 days.

Table 3.1: Aggregation of measured values to a mobility model

	Value	Unit	Description
<b>Activity</b>	time in room	s	average time a person is active within the FOV
	velocity	m/s	average walking speed
<b>Gait</b>	duration	s	total time the person walked within the FOV
	distance	m	total distance the person walked
	step time	s	average duration of steps
	stride time	s	average time of a gait cycle
	cadence	steps/min	average number of steps
	single support	%	proportion to the total gait cycle of one foot solely being on the ground
	double support	%	proportion of both feet being on the ground
	stance phase	%	proportion of one foot being on the ground
<b>STS movement</b>	quantity	number	total number of stand-ups
	duration	s	average time required to perform STS movement
<b>Hourly data</b>	data aggregated per hour	hour	all values described above are aggregated per hour

The measurements are further aggregated per hour, which allows insights into the day’s progress. An example of hourly aggregated data is shown in Figure 3.16. Since these calculations are computationally intensive, they are not performed online during tracking. They can either be executed offline, after the measuring period has ended on an external (more powerful) device, or when interim computation is inevitable, in a time, where lots of tracks are unlikely (e.g. during night). The Interface Module allows to provide the obtained measurements. For this purpose, a lightweight CherryPy<sup>7</sup> is

<sup>7</sup><http://cherrypy.org> (accessed 03-2018)

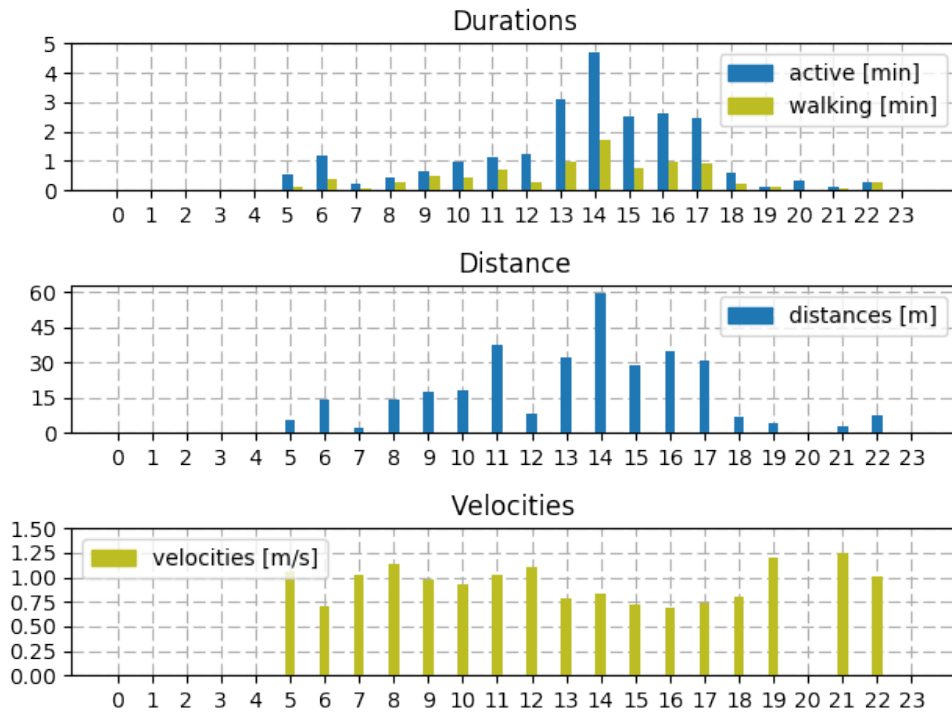


Figure 3.16: Example of diurnal statistics hourly aggregated to examine the progress over the day.

implemented, providing a REST interface via the wireless LAN access point of the SBC. The connection is SSL encrypted and requires the accessing party to authorize with a key. This ensures that only certain persons can access the obtained measurements of the monitored person. The REST interface allows to export the mobility model for a certain day, but also the aggregation of a number of models covering a wider timespan. Hence, also the aggregation time span can be set using the interface.





# Results and Discussion

In this chapter experiments are described to evaluate (i) the scale-space filtering and ML approach for gait event detection and their respective estimation of gait cycle components, (ii) the gait velocity, distance, and duration measurement, (iii) the threshold and ML approaches for stand-up detection, and (iv) the stand-up duration measurement. In order to evaluate the approaches, two datasets of persons performing stand-ups, ADL, and walks is recorded. The datasets are acquired to set up the sensor at the intended height for the DPT and to obtain straight as well as angular walks, and stand-ups combined with ADL. The achieved results are presented and compared to related work, based on the MAE. The application to real world data is tested in an 8-week field trial with 4 older adults. The aggregated measurements are compared to the outcome of physiotherapeutic assessment tests.

## 4.1 Datasets

To train the ML models and test the proposed methods, data is acquired using a depth sensor and a depth image recorder, obtaining 30 frames per second. The STS dataset focuses mainly on STS transitions in combination with ADL, while the 4-Paths dataset focuses on gait from different angles. Both datasets are acquired under laboratory conditions to ensure reproducibility.

### 4.1.1 STS Dataset

This dataset<sup>8</sup> depicts six different persons performing mainly STS transitions in combination with other activities as listed in Table 4.1, and contains 137 sequences in total. Figure 4.1 shows an example sequence of an STS movement, which begins with trunk flexion, continues with knee extension and ends with full trunk extension and an upright

---

<sup>8</sup>Due to confidentiality requirements, this dataset is not publicly available.

position. In order to train and further evaluate ML algorithms, the start and end of the STS movements are manually annotated. This is a challenging task, since the exact frame, where the movement starts/ends, is hard to identify from visualized depth images only. Further, the start is defined as the beginning of the trunk flexion [63], but since the person also moves during sitting and does not sit straight all the time, there occur fluent transitions between movements while sitting and the stand-up. The same problem arises at the end of the movement, which is defined as full trunk extension and standing position [63]: this is only valid, if the person stays still after performing the stand-up; if the person starts to walk, there is either no full trunk extension, due to a forward tilt while walking, or full extension occurs after the first stride phase or after a turn. This phase is either included in the stand-up movement and hence, extends the duration of the stand-up, or it is excluded to fit the STS transitions without walking. In this dataset, the first stride phase of STW movements is excluded and the end of a stand-up is estimated after the trunk is mainly extended before the stride phase begins. The person tracker is applied to the recorded sequences to extract the corresponding movement features, which leads to 151 person tracks. The number of tracks is higher than the amount of sequences, since the tracker drops the track, if the person does not move for a lengthy period of time, and creates a new track, when the person starts moving again.

Table 4.1: Sequences included in the STS dataset

<b>Task</b>	<b>Number of Sequences</b>
Walking & stand-up	52
Stand-up using walking aid	14
Carrying chair & stand-up	29
Walking	23
Walking with walking aid	19

#### 4.1.2 4-Paths Dataset

This dataset consists of persons walking at constant speed on 4 paths that were marked on the floor. The paths are depicted in Figure 4.2. Path I is a straight walking path of 3.7m length and passes the depth sensor perpendicularly. Path II is a 3m straight path and runs frontal towards the depth sensor. Path III is also straight, passes the depth sensor diagonally and measures 3.9m. Path IV runs semicircular to the depth sensor with a perimeter of 5.34m. In order to ensure constant passing velocity, the persons start 1m before and stop 1m after each path to avoid acceleration and deceleration, except from path II due to space reasons. The sensor is mounted at a height of 2.1m. Laser measurement is used to capture the length of each path. 10 persons conduct all 4 walks, 12 were recorded twice, summing up to a total of 52 recorded walks. The test persons performing the walks have no known disabilities influencing their gait. The subjects

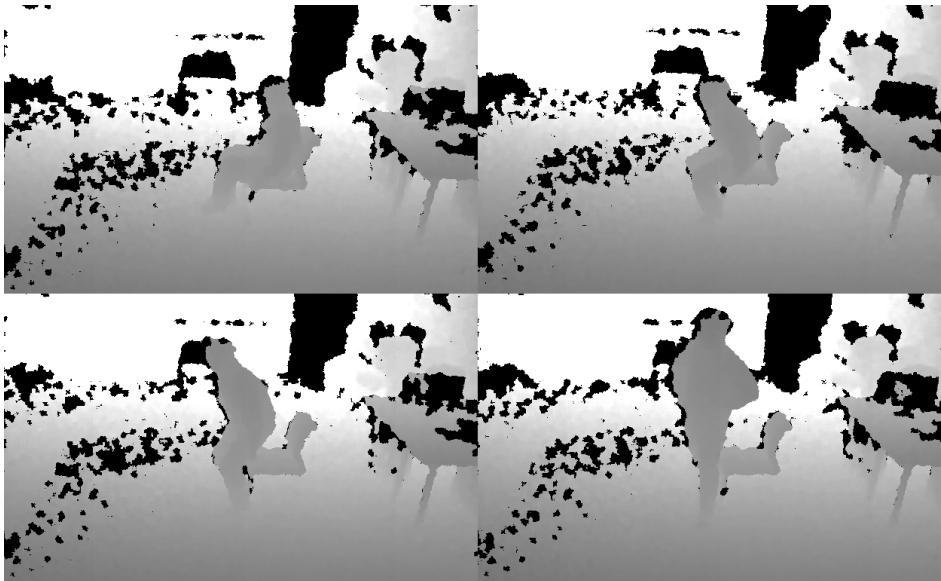


Figure 4.1: Depth sequence showing a sit-to-stand transfer.

consisted of 2 female and 8 male persons with a mean age of  $33.4 \pm 8.4$  years. The DPT is applied to all recordings to obtain motion information. To train the machine learning algorithms and perform automated evaluation all tracks are manually annotated: HS and TO events are marked using the depth sequences. Figure 4.3 shows a sequence of a gait cycle. Additionally, the duration is measured using an SW, which allows for calculation of the respective average gait velocity using the length of each path:

$$\bar{v}_{Manual} = \frac{d_{Laser}}{\Delta t_{SW}},$$

where  $d_{Laser}$  is the path's distance and  $\Delta t_{SW}$  is a person's walking duration measured by SW.

## 4.2 Gait Velocity, Distance, and Duration Evaluation

The 4-Paths dataset is also used for evaluation of the velocity, distance, and duration measurement. The resulting average walking velocities are compared to the SW measured values and the respective deviation is calculated. The Pearson's correlation coefficient is 0.93, which shows a strong correlation between the manually annotated and predicted values. The results can be seen in Table 4.2 for each of the 4 paths separately. As can be seen, the difference of the averages amount to 2.19-5.58cm/s. Especially path IV shows that the velocity estimation is robust to angular change while walking. Varsanik et al. [138] describe a similar approach to measure gait velocity using a passive gait non-wearable indoor system, utilizing a Kinect. They report a difference between human measurement using SW and the automated approach of 9.7cm/s. Hence, the approach

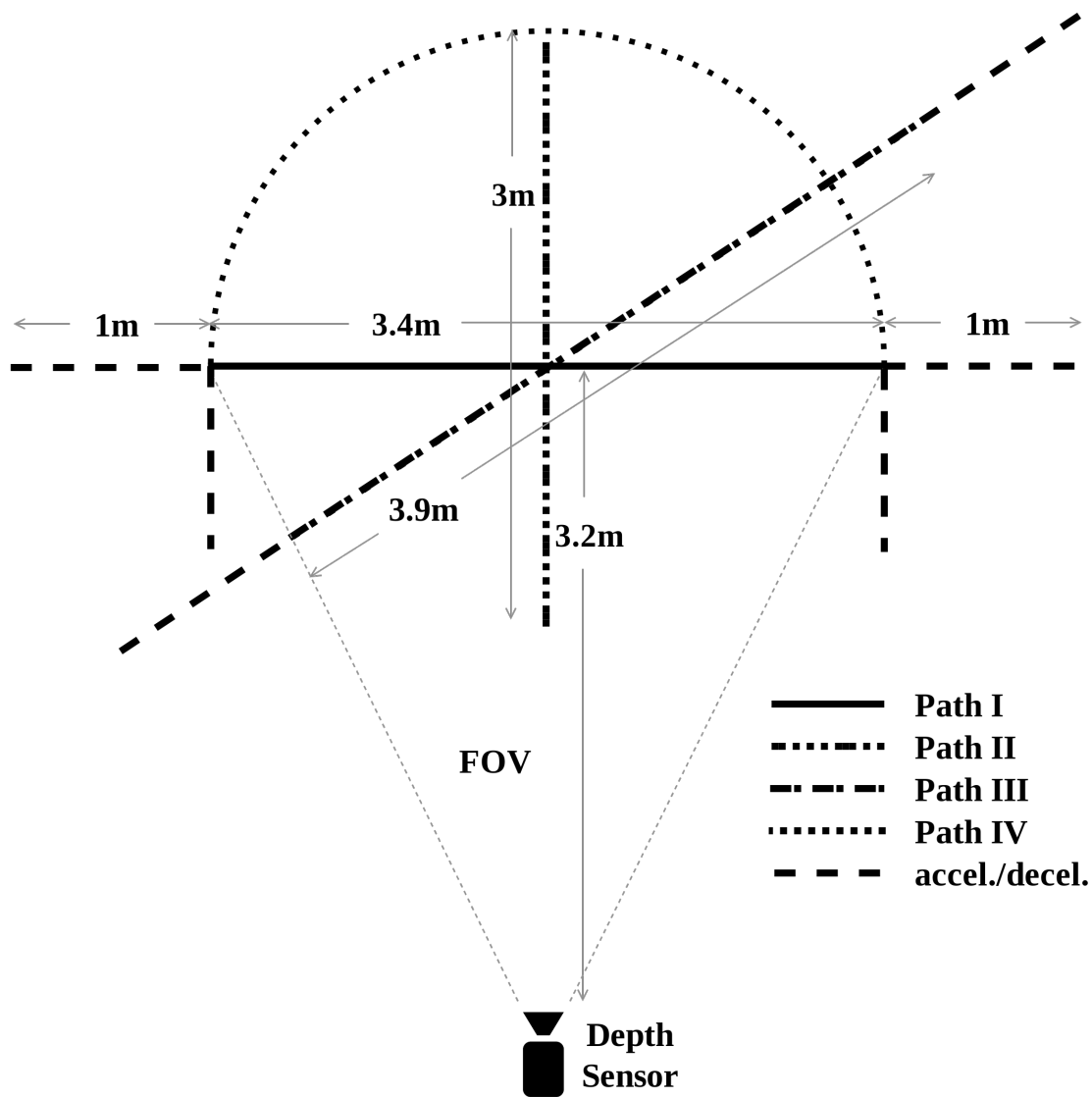


Figure 4.2: Diagram of acquisition setup for the 4-Paths dataset: The FOV covers the measurement area including the walking paths. The dashed lines show the acceleration and deceleration segment.

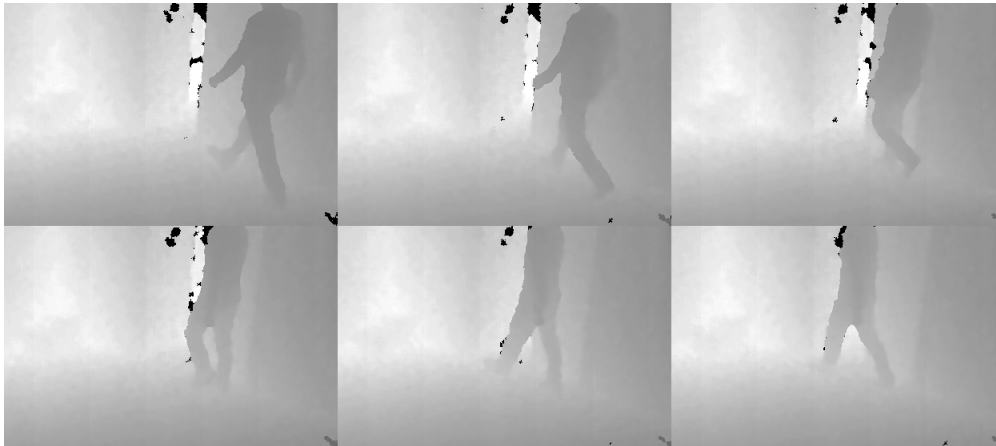


Figure 4.3: Depth sequence of 4-Paths dataset showing part of a gait cycle.

described is comparable with state-of-the-art methods. It has to be noted, that SW measurements of human timers show statistical significant variations [138]. Additionally, the distance captured using the tracker is compared to the distance measured using laser measurement. The result is shown in Table 4.2 for each walk. It can be seen, that the angle of the depth sensor to the walking path has no significant influence. Further, direction changes during walking (path IV) show no effect on the accuracy, having a smaller deviation than the other (straight) paths. Table 4.2 shows further the deviations of the duration measurement. Figure 4.4 depicts the deviations for each walk. Doppelbauer [118] achieves a MAE of 0.9cm/s-2.81cm/s using depth data, and 1.52cm/s-3.47cm/s using skeleton data evaluating his gait speed measurement. Hence, the results of Doppelbauer [118] are comparable to those achieved by the proposed measurement method.

Table 4.2: Comparison of MAE of Velocity, Distance, and Duration Measurement

<b>Path</b>	<b>Velocity Error [cm/s]</b>	<b>Distance Error [cm]</b>	<b>Duration Error [s]</b>
Path I (Straight Orthogonal)	2.19	31.35	0.38
Path II (Straight Frontal)	3.04	25.93	0.41
Path III (Straight Diagonal)	5.58	15.74	0.01
Path IV (Semi Circular)	3.76	8.88	0.28
<b>Mean Error</b>	3.64	20.48	0.27

#### 4. RESULTS AND DISCUSSION

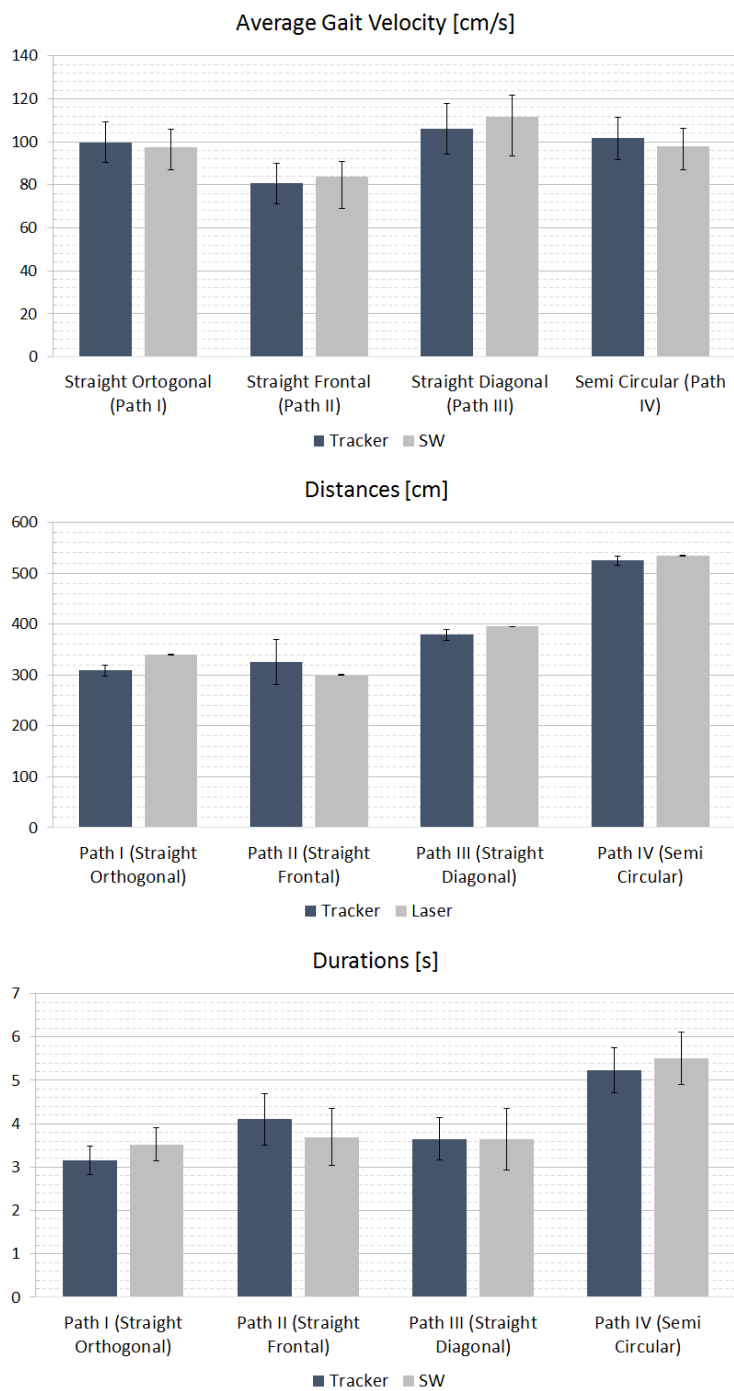


Figure 4.4: Calculated average velocities (top), distances (middle), and durations (bottom) compared to manual measurements.

### 4.3 Gait Event Evaluation

For evaluation of the gait event identification algorithms, the 4-Paths dataset is used. The subset applied for testing of the machine learning algorithm is also used to evaluate the scale-space filtering approach for better comparison.

#### 4.3.1 Scale-Space Filtering Evaluation

The gait event demarcation algorithm of González et al. [132] is applied to 10 tracks of the 4-Paths dataset, but using the signal data from the DPT as input. The algorithm detects on average 2 TO and HS events less than annotated. This effect might occur due the manual annotation of gait events, where the person is partly occluded and thus the person track starts later or stops earlier not including the corresponding event. The MAE of predicted events to the nearest manually annotated event is  $0.16s \pm 0.08s$  for HS and  $0.13s \pm 0.09s$  for TO events. The accuracies of gait parameters deduced from these gait events are outlined in Table 4.3.

Table 4.3: Temporal Gait Parameters Obtained Using Scale-Space Approach

Gait Parameter	Annotated Value	Predicted Value	MAE
Step Time [s]	$0.61 \pm 0.03$	$0.41 \pm 0.23$	0.26
Stride Time [s]	$1.21 \pm 0.06$	$0.76 \pm 0.45$	0.55
Cadence [#steps/min]	$113.49 \pm 7.87$	$215.94 \pm 101.47$	108.74
Single Support [%]	$32.64 \pm 1.78$	$21.32 \pm 16.10$	15.83
Double Support [%]	$17.83 \pm 1.91$	$29.82 \pm 21.14$	17.41
Stance Phase [%]	$50.62 \pm 0.73$	$51.96 \pm 10.38$	6.97

#### 4.3.2 Machine Learning Approach

In order to train the RF, the annotated tracks of the 4-Paths dataset are randomly partitioned into a train and test set at a ratio of 80% to 20%. The partitioning into independent training and test sets allows for generalization and avoids that the classifier knows every feature vector (overfitting). 20% of the training set are further used as validation set to optimize the predictions of the ML algorithm. The test set contains 10 tracks, which corresponds to 1,252 feature vectors and is the same test set applied for testing the scale-space filtering. The evaluation on the test set achieves an accuracy of 66.22% of correct predicted vectors. For further evaluation the manually labeled position of events (HS and TO) within a track is compared to the predicted position, which results in a deviation of  $0.16s \pm 0.20s$  for HS events and  $0.16s \pm 0.17s$  for TO events. However, not all events are detected, which leads to an irregular gait sequence that requires further optimization. After application of the optimization algorithm described in Section 3.2.2,

following results are achieved: the average quantity of predicted HS occurrences per track is  $-0.3 \pm 1.3$  compared to the annotated events, the average quantity of TO occurrences is  $-0.3 \pm 1.1$ . The deviation of the resulting regular gait sequences is  $0.18s \pm 0.19s$  for HS and  $0.18s \pm 0.18s$  for TO events. The obtained gait events are used to derive additional temporal gait parameters. Table 4.4 presents the achieved accuracies of the determined temporal gait parameters. Although the deviation of predicted to labeled gait events is comparable (HS:  $0.16s$  and  $0.18s$ , TO:  $0.13s$  and  $0.18s$ ), the results show clearly, that the ML approach performs better on estimation of the temporal gait parameters than the scale-space filtering approach.

Table 4.4: Temporal Gait Parameters Obtained Using Machine Learning Approach

<b>Gait Parameter</b>	<b>Annotated Value</b>	<b>Predicted Value</b>	<b>MAE</b>	<b>Difference Healthy/Pre-Frail [132]</b>
Step Time [s]	$0.61 \pm 0.03$	$0.55 \pm 0.03$	0.06	0.08
Stride Time [s]	$1.21 \pm 0.06$	$1.11 \pm 0.05$	0.10	0.11
Cadence [#steps/min]	$113.49 \pm 7.87$	$122.91 \pm 7.02$	9.42	7.09
Single Support [%]	$32.64 \pm 1.78$	$37.22 \pm 4.42$	4.58	2.8
Double Support [%]	$17.83 \pm 1.91$	$12.72 \pm 4.46$	5.11	2.77
Stance Phase [%]	$50.62 \pm 0.73$	$49.93 \pm 0.14$	0.69	2.98

González et al. [139] describe an approach using lower extremity tracking with the Kinect to measure gait parameters and compare the results to sensitive floor analysis. They achieve a MAE of  $0.22s \pm 0.20s$  for step time and  $0.27s \pm 0.28s$  for stride time. Hence, the deviation of  $0.06s$  and  $0.10s$  respectively of the presented solution achieves better results. In [132], González et al. evaluate their method by comparing temporal gait parameters of a young adult group to those of a pre-frail group and capture mean differences between these groups as shown in Table 4.4. Although the differences of single and double support are smaller than the errors of the proposed method, the other parameters' errors show that a distinction can be possible. Especially a distinction between healthy adults and frail adults, which is shown to significantly correlate with gait parameters [19], should be possible, but requires further evaluation. González et al. [132] achieve more precise distinction due to the higher sampling rate (70Hz). Further, in the DPT a Kalman filter [140] is applied, which smoothes the signal and hence removes acceleration peaks important for gait analysis. Doppelbauer [118], who describes an approach to estimate gait parameters using a Kinect, achieves MAE for step and stride times of  $0.04s$ - $0.28s$  and  $0.05s$ - $0.33s$  respectively using depth data, as well as  $0.08s$ - $0.21s$



and 0.08s-0.25s using skeleton data. Hence the proposed approach based on the data of the COM (0.06s and 0.1s) achieves comparable results.

## 4.4 Stand-Up Detection Evaluation

For evaluation of the stand-up recognition and measurement the STS dataset is used to train the SVM and RF. The dataset is split into multiple training and test sets in order to evaluate the different ML approaches. The feature vectors containing both start and end of the STS phase consists of 360 features respectively (3 features \* 8 seconds \* 15 frames per second). The dataset is split into 18,534 training vectors equally partitioned into two classes: no stand-up and stand-up contained. The according test set includes 4,660 vectors. The vectors containing the STS start sequence only, or the end sequence only are shorter with a length of 90 (3 features \* 2 seconds \* 15 frames per second). The vectors of these sequences sum up to 1,904 each, partitioned into both classes: sequence contained (start/end) and no sequence contained. Figure 4.5 shows the Receiver Operating Characteristic (ROC) curve for each of the trained ML algorithm. The ROC curve shows the relation of the true positive to the false positive rate, the diagonal line indicates equal amount of false positives and true positives. Hence, best results are located in the top left corner. This shows, that the SVM classifier in general achieves worse results compared to the RF. The best result is obtained by the RF containing the whole STS sequence. The result indicates a perfect work efficiency of this classifier, however this is achieved having no person occlusions in the scenes of the dataset and the characteristics of the seating facility (height, softness, armrest, etc.) remain the same. In practice, this is not always possible, since the installation environment varies from apartment to apartment.

The result is compared to the outcome of the threshold approach, which is applied to 3,002 vectors of the dataset, equally partitioned into both classes. The threshold approach is applied with 2.5s suppression time and 50% of the maximum COM as obtained by the grid search optimization. Due to the application of a sliding window, the threshold approach has to be applied to a full track, whereas the ML algorithms can be applied to extracted, shuffled feature vectors. Thus, the Confusion Matrix (CM) of the threshold approach and the RF trained with the whole STS sequence are compared in Figure 4.6. The CM contrasts the predictions of an algorithm to the true values, in this case: stand-up and no stand-up. The CM shows, that both approaches have the potential to detect stand-ups, but the ML method has a better true positive and true negative rate and is hence superior to the threshold approach. Banerjee et al. [141] describe an approach to detect stand-ups using fuzzy clustering of video data. Compared to a marker-based system, their method achieves 94.6% accuracy. This is comparable to the proposed method achieving 99.6% on the STS dataset. Although the dataset contains unconstrained stand-ups, a performance in practice does not achieve these results, due to occlusions and varying environments and sensor positions.

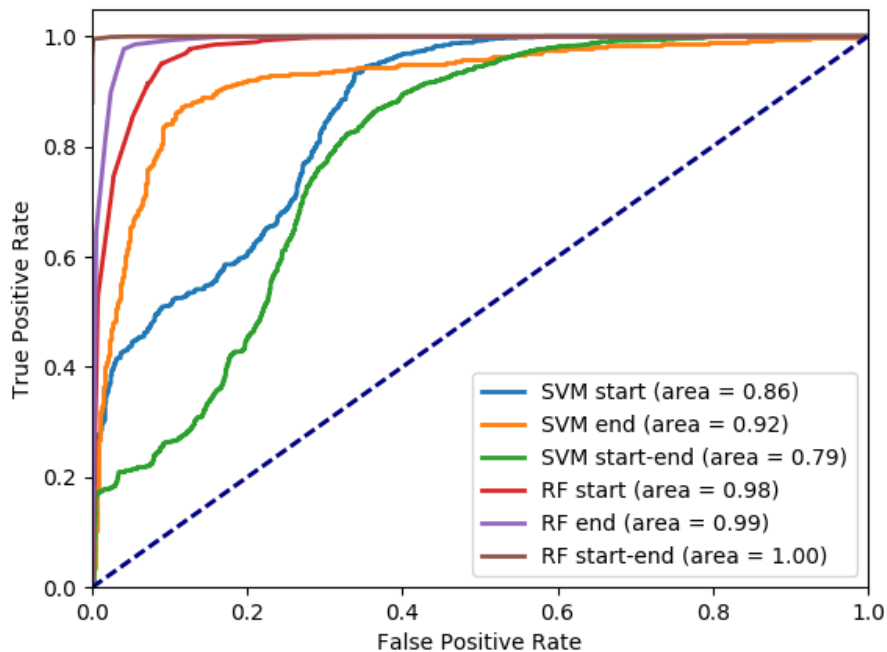


Figure 4.5: ROC curve of all machine learning algorithms.

## 4.5 Stand-Up Measurement Evaluation

Since the stand-up measurement represents a different problem from stand-up detection, all tracks of the STS dataset containing stand-ups can be used for evaluation, without splitting into training and test set. In total, the amount of annotated stand-up sequences used is 95. To obtain the accuracy of the measurement method, the predicted STS duration is compared to the duration resulting from the annotated start and end points. The MAE is  $0.57s \pm 0.33s$ , the distribution is depicted in Figure 4.7. In this Figure the result is compared to the error rates obtained by Ejupi et al. [116] and Banerjee et al. [133]. Ejupi et al. [116] compare their Kinect STS measurement approach to SW measurement. They use a standardized setup for capturing the STS transitions of fallers and non-fallers conducting the 5tSTS test, thus the obtained durations are divided by 5 to receive values comparable to the described method. The approach of Banerjee et al. [133] measuring STS transfers using voxel height and ellipse fitting achieves average errors of 0.45-0.75s compared to SW measurement depending on the camera angle. The described method performs 0.07-0.13s worse than the method of Ejupi et al. [116], but 0.07-0.38s better than the method of Banerjee et al. [133]. This is an acceptable result, considering the fact, that the sequences in the STS dataset are less constrained than the sequences of Ejupi et al. [116], since it captures stand-up movements in combination with other activities and the orientation of the test persons to the depth sensor varies.

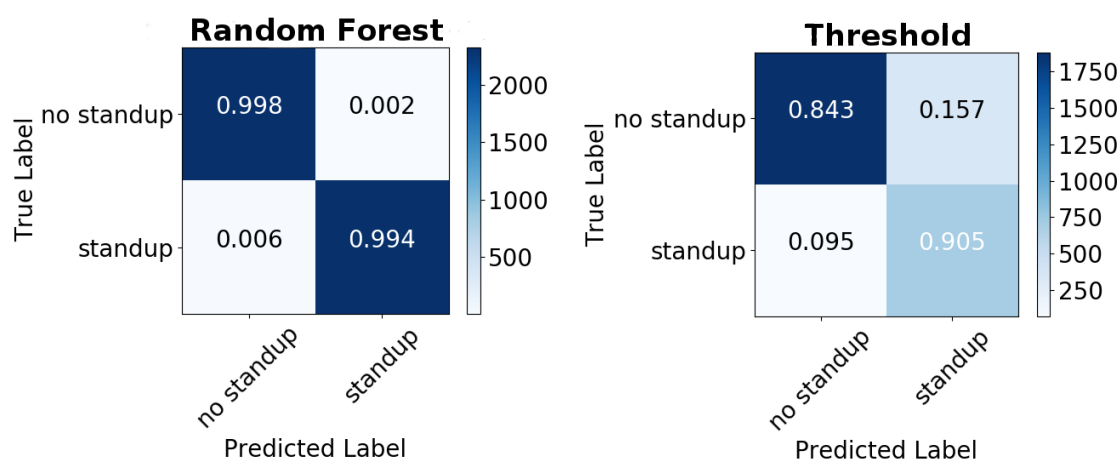


Figure 4.6: Comparison of the CM of RF (left) and threshold approach (right): RF shows a higher true positive and true negative rate.

## 4.6 Field Test

In order to test the described methods in practice, a field trial has been conducted as part of an ongoing Ambient Assisted Living Joint Programme<sup>9</sup> project. In this evaluation phase, 4 systems have been installed, each in the living room of an elderly person. The persons, two female and two male test users, live alone and have no diagnosed cognitive decline. They do not use assistive walking devices within their apartments and their age ranges from 77 to 88 years. During the test period of 8 weeks, a physiotherapist visited them to conduct physical assessments at the beginning (week 0), in the middle of the test phase (week 4), and after the trial phase (week 8). The conducted tests include a variation of the six-metre-walk test [51] using 3 meters, and a variation of the STS test [55] with 3 consecutive stand-ups. Due to a technical problem impeding regular reboot of the system, there was a data loss, which led to following amount of captured days: user 1 - 26 days, user 2 - 37 days, user 3 - 15 days, user 4 - 43 days.

The results of this test phase averaged over the total testing time, presented in Table 4.5, show slower gait velocity and longer stand-up durations when the persons are alone in their homes in comparison to the measurements of the physiotherapist. Hence, the unsupervised in-home movement is slower than the movement in supervised tests. This reflects the users' behavior change due to the test situation created during physical assessments, although conducted in the homes of the persons [21, 23], and corresponds further to the difference between IGS and HGS as described by Stone and Skubic [24]: The correlation of the average gait speed at home to the TUGT is higher in comparison to measured gait velocity on a predefined path at home. In Figure 4.8, which depicts these results, it can be seen, that the standard deviation between the physiotherapist's tests are larger than those obtained by the system. This signifies either measurement errors or

<sup>9</sup><http://www.aal-europe.eu> (accessed 03-2018)

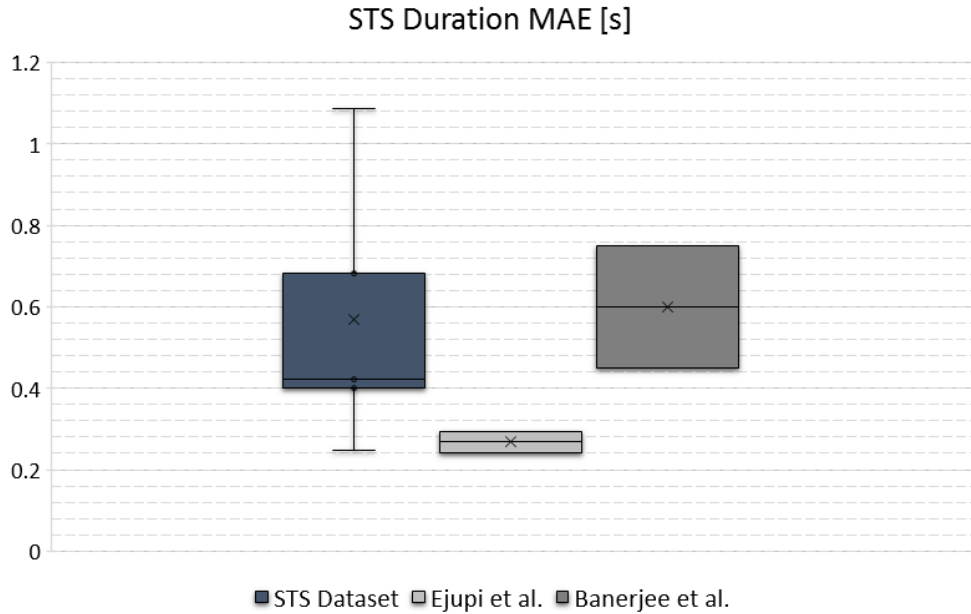


Figure 4.7: MAE of predicted to manually annotated STS durations. Left: error range on STS dataset, center: error range measuring non-fallers and fallers by Ejupi et al. [116], right: range of error depending on camera angle evaluated by Banerjee et al. [133].

Table 4.5: Comparison of System Measurement to Physiotherapist’s Measurement

	User	System	Physiotherapist	MAE
<b>Gait Velocity [m/s]</b>	User 1	0.40±0.04	0.45±0.05	0.05
	User 2	0.51±0.06	0.84±0.02	0.33
	User 3	0.37±0.02	0.82±0.15	0.45
	User 4	0.54±0.05	0.96±0.11	0.42
<b>STS Duration [s]</b>	User 1	2.55±0.27	2.41±0.40	0.14
	User 2	2.45±0.27	1.78±0.14	0.67
	User 3	2.31±0.27	1.27±0.76	1.04
	User 4	2.43±0.27	1.45±0.81	0.98

high variations in user performance. The physiotherapist conducting the tests reported, that especially user 3 and 4 misunderstood the instructions in the second and third assessment: instead of performing the tests at habitual speed, they tried to perform best. This behavior change while being actively tested is a known problem in research, called attention bias [142]. Attention bias is a subtype of measurement bias and occurs, when persons are aware that they are being tested, leading to increased performance [21, 142]. This explains the high variance in the physiotherapist’s measurement results of these

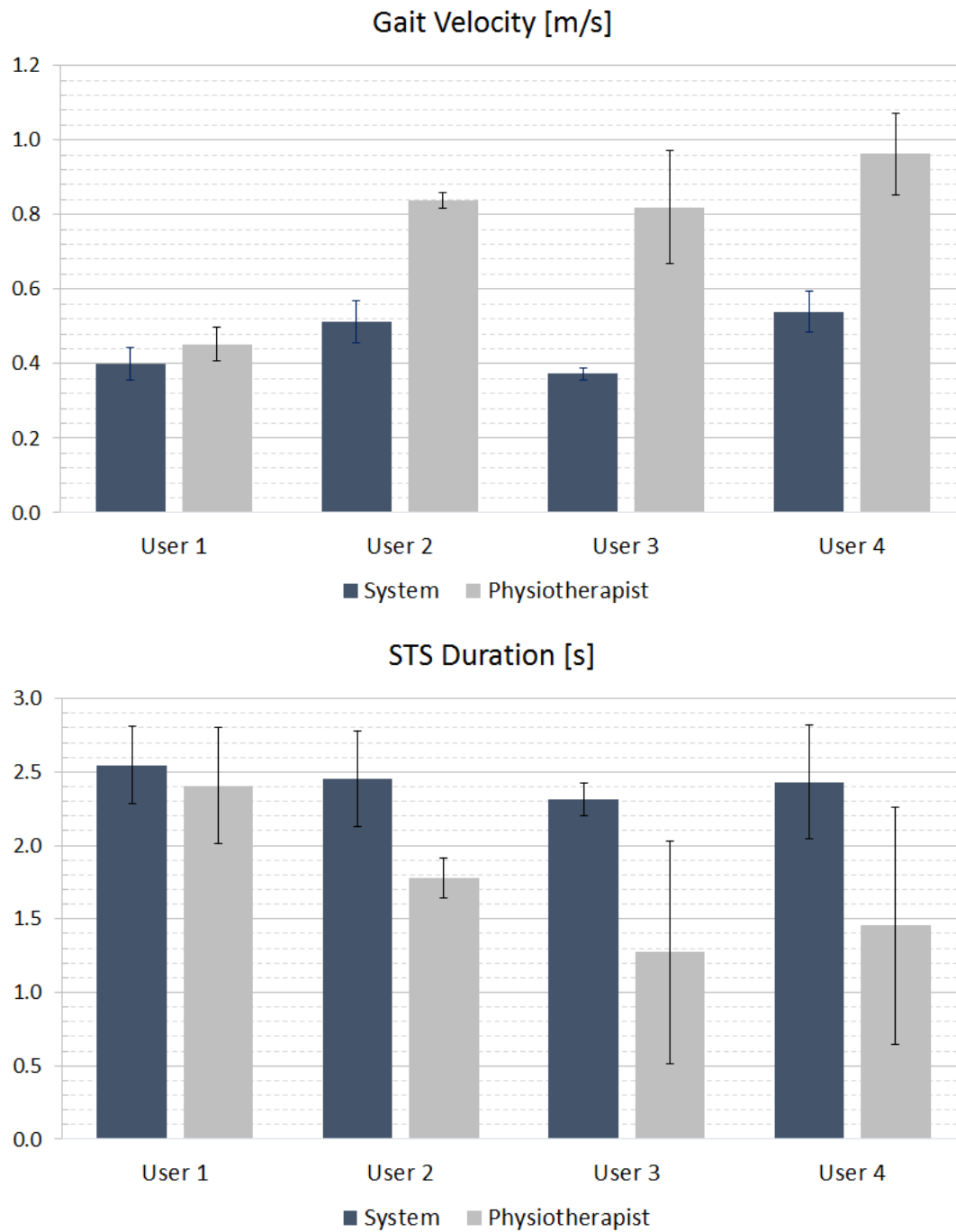


Figure 4.8: Gait velocity and STS duration results of field test: Habitual movement is slower, than the values measured by the clinician.

users and shows the influence of human elements, such as wording and understanding of instructions.

The gait velocities are further averaged over 6 days in the temporal proximity of the corresponding assessment test: for the first test, 6 days after the assessment are aggregated; for the second test, 3 days before and 3 days after the test are combined; for the last test, 6 days before the assessment are aggregated. The result is shown per user in Figure 4.9. While the assessment tests constitute snapshots in the physiological level of the test persons, the averaged values represent an aggregated time span. Hence, the behavior change is also apparent in Figure 4.9: while the physiotherapist's velocity measurement of user 1 and 2 show only minor changes between the first and the other two assessments (min: 0.01m/s, max: 0.09m/s), user 3 and 4 show an increase between 0.05m/s and 0.27m/s. Based on the cut-off value described by Stone and Skubic [24] of 0.5m/s, user 1 and user 3 are prone to falling. However, the physiotherapist assessed an increased fall risk only for user 1. The low IGS of user 3 is explainable by the installation environment: in the apartment of this user, there is a lot of furniture the user has to avoid while walking, leading to decreased gait velocity, while for the physiotherapeutical gait test, the furniture was re-arranged to enable the 3m walking test. This points to a problem when installing in unconstrained environments, like apartments of users. This is also reported by Stone and Skubic [119], who state that the furniture inside the apartment as well as the position of sensor within the apartment influences the captured movements and hence the analysis results.

The average STS duration is aggregated in the same way as the gait velocity around the three assessment tests and shown in Figure 4.10. It can be seen, that the performance of user 1 is comparable to the physiotherapeutical test, while the others perform better, when tested by the physiotherapist. The physiotherapist reported, that the user tried to perform better, but due to the physical condition, was not able. Further, there are high standard deviations visible in the diagram, indicating that the persons' stand-up behavior varied. On the one hand, this occurs "normal" stand-ups compared to external influences (e.g. door bell rings). On the other hand, the characteristics of the seating facility, such as arm rests, softness, height, influence the STS movement performance [65]. Further, the behavior change is again visible: the differences between the first and the other tests results in 0.08s-0.75s for user 1 and 2, while the difference of user 3 and 4 results in 1.04-1.50s.

The results show, that the proposed approaches are able to measure gait cycle components more accurate than using vision-based lower extremity tracking and are comparable to the results achieved with wearable accelerometers. The measurement of the STS transition durations is comparable to vision-based state-of-the-art approaches. The evaluation in practice shows higher accuracy for gait velocity than stand-up duration estimation, and that the installation environment affects the results. This suggests, that the progress of a person's mobility parameters over time is preferable to the use of snapshots for the assessment of the health level.

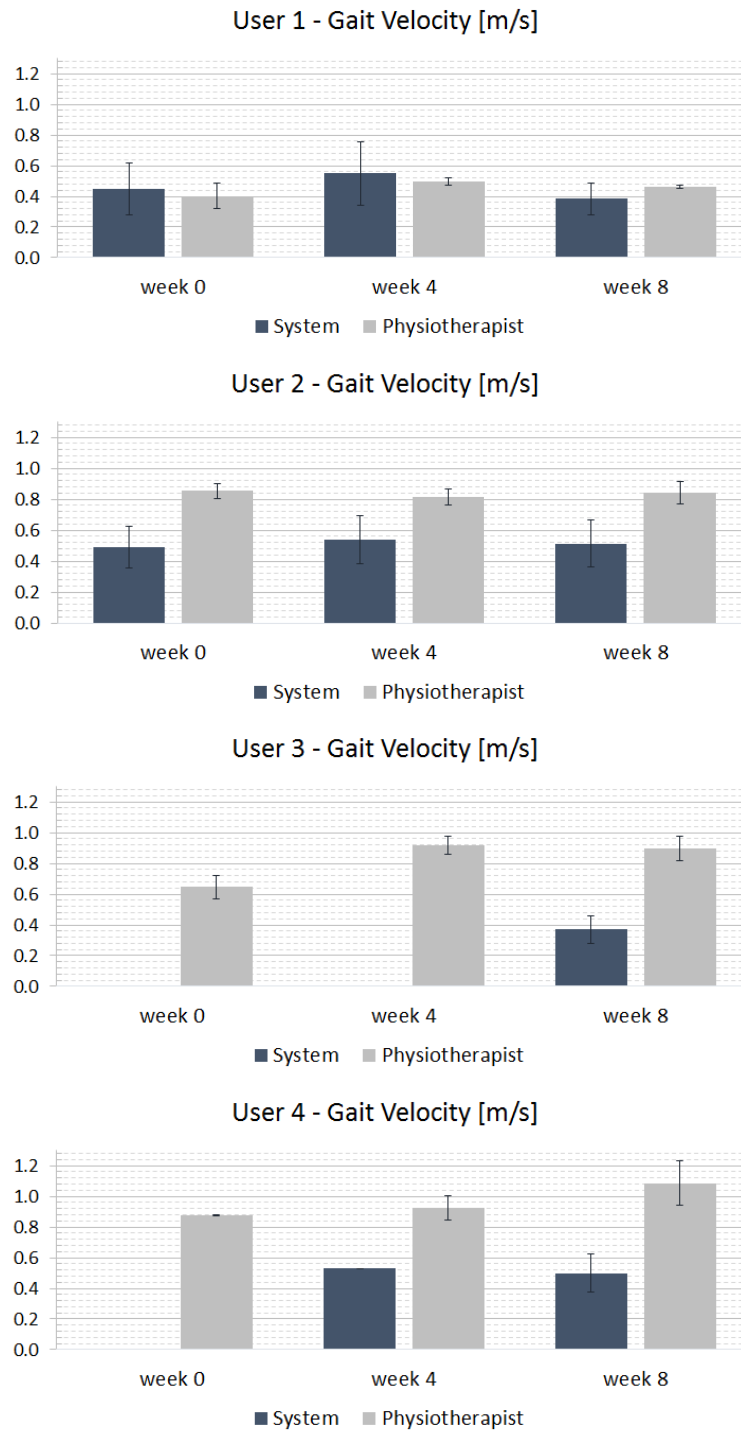


Figure 4.9: Comparison of average gait velocity per user measured by physiotherapist compared to aggregated system measurements (higher is better). The missing bars are due to the occurred loss of data during the test.

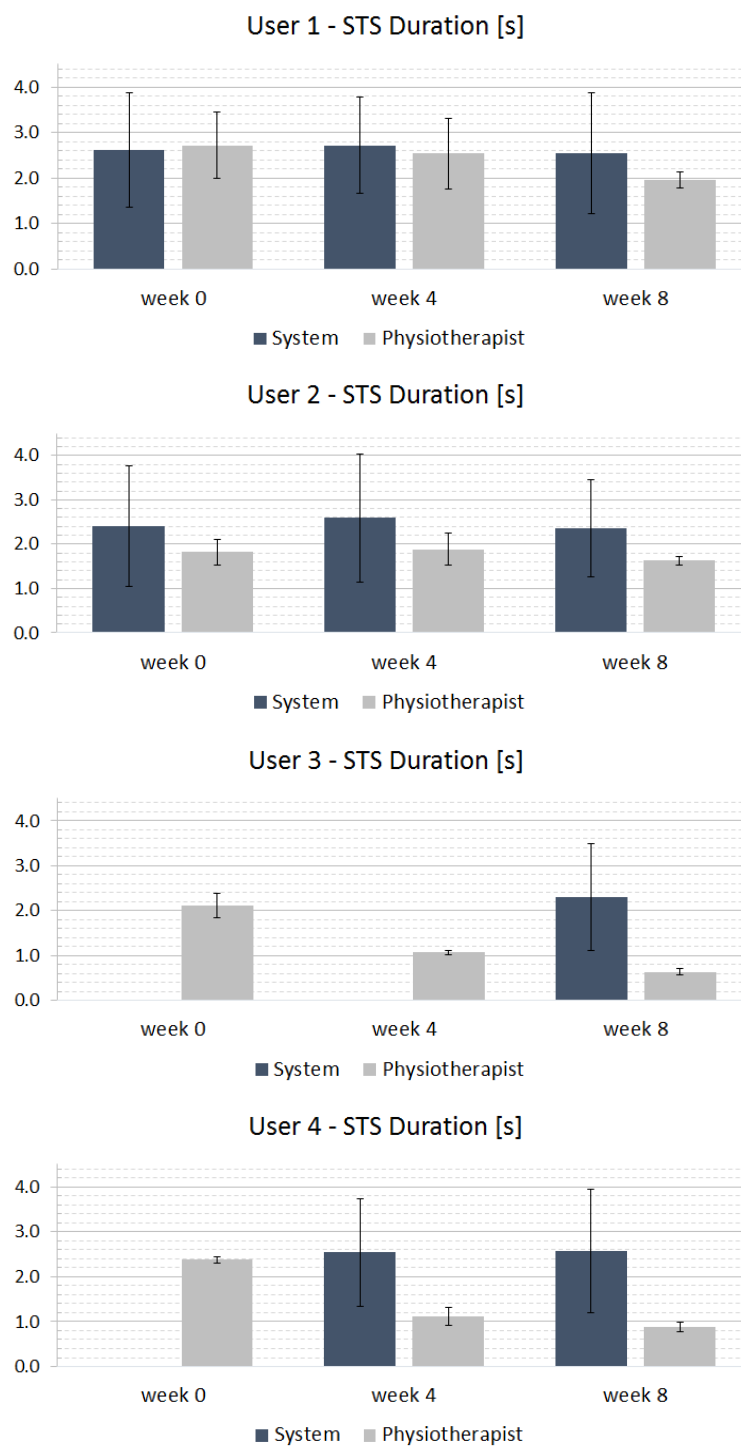


Figure 4.10: Comparison of average STS duration per user measured by physiotherapist compared to aggregated system measurements (lower is better).



## Conclusion & Future Work

In this work, persons' fitness level was measured by analyzing gait and STS performance. The analysis was based on a non-intrusive tracking method, that allows plug-and-play for installation in the homes of older adults and enables further the acquisition of habitual in-home movement.

Two depth-datasets were acquired for training of the ML algorithm, and evaluation of the described approaches. The STS dataset comprises 137 sequences of persons performing STS transitions combined with ADL. The starts and endings of STS transition phases were manually annotated. The 4-Paths dataset includes walks of 10 healthy adults, walking on 4 predefined paths: orthogonal, diagonal, frontal, and semi-circular. All gait events (HS, TO) were manually labeled.

The first approach focused on gait analysis and extracted following parameters: gait velocity, distance, and duration. Especially, gait velocity shows robust estimation, independent of the person's orientation in respect to the 3D sensor. Additionally, a scale-space filtering and a ML approach for gait event detection were compared, and the gait events further used for estimation of gait cycle components. The results show, that the ML approach in combination with an optimization algorithm performs better when comparing the gait cycle components. The estimation of the gait cycle parts is comparable to the estimation using a wearable accelerometer.

The second approach compared a thresholding to ML approaches for STS movement detection and proposes a curve-fitting approach for measurement of the duration. The evaluation shows best results using an RF for detection of stand-ups. The duration measurement is comparable to state-of-the-art methods.

A holistic system including the described algorithms was presented and evaluated in an 8-week field trial with 4 older adults. Compared to assessment tests conducted by a physiotherapist, the test showed slower in-home movements, indicating that persons change their behavior in the assessments due to the created test situation. Additionally,

the trial revealed, that human factors, e.g. wording during test explanations, and the test environment, such as furniture in the apartment, influence the results.

To sum up, mobility parameter estimation using solely the COM of person tracks is possible and achieves robust results regarding the orientation of the person to the 3D sensor. In order to allow more accurate estimation of gait cycle parts, future work will focus on the integration of the DPT without the application of the Kalman filter [140]. In addition, access to the captured point cloud of a person allows the implementation of algorithms able to distinguish between persons as suggested by Stone and Skubic [119]. This allows application of the system in multi-user environments, such as multi-person households or senior residents.

# List of Figures

1.1	The United Nations prospects of world population . . . . .	2
1.2	Scene visualization of depth information as gray values . . . . .	3
2.1	Vulnerability of elderly people to minor health problems . . . . .	6
2.2	Predictors for adverse health outcomes: frailty syndrome, disability, co-morbidity . . . . .	7
2.3	Life expectancy in relation to age and gait speed . . . . .	9
2.4	The gait cycle consists of two main phases: stance phase and swing phase	13
2.5	Phases of the STS transition . . . . .	14
2.6	Example for wearable sensors placed on various body parts . . . . .	17
2.7	Examples for non-wearable sensors . . . . .	21
2.8	Mapping of TUG time to IGS . . . . .	24
2.9	Operating principles of SL and TOF depth sensor . . . . .	27
2.10	Conversion from depth map to plan-view . . . . .	28
3.1	Overview of the proposed approaches . . . . .	32
3.2	Orientation of the coordinate system after projection to plan view . . . . .	33
3.3	Illustration of walking path its enclosed angle . . . . .	34
3.4	Comparison of the signal origins . . . . .	35
3.5	Vertical acceleration $\ddot{y}$ and the smoothed signals $\hat{y}_{\sigma=50}$ , $\hat{y}_{\sigma=100}$ . . . . .	36
3.6	Annotated and predicted HS and TO events . . . . .	37
3.7	Height track with minimum and maximum of the detected stand-up using the threshold approach . . . . .	39
3.8	Track containing all detected stand-ups . . . . .	40
3.9	Overview of the STS duration measurement steps . . . . .	41
3.10	Smoothing of track slice . . . . .	41
3.11	Curve sketching . . . . .	42
3.12	Back-projection after curve sketching . . . . .	43
3.13	Stand-up in the original track . . . . .	43
3.14	Hardware example . . . . .	44
3.15	Modular Architecture . . . . .	45
3.16	Example of diurnal statistics hourly aggregated . . . . .	47
4.1	Depth sequence showing a sit-to-stand transfer . . . . .	51
		67

4.2	Diagram of acquisition setup for the 4-Paths dataset . . . . .	52
4.3	Depth sequence of 4-Paths dataset showing part of a gait cycle . . . . .	53
4.4	Calculated average velocities, distances, and durations . . . . .	54
4.5	ROC curve of all machine learning algorithms . . . . .	58
4.6	Comparison of Random Forest and Threshold Approach . . . . .	59
4.7	MAE of predicted to manually annotated STS durations . . . . .	60
4.8	Gait velocity and STS duration results of field test . . . . .	61
4.9	Comparison of average gait velocity per user . . . . .	63
4.10	Comparison of average STS duration per user . . . . .	64

# List of Tables

2.1	Characteristics of the Frailty Index and the Frailty Phenotype . . . . .	8
2.2	Examples of mobility assessment tests . . . . .	10
2.3	Examples of fall risk assessment tests . . . . .	15
2.4	Wearable Assessments . . . . .	20
2.5	Wearable Assessments . . . . .	25
3.1	Aggregation of measured values to a mobility model . . . . .	46
4.1	Sequences included in the STS dataset . . . . .	50
4.2	Comparison of MAE of Velocity, Distance, and Duration Measurement . .	53
4.3	Temporal Gait Parameters Obtained Using Scale-Space Approach . . . .	55
4.4	Temporal Gait Parameters Obtained Using Machine Learning Approach .	56
4.5	Comparison of System Measurement to Physiotherapist's Measurement .	60



# Acronyms

**5tSTS** 5 times Sit-To-Stand test. 10, 11, 16–18, 20, 21, 24, 25, 58

**ADL** Activities of Daily Living. 5, 6, 8–10, 49, 65

**AIGS** Average In-home Gait Speed. 23–25

**CM** Confusion Matrix. 57, 59

**COM** Center Of Mass. 31, 34, 35, 38, 57, 66

**DPT** Depth based Person Tracker. 26, 28, 31, 32, 34–36, 39, 44, 49, 51, 55, 56, 66

**FOV** Field Of View. 16, 44, 46, 52

**HGS** Habitual Gait Speed. 23–25, 59

**HS** Heel Strike. 12, 35–37, 51, 55, 56, 65

**IGS** In-home Gait Speed. 23–25, 59, 62, 67

**iTUGT** instrumented Timed Up and Go Test. 16, 17, 21

**MAE** Mean Average Error. 4, 23, 49, 53, 55, 56, 58, 60, 68, 69

**ML** Machine Learning. 38, 39, 49, 50, 55–57, 65

**PD** Parkinson’s Disease. 16, 17, 19

**RF** Random Forest. 28, 37, 38, 55, 57, 59, 65

**ROC** Receiver Operating Characteristic. 57, 58, 68

**SBC** Single Board Computer. 44, 47

**SL** Structured Light. 25–27, 67

**SPPB** Short Physical Performance Battery. 12, 13, 18, 24, 34, 38

**STS** Sit-To-Stand. 3, 4, 10–14, 16, 18, 20, 22, 25, 29, 31, 32, 37–41, 43, 44, 46, 49, 50, 57–62, 64, 65, 67–69

**STW** Sit-To-Walk. 13, 14, 50

**SVM** Support Vector Machine. 38, 57

**SW** Stop-Watch. 17, 21–24, 51, 53, 58

**TO** Toe Off. 12, 35–37, 51, 55, 56, 65

**TOF** Time-Of-Flight. 25–27, 67

**TUG** Timed Up and Go. 22–25, 67

**TUGT** Timed Up and Go Test. 2, 10, 13, 15–17, 20–25, 34, 37, 59



# Bibliography

- [1] U. Nations, “World population ageing: 1950-2050,” *New York: Department of Economic and Social Affairs*, pp. 11–14, 2002.
- [2] U. Nations, “World population prospects: The 2017 revision, key findings and advance tables,” *Department of Economic and Social Affairs, Population Division*, 2017.
- [3] U. Nations, “World population ageing: 1950-2050,” *New York: Department of Economic and Social Affairs*, pp. 90–98, 2002.
- [4] J. C. Millán-Calenti, J. Tubío, S. Pita-Fernández, I. González-Abraldes, T. Lorenzo, T. Fernández-Arruty, and A. Maseda, “Prevalence of functional disability in activities of daily living (adl), instrumental activities of daily living (iadl) and associated factors, as predictors of morbidity and mortality,” *Archives of gerontology and geriatrics*, vol. 50, no. 3, pp. 306–310, 2010.
- [5] H. Sun, V. De Florio, N. Gui, and C. Blondia, “Promises and challenges of ambient assisted living systems,” in *Sixth International Conference on Information Technology: New Generations (ITNG'09)*, pp. 1201–1207, IEEE, 2009.
- [6] S. McLean, A. Sheikh, K. Cresswell, U. Nurmatov, M. Mukherjee, A. Hemmi, and C. Pagliari, “The impact of telehealthcare on the quality and safety of care: a systematic overview,” *PLoS One*, vol. 8, no. 8, p. e71238, 2013.
- [7] P. Eland-de Kok, H. van Os-Medendorp, A. Vergouwe-Meijer, C. Bruijnzeel-Koomen, and W. Ros, “A systematic review of the effects of e-health on chronically ill patients,” *Journal of clinical nursing*, vol. 20, no. 21-22, pp. 2997–3010, 2011.
- [8] G. Demiris, B. K. Hensel, M. Skubic, and M. Rantz, “Senior residents’ perceived need of and preferences for “smart home” sensor technologies,” *International journal of technology assessment in health care*, vol. 24, no. 01, pp. 120–124, 2008.
- [9] J. Favela and X. Alamán, “Special theme: ambient assisted living for mobility: safety, well-being and inclusion,” *Personal and Ubiquitous Computing*, pp. 1–2, 2013.

- [10] A. Clegg, J. Young, S. Iliffe, M. O. Rikkert, and K. Rockwood, “Frailty in elderly people,” *The Lancet*, vol. 381, no. 9868, pp. 752–762, 2013.
- [11] K. Bandeen-Roche, C. L. Seplaki, J. Huang, B. Buta, R. R. Kalyani, R. Varadhan, Q.-L. Xue, J. D. Walston, and J. D. Kasper, “Frailty in older adults: a nationally representative profile in the united states,” *The Journals of Gerontology Series A: Biological Sciences and Medical Sciences*, vol. 70, no. 11, pp. 1427–1434, 2015.
- [12] J. E. Morley, B. Vellas, G. A. Van Kan, S. D. Anker, J. M. Bauer, R. Bernabei, M. Cesari, W. Chumlea, W. Doehner, J. Evans, *et al.*, “Frailty consensus: a call to action,” *Journal of the American Medical Directors Association*, vol. 14, no. 6, pp. 392–397, 2013.
- [13] L. P. Fried, C. M. Tangen, J. Walston, A. B. Newman, C. Hirsch, J. Gottdiener, T. Seeman, R. Tracy, W. J. Kop, G. Burke, *et al.*, “Frailty in older adults: evidence for a phenotype,” *The Journals of Gerontology Series A: Biological Sciences and Medical Sciences*, vol. 56, no. 3, pp. M146–M157, 2001.
- [14] G. Zuliani, C. Soavi, M. Maggio, F. De Vita, A. Cherubini, and S. Volpato, “Counteracting inflammation and insulin resistance with diet and exercise: A strategy for frailty prevention?,” *European Geriatric Medicine*, vol. 6, no. 3, pp. 220–231, 2015.
- [15] S. Ilinca and S. Calciolari, “The patterns of health care utilization by elderly europeans: frailty and its implications for health systems,” *Health services research*, vol. 50, no. 1, pp. 305–320, 2015.
- [16] D. H. Davis, M. R. Rockwood, A. B. Mitnitski, and K. Rockwood, “Impairments in mobility and balance in relation to frailty,” *Archives of gerontology and geriatrics*, vol. 53, no. 1, pp. 79–83, 2011.
- [17] E. Gianaria, M. Grangetto, M. Roppolo, A. Mulasso, and E. Rabaglietti, “Kinect-based gait analysis for automatic frailty syndrome assessment,” in *IEEE International Conference on Image Processing (ICIP)*, pp. 1314–1318, IEEE, 2016.
- [18] D. Podsiadlo and S. Richardson, “The timed “up & go”: a test of basic functional mobility for frail elderly persons,” *Journal of the American geriatrics Society*, vol. 39, no. 2, pp. 142–148, 1991.
- [19] M. Schwenk, J. Mohler, C. Wendel, M. Fain, R. Taylor-Piliae, B. Najafi, *et al.*, “Wearable sensor-based in-home assessment of gait, balance, and physical activity for discrimination of frailty status: baseline results of the arizona frailty cohort study,” *Gerontology*, vol. 61, no. 3, pp. 258–267, 2015.
- [20] T. S. Alexandre, D. M. Meira, N. C. Rico, and S. K. Mizuta, “Accuracy of timed up and go test for screening risk of falls among community-dwelling elderly,” *Brazilian Journal of Physical Therapy*, vol. 16, no. 5, pp. 381–388, 2012.

- [21] T. Frenken, B. Vester, M. Brell, and A. Hein, “atug: Fully-automated timed up and go assessment using ambient sensor technologies,” in *5th International Conference on Pervasive Computing Technologies for Healthcare (PervasiveHealth)*, pp. 55–62, IEEE, 2011.
- [22] R. C. van Lummel, S. Walgaard, A. B. Maier, E. Ainsworth, P. J. Beek, and J. H. van Dieën, “The instrumented sit-to-stand test (ists) has greater clinical relevance than the manually recorded sit-to-stand test in older adults,” *PloS one*, vol. 11, no. 7, p. e0157968, 2016.
- [23] H.-K. Kuo, S. G. Leveille, Y.-H. Yu, and W. P. Milberg, “Cognitive function, habitual gait speed, and late-life disability in the national health and nutrition examination survey (nhanes) 1999–2002,” *Gerontology*, vol. 53, no. 2, pp. 102–110, 2007.
- [24] E. E. Stone and M. Skubic, “Mapping kinect-based in-home gait speed to tug time: a methodology to facilitate clinical interpretation,” in *7th International Conference on Pervasive Computing Technologies for Healthcare (PervasiveHealth)*, pp. 57–64, IEEE, 2013.
- [25] M. Gabel, R. Gilad-Bachrach, E. Renshaw, and A. Schuster, “Full body gait analysis with kinect,” in *Annual International Conference of the IEEE Engineering in Medicine and Biology Society*, pp. 1964–1967, IEEE, 2012.
- [26] P. C. Shih, K. Han, E. S. Poole, M. B. Rosson, and J. M. Carroll, “Use and adoption challenges of wearable activity trackers,” *IConference Proceedings*, 2015.
- [27] C. Rougier, E. Auvinet, J. Rousseau, M. Mignotte, and J. Meunier, “Fall detection from depth map video sequences,” *Toward useful services for elderly and people with disabilities*, pp. 121–128, 2011.
- [28] S. Studenski, S. Perera, K. Patel, C. Rosano, K. Faulkner, M. Inzitari, J. Brach, J. Chandler, P. Cawthon, E. B. Connor, *et al.*, “Gait speed and survival in older adults,” *Jama*, vol. 305, no. 1, pp. 50–58, 2011.
- [29] Y.-Y. Cheng, S.-H. Wei, P.-Y. Chen, M.-W. Tsai, I.-C. Cheng, D.-H. Liu, and C.-L. Kao, “Can sit-to-stand lower limb muscle power predict fall status?,” *Gait & posture*, vol. 40, no. 3, pp. 403–407, 2014.
- [30] S. Allin and A. Mihailidis, “Sit to stand detection and analysis,” in *AAAI Fall Symposium: AI in Eldercare: New Solutions to Old Problems*, pp. 1–3, 2008.
- [31] K. Rockwood, M. Andrew, and A. Mitnitski, “A comparison of two approaches to measuring frailty in elderly people,” *The Journals of Gerontology Series A: Biological Sciences and Medical Sciences*, vol. 62, no. 7, pp. 738–743, 2007.
- [32] X. Chen, G. Mao, and S. Leng, “Frailty syndrome: An overview,” *Clinical Interventions in Aging*, vol. 9, pp. 433–441, 2014.

- [33] K. Rockwood, X. Song, C. MacKnight, H. Bergman, D. B. Hogan, I. McDowell, and A. Mitnitski, "A global clinical measure of fitness and frailty in elderly people," *Canadian Medical Association Journal*, vol. 173, no. 5, pp. 489–495, 2005.
- [34] P.-O. Lang, J.-P. Michel, and D. Zekry, "Frailty syndrome: a transitional state in a dynamic process," *Gerontology*, vol. 55, no. 5, pp. 539–549, 2009.
- [35] A. E. Sales, "Comorbidities, frailty, and "pay-off time"," *Medical Care*, vol. 47, no. 6, pp. 607–609, 2009.
- [36] L. P. Fried, E. C. Hadley, J. D. Walston, A. B. Newman, J. M. Guralnik, S. Studenski, T. B. Harris, W. B. Ershler, and L. Ferrucci, "From bedside to bench: research agenda for frailty," *Science's SAGE KE*, vol. 2005, no. 31, p. pe24, 2005.
- [37] L. Ferrucci, J. M. Guralnik, S. Studenski, L. P. Fried, G. B. Cutler, and J. D. Walston, "Designing randomized, controlled trials aimed at preventing or delaying functional decline and disability in frail, older persons: a consensus report," *Journal of the American Geriatrics Society*, vol. 52, no. 4, pp. 625–634, 2004.
- [38] M. Cesari, G. Gambassi, G. Abellan van Kan, and B. Vellas, "The frailty phenotype and the frailty index: different instruments for different purposes," *Age and ageing*, vol. 43, no. 1, pp. 10–12, 2013.
- [39] S. D. Searle, A. Mitnitski, E. A. Gahbauer, T. M. Gill, and K. Rockwood, "A standard procedure for creating a frailty index," *BMC geriatrics*, vol. 8, no. 1, p. 24, 2008.
- [40] L. P. Fried, L. Ferrucci, J. Darer, J. D. Williamson, and G. Anderson, "Untangling the concepts of disability, frailty, and comorbidity: implications for improved targeting and care," *The Journals of Gerontology Series A: Biological Sciences and Medical Sciences*, vol. 59, no. 3, pp. M255–M263, 2004.
- [41] K. Bandeen-Roche, Q.-L. Xue, L. Ferrucci, J. Walston, J. M. Guralnik, P. Chaves, S. L. Zeger, and L. P. Fried, "Phenotype of frailty: characterization in the women's health and aging studies," *The Journals of Gerontology Series A: Biological Sciences and Medical Sciences*, vol. 61, no. 3, pp. 262–266, 2006.
- [42] S. D. Searle and K. Rockwood, "Frailty and the risk of cognitive impairment," *Alzheimer's research & therapy*, vol. 7, no. 1, p. 54, 2015.
- [43] D. M. Jones, X. Song, and K. Rockwood, "Operationalizing a frailty index from a standardized comprehensive geriatric assessment," *Journal of the American Geriatrics Society*, vol. 52, no. 11, pp. 1929–1933, 2004.
- [44] D. Wieland and V. Hirth, "Comprehensive geriatric assessment," *Cancer Control*, vol. 10, no. 6, pp. 454–462, 2003.

- [45] K. Rockwood and A. Mitnitski, "Frailty in relation to the accumulation of deficits," *The Journals of Gerontology Series A: Biological Sciences and Medical Sciences*, vol. 62, no. 7, pp. 722–727, 2007.
- [46] K. Delbaere, G. Crombez, G. Vanderstraeten, T. Willems, and D. Cambier, "Fear-related avoidance of activities, falls and physical frailty. a prospective community-based cohort study," *Age and ageing*, vol. 33, no. 4, pp. 368–373, 2004.
- [47] M. Montero-Odasso, M. Schapira, C. Varela, C. Pitteri, E. R. Soriano, R. Kaplan, L. A. Camera, and L. Mayorga, "Gait velocity in senior people an easy test for detecting mobility impairment in community elderly," *Journal of Nutrition Health and Aging*, vol. 8, no. 5, pp. 340–343, 2004.
- [48] F. Zhang, L. Ferrucci, E. Culham, E. J. Metter, J. Guralnik, and N. Deshpande, "Performance on five times sit-to-stand task as a predictor of subsequent falls and disability in older persons," *Journal of aging and health*, vol. 25, no. 3, pp. 478–492, 2013.
- [49] J. Anders, U. Dapp, S. Laub, and W. von Renteln-Kruse, "Impact of fall risk and fear of falling on mobility of independently living senior citizens transitioning to frailty: screening results concerning fall prevention in the community," *Zeitschrift fur Gerontologie und Geriatrie*, vol. 40, no. 4, pp. 255–267, 2007.
- [50] A. Tiedemann, H. Shimada, C. Sherrington, S. Murray, and S. Lord, "The comparative ability of eight functional mobility tests for predicting falls in community-dwelling older people," *Age and ageing*, vol. 37, no. 4, pp. 430–435, 2008.
- [51] H. S. Lam, F. W. Lau, G. K. Chan, and K. Sykes, "The validity and reliability of a 6-metre timed walk for the functional assessment of patients with stroke," *Physiotherapy theory and practice*, vol. 26, no. 4, pp. 251–255, 2010.
- [52] T. Abe, Y. Soma, N. Kitano, T. Jindo, A. Sato, K. Tsunoda, T. Tsuji, and T. Okura, "Change in hand dexterity and habitual gait speed reflects cognitive decline over time in healthy older adults: a longitudinal study," *Journal of physical therapy science*, vol. 29, no. 10, pp. 1737–1741, 2017.
- [53] R. W. Bohannon, "Reference values for the timed up and go test: a descriptive meta-analysis," *Journal of geriatric physical therapy*, vol. 29, no. 2, pp. 64–68, 2006.
- [54] K. Berg, S. Wood-Dauphine, J. Williams, and D. Gayton, "Measuring balance in the elderly: preliminary development of an instrument," *Physiotherapy Canada*, vol. 41, no. 6, pp. 304–311, 1989.
- [55] M. Csuka and D. J. McCarty, "Simple method for measurement of lower extremity muscle strength," *The American journal of medicine*, vol. 78, no. 1, pp. 77–81, 1985.

- [56] R. W. Bohannon, “Comfortable and maximum walking speed of adults aged 20–79 years: reference values and determinants,” *Age and ageing*, vol. 26, no. 1, pp. 15–19, 1997.
- [57] J. M. Guralnik, E. M. Simonsick, L. Ferrucci, R. J. Glynn, L. F. Berkman, D. G. Blazer, P. A. Scherr, and R. B. Wallace, “A short physical performance battery assessing lower extremity function: association with self-reported disability and prediction of mortality and nursing home admission,” *Journal of gerontology*, vol. 49, no. 2, pp. M85–M94, 1994.
- [58] J. Cabrero-García, C. L. Muñoz-Mendoza, M. J. Cabañero-Martínez, L. González-Llopis, J. D. Ramos-Pichardo, and A. Reig-Ferrer, “Valores de referencia de la short physical performance battery para pacientes de 70 y más años en atención primaria de salud,” *Atención Primaria*, vol. 44, no. 9, pp. 540–548, 2012.
- [59] T. A. Wren, G. E. Gorton, S. Ounpuu, and C. A. Tucker, “Efficacy of clinical gait analysis: A systematic review,” *Gait & posture*, vol. 34, no. 2, pp. 149–153, 2011.
- [60] S. Lord, P. Halligan, and D. Wade, “Visual gait analysis: the development of a clinical assessment and scale,” *Clinical rehabilitation*, vol. 12, no. 2, pp. 107–119, 1998.
- [61] X. Xu, R. W. McGorry, L.-S. Chou, J.-h. Lin, and C.-c. Chang, “Accuracy of the microsoft kinect™ for measuring gait parameters during treadmill walking,” *Gait & posture*, vol. 42, no. 2, pp. 145–151, 2015.
- [62] J. Perry, J. R. Davids, *et al.*, “Gait analysis: normal and pathological function,” *Journal of Pediatric Orthopaedics*, vol. 12, no. 6, p. 815, 1992.
- [63] P. J. Millington, B. M. Myklebust, G. M. Shambes, *et al.*, “Biomechanical analysis of the sit-to-stand motion in elderly persons,” *Arch Phys Med Rehabil*, vol. 73, no. 7, pp. 609–17, 1992.
- [64] S. R. Lord, S. M. Murray, K. Chapman, B. Munro, and A. Tiedemann, “Sit-to-stand performance depends on sensation, speed, balance, and psychological status in addition to strength in older people,” *The Journals of Gerontology Series A: Biological Sciences and Medical Sciences*, vol. 57, no. 8, pp. M539–M543, 2002.
- [65] W. G. Janssen, H. B. Bussmann, and H. J. Stam, “Determinants of the sit-to-stand movement: a review,” *Physical therapy*, vol. 82, no. 9, pp. 866–879, 2002.
- [66] R. Van Lummel, E. Ainsworth, J. Hausdorff, U. Lindemann, P. Beek, and J. Van Dieen, “Validation of seat-off and seat-on in repeated sit-to-stand movements using a single-body-fixed sensor,” *Physiological measurement*, vol. 33, no. 11, p. 1855, 2012.

- [67] E. Papa and A. Cappozzo, "Sit-to-stand motor strategies investigated in able-bodied young and elderly subjects," *Journal of biomechanics*, vol. 33, no. 9, pp. 1113–1122, 2000.
- [68] M. Galli, V. Cimolin, M. Crivellini, and I. Campanini, "Quantitative analysis of sit to stand movement: experimental set-up definition and application to healthy and hemiplegic adults," *Gait & Posture*, vol. 28, no. 1, pp. 80–85, 2008.
- [69] G. D. Baer and A. M. Ashburn, "Trunk movements in older subjects during sit-to-stand," *Archives of Physical Medicine and Rehabilitation*, vol. 76, no. 9, pp. 844–849, 1995.
- [70] K. Kerr, J. White, D. Barr, and R. Mollan, "Analysis of the sit-stand-sit movement cycle in normal subjects," *Clinical Biomechanics*, vol. 12, no. 4, pp. 236–245, 1997.
- [71] M. Gross, P. Stevenson, S. Charette, G. Pyka, and R. Marcus, "Effect of muscle strength and movement speed on the biomechanics of rising from a chair in healthy elderly and young women," *Gait & posture*, vol. 8, no. 3, pp. 175–185, 1998.
- [72] P.-T. Cheng, M.-Y. Liaw, M.-K. Wong, F.-T. Tang, M.-Y. Lee, and P.-S. Lin, "The sit-to-stand movement in stroke patients and its correlation with falling," *Archives of physical medicine and rehabilitation*, vol. 79, no. 9, pp. 1043–1046, 1998.
- [73] A. Kerr, B. Durward, and K. Kerr, "Defining phases for the sit-to-walk movement," *Clinical biomechanics*, vol. 19, no. 4, pp. 385–390, 2004.
- [74] M. Kouta, K. Shinkoda, and N. Kanemura, "Sit-to-walk versus sit-to-stand or gait initiation: biomechanical analysis of young men," *Journal of Physical Therapy Science*, vol. 18, no. 2, pp. 201–206, 2006.
- [75] A. Magnan, B. J. McFadyen, and G. St-Vincent, "Modification of the sit-to-stand task with the addition of gait initiation," *Gait & Posture*, vol. 4, no. 3, pp. 232–241, 1996.
- [76] M. Mubashir, L. Shao, and L. Seed, "A survey on fall detection: Principles and approaches," *Neurocomputing*, vol. 100, pp. 144–152, 2013.
- [77] J. Templer and B. R. Connell, "Environmental and behavioral factors in falls among the elderly," *Journal of Rehabilitation Research and Development*, vol. 30, p. 92, 1994.
- [78] A. Nowak and R. E. Hubbard, "Falls and frailty: lessons from complex systems," *Journal of the Royal Society of Medicine*, vol. 102, no. 3, pp. 98–102, 2009.
- [79] J. B. Nielsen, "How we walk: central control of muscle activity during human walking," *The Neuroscientist*, vol. 9, no. 3, pp. 195–204, 2003.

- [80] K. A. McMichael, J. Vander Bilt, L. Lavery, E. Rodriguez, and M. Ganguli, "Simple balance and mobility tests can assess falls risk when cognition is impaired," *Geriatric Nursing*, vol. 29, no. 5, pp. 311–323, 2008.
- [81] S. Mathias, U. Nayak, and B. Isaacs, "Balance in elderly patients: the " get-up and go" test.," *Archives of physical medicine and rehabilitation*, vol. 67, no. 6, pp. 387–389, 1986.
- [82] D. J. Rose, C. J. Jones, and N. Lucchese, "Predicting the probability of falls in community-residing older adults using the 8-foot up-and-go: a new measure of functional mobility," *Journal of Aging and Physical Activity*, vol. 10, no. 4, pp. 466–475, 2002.
- [83] J. C. Wall, C. Bell, S. Campbell, and J. Davis, "The timed get-up-and-go test revisited: measurement of the component tasks," *Journal of rehabilitation research and development*, vol. 37, no. 1, p. 109, 2000.
- [84] M. O'brien, K. Power, S. Sanford, K. Smith, and J. Wall, "Temporal gait patterns in healthy young and elderly females," *Physiother Can*, vol. 35, no. 6, pp. 323–26, 1983.
- [85] P. W. Duncan, D. K. Weiner, J. Chandler, and S. Studenski, "Functional reach: a new clinical measure of balance," *Journal of gerontology*, vol. 45, no. 6, pp. M192–M197, 1990.
- [86] B. Allen, R. Derveloy, K. Lowry, H. Handley, N. Fell, W. Gasior, G. Yu, and M. Sarti, "Evaluation of fall risk for post-stroke patients using bluetooth low-energy wireless sensor," in *IEEE Global Communications Conference (GLOBECOM)*, pp. 2598–2603, IEEE, 2013.
- [87] J. M. Morse, R. M. Morse, and S. J. Tylko, "Development of a scale to identify the fall-prone patient," *Canadian Journal on Aging/La Revue canadienne du vieillissement*, vol. 8, no. 4, pp. 366–377, 1989.
- [88] R. Schwendimann, S. De Geest, and K. Milisen, "Evaluation of the morse fall scale in hospitalised patients," *Age and ageing*, vol. 35, no. 3, pp. 311–313, 2006.
- [89] A. Muro-de-la Herran, B. Garcia-Zapirain, and A. Mendez-Zorrilla, "Gait analysis methods: An overview of wearable and non-wearable systems, highlighting clinical applications," *Sensors*, vol. 14, no. 2, pp. 3362–3394, 2014.
- [90] Y. S. Delahoz and M. A. Labrador, "Survey on fall detection and fall prevention using wearable and external sensors," *Sensors*, vol. 14, no. 10, pp. 19806–19842, 2014.
- [91] H. Sayuti, R. A. Rashid, A. L. Mu'azzah, A. Hamid, N. Fisal, M. Sarijari, A. Mohd, K. M. Yusof, and R. A. Rahim, "Lightweight priority scheduling scheme for



- smart home and ambient assisted living system,” *International Journal of Digital Information and Wireless Communications (IJDIWC)*, vol. 4, no. 1, pp. 114–123, 2014.
- [92] S. Patel, H. Park, P. Bonato, L. Chan, and M. Rodgers, “A review of wearable sensors and systems with application in rehabilitation,” *Journal of neuroengineering and rehabilitation*, vol. 9, no. 1, p. 21, 2012.
- [93] E. D. De Bruin, A. Hartmann, D. Uebelhart, K. Murer, and W. Zijlstra, “Wearable systems for monitoring mobility-related activities in older people: a systematic review,” *Clinical rehabilitation*, vol. 22, no. 10-11, pp. 878–895, 2008.
- [94] W. Tao, T. Liu, R. Zheng, and H. Feng, “Gait analysis using wearable sensors,” *Sensors*, vol. 12, no. 2, pp. 2255–2283, 2012.
- [95] J. J. Kavanagh and H. B. Menz, “Accelerometry: a technique for quantifying movement patterns during walking,” *Gait & posture*, vol. 28, no. 1, pp. 1–15, 2008.
- [96] A. Weiss, T. Herman, M. Plotnik, M. Brozgol, N. Giladi, and J. Hausdorff, “An instrumented timed up and go: the added value of an accelerometer for identifying fall risk in idiopathic fallers,” *Physiological measurement*, vol. 32, no. 12, p. 2003, 2011.
- [97] E. P. Doheny, C. W. Fan, T. Foran, B. R. Greene, C. Cunningham, and R. A. Kenny, “An instrumented sit-to-stand test used to examine differences between older fallers and non-fallers,” in *Annual International Conference of the IEEE Engineering in Medicine and Biology Society, EMBC*, pp. 3063–3066, IEEE, 2011.
- [98] A. Salarian, F. B. Horak, C. Zampieri, P. Carlson-Kuhta, J. G. Nutt, and K. Aminian, “itug, a sensitive and reliable measure of mobility,” *IEEE Transactions on Neural Systems and Rehabilitation Engineering*, vol. 18, no. 3, pp. 303–310, 2010.
- [99] A. F. R. Kleiner, I. Pacifici, A. Vagnini, F. Camerota, C. Celletti, F. Stocchi, M. F. De Pandis, and M. Galli, “Timed up and go evaluation with wearable devices: Validation in parkinson’s disease,” *Journal of Bodywork and Movement Therapies*, 2017.
- [100] S. Mellone, C. Tacconi, and L. Chiari, “Validity of a smartphone-based instrumented timed up and go,” *Gait & posture*, vol. 36, no. 1, pp. 163–165, 2012.
- [101] T. E. Group, “Euroqol-a new facility for the measurement of health-related quality of life,” *Health policy*, vol. 16, no. 3, pp. 199–208, 1990.
- [102] H. B. Mann and D. R. Whitney, “On a test of whether one of two random variables is stochastically larger than the other,” *The annals of mathematical statistics*, pp. 50–60, 1947.

- [103] F. Wilcoxon, "Individual comparisons by ranking methods," *Biometrics bulletin*, vol. 1, no. 6, pp. 80–83, 1945.
- [104] M. El-Gohary, S. Pearson, J. McNames, M. Mancini, F. Horak, S. Mellone, and L. Chiari, "Continuous monitoring of turning in patients with movement disability," *Sensors*, vol. 14, no. 1, pp. 356–369, 2013.
- [105] M. Mancini, H. Schlueter, M. El-Gohary, N. Mattek, C. Duncan, J. Kaye, and F. B. Horak, "Continuous monitoring of turning mobility and its association to falls and cognitive function: A pilot study," *Journals of Gerontology Series A: Biomedical Sciences and Medical Sciences*, vol. 71, no. 8, pp. 1102–1108, 2016.
- [106] O. D. Lara and M. A. Labrador, "A survey on human activity recognition using wearable sensors.," *IEEE Communications Surveys and Tutorials*, vol. 15, no. 3, pp. 1192–1209, 2013.
- [107] C. Debes, A. Merentitis, S. Sukhanov, M. Niessen, N. Frangiadakis, and A. Bauer, "Monitoring activities of daily living in smart homes: Understanding human behavior," *IEEE Signal Processing Magazine*, vol. 33, no. 2, pp. 81–94, 2016.
- [108] G. Feng, J. Mai, Z. Ban, X. Guo, and G. Wang, "Floor pressure imaging for fall detection with fiber-optic sensors," *IEEE Pervasive Computing*, vol. 15, no. 2, pp. 40–47, 2016.
- [109] U. Givon, G. Zeilig, and A. Achiron, "Gait analysis in multiple sclerosis: characterization of temporal–spatial parameters using gaitrite functional ambulation system," *Gait & posture*, vol. 29, no. 1, pp. 138–142, 2009.
- [110] B. Jansen, F. Temmermans, and R. Deklerck, "3d human pose recognition for home monitoring of elderly," in *29th Annual International Conference of the IEEE Engineering in Medicine and Biology Society*, pp. 4049–4051, IEEE, 2007.
- [111] E. E. Stone and M. Skubic, "Fall detection in homes of older adults using the microsoft kinect," *IEEE journal of biomedical and health informatics*, vol. 19, no. 1, pp. 290–301, 2015.
- [112] R. Planinc and M. Kampel, "Introducing the use of depth data for fall detection," *Personal and ubiquitous computing*, vol. 17, no. 6, pp. 1063–1072, 2013.
- [113] R. Planinc, A. A. Chaaraoui, M. Kampel, and F. Florez-Revuelta, "Computer vision for active and assisted living," *Active and Assisted Living: Technologies and Applications*, p. 57, 2016.
- [114] S. Vernon, K. Paterson, K. Bower, J. McGinley, K. Miller, Y.-H. Pua, and R. A. Clark, "Quantifying individual components of the timed up and go using the kinect in people living with stroke," *Neurorehabilitation and neural repair*, vol. 29, no. 1, pp. 48–53, 2015.

- [115] J. Shotton, T. Sharp, A. Kipman, A. Fitzgibbon, M. Finocchio, A. Blake, M. Cook, and R. Moore, “Real-time human pose recognition in parts from single depth images,” *Communications of the ACM*, vol. 56, no. 1, pp. 116–124, 2013.
- [116] A. Ejupi, M. Brodie, Y. J. Gschwind, S. R. Lord, W. L. Zagler, and K. Delbaere, “Kinect-based five-times-sit-to-stand test for clinical and in-home assessment of fall risk in older people,” *Gerontology*, vol. 62, no. 1, pp. 118–124, 2016.
- [117] R. J. Gobbens, M. A. van Assen, K. G. Luijkx, M. T. Wijnen-Sponselee, and J. M. Schols, “The tilburg frailty indicator: psychometric properties,” *Journal of the American Medical Directors Association*, vol. 11, no. 5, pp. 344–355, 2010.
- [118] S. Doppelbauer, “Mobility analysis for frailty syndrome assessment,” Master’s thesis, TU Wien, 2017.
- [119] E. E. Stone and M. Skubic, “Unobtrusive, continuous, in-home gait measurement using the microsoft kinect,” *IEEE Transactions on Biomedical Engineering*, vol. 60, no. 10, pp. 2925–2932, 2013.
- [120] E. Stone, M. Skubic, M. Rantz, C. Abbott, and S. Miller, “Average in-home gait speed: Investigation of a new metric for mobility and fall risk assessment of elders,” *Gait & posture*, vol. 41, no. 1, pp. 57–62, 2015.
- [121] R. A. Newton, “Balance screening of an inner city older adult population,” *Archives of physical medicine and rehabilitation*, vol. 78, no. 6, pp. 587–591, 1997.
- [122] C. Pramerdorfer, R. Planinc, M. Van Look, D. Fankhauser, M. Kampel, and M. Brandstötter, “Fall detection based on depth-data in practice,” in *European Conference on Computer Vision*, pp. 195–208, Springer, 2016.
- [123] H. Sarbolandi, D. Lefloch, and A. Kolb, “Kinect range sensing: Structured-light versus time-of-flight kinect,” *Computer Vision and Image Understanding*, vol. 139, pp. 1–20, 2015.
- [124] M. Gupta, Q. Yin, and S. K. Nayar, “Structured light in sunlight,” in *Proceedings of the IEEE International Conference on Computer Vision*, pp. 545–552, 2013.
- [125] A. Kolb, E. Barth, R. Koch, and R. Larsen, “Time-of-flight sensors in computer graphics,” in *Eurographics (STARs)*, pp. 119–134, 2009.
- [126] M. A. Fischler and R. C. Bolles, “Random sample consensus: a paradigm for model fitting with applications to image analysis and automated cartography,” *Communications of the ACM*, vol. 24, no. 6, pp. 381–395, 1981.
- [127] D. Beymer, “Person counting using stereo,” in *Workshop on Human Motion*, pp. 127–133, IEEE, 2000.
- [128] L. Breiman, “Random forests,” *Machine learning*, vol. 45, no. 1, pp. 5–32, 2001.

- [129] C. H. Papadimitriou and K. Steiglitz, *Combinatorial optimization: algorithms and complexity*. Courier Corporation, 1998.
- [130] S. E. Hardy, S. Perera, Y. F. Roumani, J. M. Chandler, and S. A. Studenski, “Improvement in usual gait speed predicts better survival in older adults,” *Journal of the American Geriatrics Society*, vol. 55, no. 11, pp. 1727–1734, 2007.
- [131] J. Verghese, R. Holtzer, R. B. Lipton, and C. Wang, “Quantitative gait markers and incident fall risk in older adults,” *The Journals of Gerontology: Series A*, vol. 64, no. 8, pp. 896–901, 2009.
- [132] I. González, J. Fontecha, R. Hervás, and J. Bravo, “Estimation of temporal gait events from a single accelerometer through the scale-space filtering idea,” *Journal of medical systems*, vol. 40, no. 12, p. 251, 2016.
- [133] T. Banerjee, M. Skubic, J. M. Keller, and C. Abbott, “Sit-to-stand measurement for in-home monitoring using voxel analysis,” *IEEE journal of biomedical and health informatics*, vol. 18, no. 4, pp. 1502–1509, 2014.
- [134] C. Cortes and V. Vapnik, “Support-vector networks,” *Machine learning*, vol. 20, no. 3, pp. 273–297, 1995.
- [135] T. K. Ho, “Random decision forests,” in *Proceedings of the Third International Conference on Document Analysis and Recognition*, vol. 1, pp. 278–282, IEEE, 1995.
- [136] A. Savitzky and M. J. Golay, “Smoothing and differentiation of data by simplified least squares procedures,” *Analytical chemistry*, vol. 36, no. 8, pp. 1627–1639, 1964.
- [137] T. Scheers, R. Philippaerts, and J. Lefevre, “Variability in physical activity patterns as measured by the sensewear armband: how many days are needed?,” *European journal of applied physiology*, vol. 112, no. 5, pp. 1653–1662, 2012.
- [138] J. S. Varsanik, Z. M. Kimmel, C. de Moor, W. Gabel, and G. A. Phillips, “Validation of an ambient measurement system (ams) for walking speed,” *Journal of Medical Engineering & Technology*, pp. 1–13, 2017.
- [139] I. González, I. H. López-Nava, J. Fontecha, A. Muñoz-Meléndez, A. I. Pérez-SanPablo, and I. Quiñones-Urióstegui, “Comparison between passive vision-based system and a wearable inertial-based system for estimating temporal gait parameters related to the gaitrite electronic walkway,” *Journal of biomedical informatics*, vol. 62, pp. 210–223, 2016.
- [140] R. E. Kalman *et al.*, “A new approach to linear filtering and prediction problems,” *Journal of basic Engineering*, vol. 82, no. 1, pp. 35–45, 1960.
- [141] T. Banerjee, J. M. Keller, M. Skubic, and C. Abbott, “Sit-to-stand detection using fuzzy clustering techniques,” in *IEEE International Conference on Fuzzy Systems (FUZZ)*, pp. 1–8, IEEE, 2010.

- [142] R. Krishna, R. Maithreyi, and K. Surapaneni, "Research bias: a review for medical students," *J Clin Diagn Res*, vol. 4, pp. 2320–2324, 2010.